

Russian Original Vol. 42, No. 1, January, 1977

July, 1977



NE

PS

SATEAZ 42(1) 1-90 (1977)



SOVIET ATOMIC ENERGY

АТОМНАЯ ЭНЕРГИЯ
(ATOMNAYA ÉNERGIYA)

TRANSLATED FROM RUSSIAN



CONSULTANTS BUREAU, NEW YORK

SOVIET ATOMIC ENERGY

Soviet Atomic Energy is a cover-to-cover translation of *Atomnaya Énergiya*, a publication of the Academy of Sciences of the USSR.

An agreement with the Copyright Agency of the USSR (VAAP) makes available both advance copies of the Russian journal and original glossy photographs and artwork. This serves to decrease the necessary time lag between publication of the original and publication of the translation and helps to improve the quality of the latter. The translation began with the first issue of the Russian journal.

Editorial Board of *Atomnaya Énergiya*:

Editor: O. D. Kazachkovskii

Associate Editor: N. A. Vlasov

A. A. Bochvar

N. A. Dollezhal'

V. S. Fursóv

I. N. Golovin

V. F. Kalinin

A. K. Krasin

V. V. Matveev

M. G. Meshcheryakov

V. B. Shevchenko

V. I. Smirnov

A. P. Zefirov

Copyright © 1977 Plenum Publishing Corporation, 227 West 17th Street, New York, N.Y. 10011. All rights reserved. No article contained herein may be reproduced, stored in a retrieval system, or transmitted, in any form or by any means, electronic, mechanical, photocopying, microfilming, recording or otherwise, without written permission of the publisher.

Consultants Bureau journals appear about six months after the publication of the original Russian issue. For bibliographic accuracy, the English issue published by Consultants Bureau carries the same number and date as the original Russian from which it was translated. For example, a Russian issue published in December will appear in a Consultants Bureau English translation about the following June, but the translation issue will carry the December date. When ordering any volume or particular issue of a Consultants Bureau journal, please specify the date and, where applicable, the volume and issue numbers of the original Russian. The material you will receive will be a translation of that Russian volume or issue.

Subscription
\$117.50 per volume (6 Issues)
2 volumes per year

Single Issue: \$50
Single Article: \$7.50

Prices somewhat higher outside the United States.

CONSULTANTS BUREAU, NEW YORK AND LONDON



227 West 17th Street
New York, New York 10011

Published monthly. Second-class postage paid at Jamaica, New York 11431.

Soviet Atomic Energy is abstracted or indexed in *Applied Mechanics Reviews*, *Chemical Abstracts*, *Engineering Index*, *INSPEC-Physics Abstracts* and *Electrical and Electronics Abstracts*, *Current Contents*, and *Nuclear Science Abstracts*.

SOVIET ATOMIC ENERGY

A translation of *Atomnaya Énergiya*

July, 1977

Volume 42, Number 1

January, 1977

CONTENTS

Engl./Russ.

ARTICLES

- ✓ Reactivity Effects in a BN-350 Reactor — V. V. Orlov, M. F. Troyanov, V. I. Matveev, G. B. Pomerantsev, N. D. Tverdovskii, G. M. Pshakin, E. M. Khalov, A. P. Ivanov, V. S. Shkol'nik, A. I. Voropaev, and A. V. Danilychev 1 3
- Model of Irradiation Creep of Ceramic Fuel Materials — V. B. Malygin, Yu. K. Bibilashvili, I. S. Golovnin, and K. V. Naboichenko 6 8
- Temperature Dependence of Erosion of Alloys of Vanadium and Niobium during Bombardment with Helium Ions — B. A. Kalin, N. M. Kirilin, A. A. Pisarev, D. M. Skorov, V. G. Tel'kovskii, and G. N. Shishkin 12 13
- Investigation of Radiation Swelling in the Zirconium-Hydrogen System — P. G. Pinchuk, V. N. Bykov, V. A. Karabash, Yu. V. Alekseev, and A. G. Vakhtin 15 16
- Estimate of Perturbations in Solving Nonuniform Neutron Transport Problems by the Monte Carlo Method — D. A. Usikov 18 19
- Measurement of Average Energies of ^{233}U , ^{235}U , and ^{239}Pu Fission Neutron Spectra by a Relative Method — L. M. Andreichuk, B. G. Basova, V. A. Korostylev, V. N. Nefedov, and D. K. Ryazanov 23 23
- Spectrum of Low-Energy Neutrons from the Spontaneous Fission of ^{252}Cr — P. P. D'yachenko, E. A. Seregina, L. S. Kutsaeva, V. M. Piksaikin, N. N. Semenova, M. Z. Tarasco, and A. Laitai 26 25
- Theory of Separation Cascades Consisting of Elements with Several Outlets — B. Sh. Dzhandzhgava, V. A. Kaminskii, N. I. Laguntsov, G. A. Sulaberidze, and V. A. Chuzhinov 30 29

REVIEWS

- ✓ Detection of Flaws in Metal of Atomic Power Plant Equipment during Operation — B. R. Brodskii and É. F. Monina 35 34

DEPOSITED PAPERS

- Optimization of the Cost of the Structural Design of the Radiation Shielding and the Sanitary-Safety Zone of Charged-Particle Accelerators — Yu. A. Bolchek and A. Ya. Yakovlev 42 41
- Theory of Unsteady γ Transport in the Small-Angle Scattering Approximation — V. S. Galishev and G. Ya. Trukhanov 43 41
- Intensity of γ Radiation from an Activated Cylinder — G. S. Vozzhenikov and A. L. Zagoryuev 44 42
- Analysis of the Procedure for Measuring Fast Monoenergetic Neutron Fluxes with Proton Recoil Proportional Counters — A. N. Davletshin and V. A. Tolstikov 44 43

LETTERS TO THE EDITOR

- Application of Direct-Charge Detectors for Power Monitoring in Water-Cooled Water-Moderated Power Reactors — L. I. Golubev, V. A. Zagadkin, M. G. Mitel'man, A. B. Morev, N. D. Rozenblyum, and V. V. Fursov 46 44

CONTENTS

(continued)

Engl./Russ.

Heat Production and Fragment Capture Cross Section in Thermal Reactors — P. E. Nemirovskii and V. A. Chepurinov	48	45
Effect of Approximating the Scattering Indicatrix and Representation of the Constants on the Results of Calculating the Field Characteristics beyond an Iron Barrier — G. Sh. Pekarskii, Yu. Ya. Katsman, and G. A. Kucher	50	47
Flow rate Measurement by Means of Correlating the Random Signals of Thermocouples in Circuits with a Natural Circulation of Coolant — V. M. Selivanov, A. D. Martynov, Yu. A. Sergeev, V. S. Sever'yanov, A. P. Solopov, V. I. Sharypin, D. Pallagi, S. Horanyi, T. Hargitai, and S. Työgyer	53	49
Neutron Resonance Parameters of ²⁴⁵ Cm for Neutron Energies in the 1-30-eV Range — T. S. Belanova, Yu. S. Zamyatnin, A. G. Kolesov, V. M. Lebedev, and V. A. Poruchikov	57	52
Effect of Pressure in Light Water and Benzene Vapors on the Total Interaction Cross Section for Slow Neutrons — V. E. Zhitarev and S. B. Stepanov	59	53
Certain Characteristics of a Personal Film Dosimeter with "K" Emulsion — M. G. Gelev, M. M. Komochkov, I. T. Mishev, Yu. V. Mokrov, and M. I. Salatskaya	61	55
Cross Sections for the Fission of ²³⁵ U and ²³⁹ Pu by 2-, 24-, 55-, and 144-keV Neutrons — K. D. Zhuravlev, N. I. Kroshkin, and L. V. Karin	62	56
Possibilities of Recording Thermal Neutrons with Cadmium Telluride Detectors — A. G. Vradii, M. I. Krapivin, L. V. Maslova, O. A. Matveev, A. Kh. Khusainov, and V. K. Shashurin	64	58
Total Cross Section Measurement for the Reaction T(t,2n) ⁴ He — V. I. Serov, S. N. Abramovich, and L. A. Morkin	66	59
CHRONICLES OF THE COMECON		
Journal of Cooperation	70	62
INFORMATION: SEMINARS, CONFERENCES, AND MEETINGS		
✓ Soviet—French Seminar on Fast Reactors — P. L. Kirillov	73	64
✓ Soviet—American Symposium on Fusion—Fission Reactors — V. I. Pistunovich and G. E. Shatalov	75	65
✓ Eighth International Conference on Nondestructive Testing — V. V. Gorskii	76	66
Chemical Equipment atACHEMA-76 Exhibition — S. M. Karpacheva	78	68
Meeting of IAEA Experts on the Technology of Inertial Plasma Confinement Systems V. M. Korzhavin and V. Yu. Galkin	80	69
Third Session of Soviet—American Coordinating Commission on Thermonuclear Energy — G. A. Eliseev	82	71
The International Conference Neutrino-76 — V. D. Khovanskii	84	72
Second Seminar on Mössbauer Spectroscopy — V. A. Povitskii	86	74
BIBLIOGRAPHY		
Problems of the Metrology of Ionizing Radiation — Reviewed by M. V. Kazarnovskii ...	88	75
É. G. Rakov, Yu. N. Tumanov, Yu. P. Butylkin, A. A. Tsvetkov, N. A. Beleshko, and E. P. Poroikov. The Principal Properties of Inorganic Fluorides — Reviewed by S. S. Rodin and Yu. V. Smirnov	89	76

The Russian press date (podpisano k pechatu) of this issue was 12/24/1976.
Publication therefore did not occur prior to this date, but must be assumed
to have taken place reasonably soon thereafter.

ARTICLES

REACTIVITY EFFECTS IN A BN-350 REACTOR

V. V. Orlov, M. F. Troyanov,
 V. I. Matveev, G. B. Pomerantsev,
 N. D. Tverdovskii, G. M. Pshakin,
 E. M. Khalov, A. P. Ivanov,
 V. S. Shkol'nik, A. I. Voropaev,
 and A. V. Danilychev

UDC 621.039:516.25:621.
 039.516.2:621.039.519

Temperature Effect of Reactivity

First measurements of the temperature effect of reactivity were carried out on a BN-350 reactor during a zero load test from December 1972 to January 1973. These measurements were of a preliminary nature and were carried out basically to estimate temperature corrections to the critical state of the reactor in experiments.

The basic difficulty in measuring the isothermal temperature coefficient is connected with the determination of the reactor temperature and stabilizing it during the measurements. Temperature control in the BN-350 reactor was achieved by means of thermocouples set above the fuel elements (~80 cm above the upper boundary of the active zone) and close to the output manifold.

The first measurements of the temperature coefficient showed a considerable scatter — $(2-6) \cdot 10^{-5} (\Delta k/k) ^\circ\text{C}^{-1}$, which was caused by the small interval of temperature measurements (5-10°C), the inaccuracy of the temperature measurements made with standard apparatus, as well as by the non-steady-state nature of the temperature field in the reactor, as evidenced by the discrepancy of thermocouple readings at different measuring points.

The most representative experiment during this run was one [1,2] in which the change in reactivity was measured on heating the reactor from 152 to 242°C and subsequently cooling it to 222°C. The experiment was carried out with continuous heating of the reactor at a rate of 3-5 deg C/h as a result of electrical heating of the primary and secondary circuits switched on to full power. The pumps in the primary circuit operated at 250 rpm, and the reactor power was maintained at a level of ≈ 100 W.

Slow heating and constant flow rate ensured a sufficiently uniform temperature field throughout the reactor volume. Uniformity of heating was controlled from the thermocouple readings and the drift of the reactivity meter [3]. Error in temperature measurements was reduced to $\pm 0.2^\circ\text{C}$ in the experiments.

Measurements of the temperature effect were repeated during the power trial. In these experiments the reactor was heated and subsequently cooled in the range 209-289°C as a result of the energy released by the operating pumps of the primary circuit and the power of the reactor itself, which was 3-5 MW. The temperature was stabilized with the aid of steam generators. Coolant circulation was achieved by the operation of four pumps working at their rated revolutions. Two loops each of the secondary and tertiary circuits were also switched in. The temperature was measured by stages corresponding to the stages of pressure in the steam generators. For reliable temperature stabilization the reactor was maintained at each stage for 3-7 h. The criterion of stabilization was a discrepancy in the thermocouple readings within the limits $\sim 1.5^\circ\text{C}$, and a drift of the reactivity meter of less than 0.01 cent/h.

The experimental results are shown in Fig.1. In processing results of the measurements the connection between the reactivity and temperature was established from readings of the thermocouples situated above the fuel elements. These were processed by the least-squares method on the assumption that the experimental errors were independent.

Translated from Atomnaya Énergiya, Vol.42, No.1, pp.3-8, January, 1977. Original article submitted April 20, 1976.

This material is protected by copyright registered in the name of Plenum Publishing Corporation, 227 West 17th Street, New York, N.Y. 10011. No part of this publication may be reproduced, stored in a retrieval system, or transmitted, in any form or by any means, electronic, mechanical, photocopying, microfilming, recording or otherwise, without written permission of the publisher. A copy of this article is available from the publisher for \$7.50.

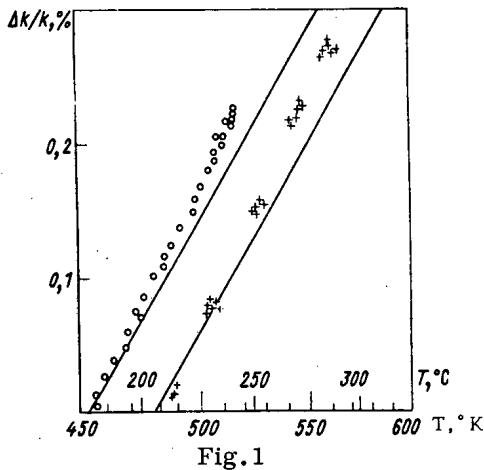


Fig. 1

Fig. 1. Variation of reactivity with isothermal heating of the reactor: —) calculations; ○ and +) first and second experiments, respectively.

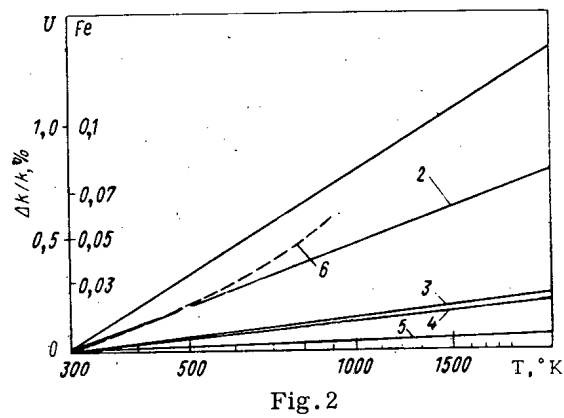


Fig. 2

Fig. 2. Doppler effect, from investigations on uranium and iron, as a function of the temperature (calculations with perturbation theory): 1) whole reactor; 2, 4) zones of low and high enrichment; 3, 5) lateral and end-face shields; 6) iron in the whole reactor.

In determining the error of the isothermal temperature coefficient of reactivity the statistical error in measurements of the temperature, reactivity, and their connection with each other was taken into account as well as the systematic error associated with the fact that the regulating devices have an efficiency that is not specified.

Processing of the experiments yielded the mean value of the isothermal temperature coefficient of reactivity in the interval 180–280°C, which was equal to $-(3.48 \pm 0.32) \cdot 10^{-5} (\Delta k/k) ^\circ\text{C}^{-1}$.

Calculated results were obtained using the catalogs of constants BNAB-70 and ARAMAKO based only on nuclear data, and the programs written in [1, 2, 4]. Calculations of the change in reactivity from the expansion of the sodium on heating (sodium component of the temperature effect) were carried out with first-order perturbation theory in one-dimensional geometry [4]. Corrections were introduced into the calculated results for changes in self-shielding factors of the medium cross sections, and changes in the reflecting properties of the end-face shields. This last correction was found by calculating the change in the effective breeding coefficient by a synthetic method in two-dimensional geometry (ARAMAKO-RADAR program) [2].

The reactivity effect with the change in geometric characteristics during heating of the reactor is negative because of the increased neutron loss. It was calculated from first-order perturbation theory using the similarity method [5].

Radial expansion, determined by the expansion of the steel slab of the lower collector, leads to a change in reactivity given by the relation $\rho_R = -0.457 (\Delta R/R)$, where R and ΔR are the radius of the active zone and its change, respectively.

The calculated value of the change in reactivity as a result of axial expansion depends on the model adopted. For the initial stage of reactor operation under consideration, it was assumed that the fuel is not attached to the shielding and can expand freely. In this case the axial expansion of the reactor is determined by the increase in height of the fuel rod. The effects of expansion of the steel structures in the axial direction and the displacement of the regulation devices relative to the active zone on heating turned out to be small compared with expansion of the fuel. The dependence of reactivity on axial expansion of the reactor is defined by the relation $\rho_H = -0.222 (\Delta H/H)$, where H and ΔH are the height of the active zone and its variation, respectively.

The Doppler effect on reactivity, caused by the temperature dependence of the resonance cross sections, was calculated from perturbation theory. Application of perturbation theory for comparatively small changes of fuel temperature allow us to take into account the change in self-shielding factors for resonance cross sections more accurately than the calculation of two reactor states with different temperatures, and is convenient for analyzing components of the Doppler effect.

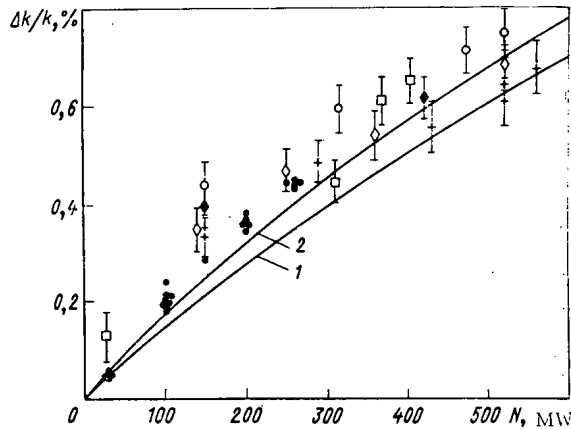


Fig. 3. Change in reactivity for change in power in the range 0-52% of the rated power: ●) measurements during a power test with power being taken up by three loops; later outputs on three (□◇) and four (+◆○) loops; 1) calculations for rated operation of the plant; 2) for operation with three loops.

It was shown in [2] that a more accurate determination of the neutron spectrum in the region below 10 keV is very important in calculating the Doppler effect. For this purpose the ARAMAKO-M-26 program was used [4], in which the group neutron delay cross sections are determined after multigroup calculations of the spectrum inside each group.

The contribution from the end-face shields was found from calculations of the change in K_{eff} by a program using a synthetic method in a two-dimensional model (ARAMAKO-RADAR program [2]).

The magnitude of the Doppler constant was calculated in the range 300-2100°K [$\Gamma(\partial k/\partial T) = 0.007$], as well as the Doppler component of the temperature effect on heating of the fuel.

Data on the temperature dependence of the capture cross sections of iron, chromium, and nickel [6] were used as a basis for determining the contribution from the Doppler effect to the change in reactivity for these materials, which constituted ~8% of the total Doppler effect. The calculated dependence of the Doppler effect on reactor temperature for uniform heating is given in Fig. 2.

Calculated data on the temperature coefficient of reactivity are given in Table 1 comparing it with the measured quantity. It can be seen that the results are roughly 10% lower than the experimental data, and are within the limits of the estimated error of measurement. The calculated quantity can be refined chiefly by increasing the accuracy of the calculations of the Doppler effect and the sodium expansion effect. With regards to the latter, the BFS [7] experiments definitely indicate that there is an excess in the calculations of the contribution from the positive component in the overall change in reactivity as the density of sodium decreases. As a result of this, the calculated temperature coefficient should turn out to be larger than that given in Table 1 after the constants are refined.

Power Reactivity Effect

For a constant coolant flow rate the power reactivity effect is determined by the same processes as the temperature effect. The difference lies in the fact that, as a result of nonuniform heat liberation, a nonuniform temperature field arises in the fuel, in connection with which the relative contribution of the various processes changes compared with the temperature effect. The Doppler component makes the basic contribution (up to ~70%) to the effect. The contribution from the change in reactor volume is determined by the axial expansion of the fuel (~20%) and by the appreciably smaller radial expansion (~5%). The contribution from the change in coolant density is also small (~5%).

The experiments for measuring the power effect were carried out with a more fully loaded active zone as compared with the zero load trial stage. The loading was carried out according to the condition for the reactor to operate at a power of ~50% of the rated power. The power effect measurements were performed while the reactor was being run up to power. Results of the power effect measurements are given in Fig. 3 for various states of the active zone with regard to fuel consumption, and for different numbers of operating loops.

In processing the experimental data, the following facts were taken into account: since the sodium temperature at the reactor input varied from one power level to another, that part of the reactivity effect due to isothermal heating of the reactor was eliminated by reducing all the states to an input temperature of 220°C, using the temperature coefficient of reactivity $3.5 \cdot 10^{-5} (\Delta k/k) ^\circ C^{-1}$; the power effect was determined as the difference in reactivity states for different power levels, all other conditions being equal (input temperature, position of the control apparatus, and coolant flow rate). The power was determined from the thermal output of the tertiary circuit.

TABLE 1. Isothermal Temperature Coefficient of Reactivity and Its Components (average value in the range 180-280°C)

Component	$10^4, \frac{\Delta k}{k} \text{ } ^\circ\text{C}^{-1}$
Sodium expansion	-0,62
Radial expansion of zone	-0,83
Axial expansion of zone (calc. from fuel)	-0,24
Doppler effect: on fuel	-1,39
on steel	-0,10
Total calc. coeff.	-3,18
Experimental value	-3,48 ± 0,32

TABLE 2. Power Effect and Its Components

Components	Total effect, $10^5 \Delta k/k$			
	rated coolant flow rate		operation on three loops	
	0-100 %	0-50 %	0-30 %	0-50 %
Sodium expansion	64	32	28	47
Radial expansion	62	31	25	41
Axial expansion	228	114	76	126
Doppler effect	729	436	336	472
Total effect	1083	613	465	686
Power coeff. in given power range, $10^5 \Delta k/k \text{ MW}$	1,083	1,22	1,55	1,37

While special measurements were being made of the power effect during a power test, a good deal of attention was paid to stabilizing the reactor state for which the effect was being determined. Thus, the experimental results have only a small scatter. When using data obtained while running the reactor up to power after shutdowns, the states were not stabilized carefully enough, and the experimental points have a greater scatter (see Fig. 3). In the comparison of calculations and experiment, the theoretical model allowed for the appropriate coolant flow rate and power level.

Corresponding to the power distribution of the active zone, the reactor was divided into zones where the flow rate was throttled in such a way that the heating of coolant in each zone and the casing temperature of the most heavily loaded fuel elements in them were roughly the same. On this basis, the sodium component of the power effect is defined as follows:

$$\rho_{Na} = \sum_{i=1}^n \left(\frac{\partial \rho}{\partial t} \right)_{Na}^i \frac{\Delta t_i}{2} + \left(\frac{\partial \rho}{\partial t} \right)_{Na}^{u.e.s.} (\Delta t_i + \Delta t_{u.e.s.i}),$$

where n is the number of throttling zones, $(\partial \rho / \partial t)_{Na}^i$ is the sodium component of the i -th zone in the isothermal temperature coefficient of reactivity, $(\partial \rho / \partial t)_{Na}^{u.e.s.}$ is the sodium component of the upper end-face shield in the isothermal coefficient of reactivity, Δt_i and $\Delta t_{u.e.s.i}$ are the mean coolant heating in the i -th zone and the upper end-face shield of this zone. This approach lets us allow accurately enough for the contribution to the power effect from each zone of the reactor in accordance with the heating of its coolant content, including the contribution from the end-face shields as well.

Radial expansion in the power effect is determined by heating of the walls of the fuel cassettes. Buckling of individual cassettes as a result of nonuniform temperature over the cassette perimeter is quite negligible. Two extreme cases were considered when analyzing the radial expansion of the reactor:

- The cassettes are set in the reactor in such a way that the gaps between them are maintained, and the cassette walls expand within the limits of the gaps. In this case the effect is minimal since the change in radius of the active zone is determined only by the expansion of the cassettes at the edges.
- The cassettes touch each other and the active zone expands like a single steel structure. As a result of this the zone assumes the shape of a truncated cone instead of a cylinder. In this case the effect is a maximum.

Since the true position of the cassettes is undetermined, the mean position was used in the calculations. It should be noted that the inaccuracy of the expansion model is unimportant for the total power effect in view of the negligible contribution made by this component. The axial component of expansion is more important. The indeterminacy of this component depends on the connection between the fuel and its jacket, and on the accuracy with which the temperature field of the fuel, and the expansion of fuel and jacket have been calculated. The calculated value of the axial component of the expansion effect was determined from the mean fuel temperature over the whole active zone. Because of the small fuel consumption it was assumed that the fuel expands independently of the jacket.

In addition to the error in determining the Doppler effect, calculations of the fuel temperature in the reactor and making allowance for its nonuniformity play an important part in calculating the Doppler component of the power effect.

The total value of the Doppler component is

$$\rho_D^N = \int_V \int_{T_0}^T \rho_D'(T, \mathbf{r}) d\mathbf{r} dT,$$

where $\rho_D'(T, \mathbf{r})$ is the Doppler coefficient of reactivity for a volume element $d\mathbf{r}$ at the fuel temperature, ρ_D^N is the total value of the Doppler component as the power is varied from zero to the rated power, V is the volume of the reactor, and T_0 and T are the fuel temperatures at zero power and at the rated power, respectively.

The fuel temperature was calculated for fresh fuel from the power distribution for the initial loading of the active zone. A component associated with the construction materials was taken into account in calculating the magnitude of the Doppler effect.

Calculated data for the power effect are given in Table 2 with a breakdown into individual components, while Fig. 3 compares calculated and experimental results for the reactivity effect as a function of power. For a power of $\sim 50\%$ the experimental value for the change in reactivity averaged over all the points is roughly 10% higher than the calculated value. At power levels of $\sim 30\%$ the discrepancy is greater, but the scatter of the points is also more important here.

In connection with the fact that the Doppler effect makes the main contribution to the change in reactivity as the power varies, the cause of values of the calculated power effect which are lower as compared with experiment must be sought above all in the calculations of the fuel temperature and of the neutron spectrum in the region below 10 keV.

Reactivity Effect Dependent on Fuel Depletion

Determining the reactivity effect connected with the change in isotope composition of the fuel on being consumed and the efficiency coefficient is of considerable interest both directly as well as from the point of view of its use together with other functionals in order to correct the constants.

Operation of the reactor at power for a fairly long time enabled us to obtain a first experimental estimate of the effect of depletion on a basis of ~ 36 effective days. The reactivity effect was defined by the difference in reactivity states of the reactor for various power outputs, but with other conditions the same (position of the rods, power, input temperature of the coolant and its flow rate).

The error in determining the depletion effect in this way is basically connected with the accuracy of determining the operation integral for the reactor at power. The experimental value for the depletion effect reduced to a single month of reactor operation at rated power (30 days at 1000 MW), came to $-(0.46 \pm 0.06)\% \Delta k/k$.

The fundamental difficulty in determining the depletion effect theoretically is connected with making sufficiently correct allowance for the nonuniformity of depletion over the active zone and the accumulation of plutonium in the shields. The calculated value of the depletion effect was found by perturbation theory from the volume integral

$$\rho_{\text{dep}} = \sum_{i=1}^n \int_V \rho_i(\mathbf{r}) \Delta A_i(\mathbf{r}) d\mathbf{r},$$

where n is the number of nuclides whose concentration changes during the process of operation, $\rho_i(\mathbf{r})$ is the efficiency of a single nucleus of the i -th nuclide at the point \mathbf{r} , $\Delta A_i(\mathbf{r})$ is the change in concentration of the i -th nuclide at the point \mathbf{r} after 30 effective days.

The calculated value of the effect obtained in this way came to $-0.411\% \Delta k/k$ (depletion of ^{235}U and ^{238}U , -1.25 and $0.065\% \Delta k/k$; accumulation of ^{236}U , fission fragments, and ^{239}Pu , -0.046 , -0.149 , and $0.972\% \Delta k/k$, respectively).

Comparison of calculation and experiment shows that they agree well enough within the limits of experimental error.

CONCLUSIONS

The experiments were the first check on values of the temperature and power reactivity effects and the depletion effect for a fast power reactor. These results and their theoretical analysis enable us to estimate

the reactivity balance in a BN-350 reactor, and to check and refine the methods of calculation. The models and methods used for calculations in designing fast power reactors turned out to be effective and gave quite satisfactory results.

Calculations of the temperature and power reactivity effects somewhat underestimate their values (by $\approx 15\%$). The largest error in the temperature effect comes from the Doppler and sodium components, and in the power effect from the Doppler effect and the indeterminacy in temperature field calculations.

Calculations give a fairly good estimate of the depletion effect also, although in this case obvious care has to be exercised in choosing the method of calculation. This fact is connected with the necessity of correctly allowing for nonuniformity of fuel depletion and the accumulation of plutonium.

Investigation of the reactivity effect for prolonged use of the reactor is of great practical and theoretical interest. The effect of depletion and change in structure of the fuel pellets on the temperature and power effects, the nonlinear nature of the power effect, and the influence of plutonium accumulation on the reactivity effects in the reactor, all these are questions of reactor physics the study of which allows us to increase the accuracy of physical calculations in designing fast power reactors.

LITERATURE CITED

1. V. V. Orlov, *At. Energ.*, 36, No.2, 97 (1974).
2. V. V. Orlov et al., in: *Fast Reactor Power Stations*, BNES, London (1974), p.255.
3. B. G. Dubovskii et al., *At. Energ.*, 36, No.2, 104 (1974).
4. I. P. Markelov et al., *Collected Proceedings on Programming and Methods of Physical Calculations of Fast Reactors SEV* [in Russian], NIAR, Dimitrovgrad (1975), p.34.
5. V. V. Orlov et al., *Kernenergie*, 12, No.4, 112 (1969).
6. H. Takano and V. Ishiguro, in: *EACRP Working Group Meeting, "The keV capture of structural materials Ni, Fe, Cr," Karlsruhe* (1973), KFK-2046, p.317.
7. V. V. Orlov et al., in: *Proceedings of International Symposium on Physics of Fast Reactors, Vol.1, Tokyo, 16-19 Oct. (1973)*, p.571.

MODEL OF IRRADIATION CREEP OF CERAMIC FUEL MATERIALS

V. B. Malygin, Yu. K. Bibilashvili,
I. S. Golovnin, and K. V. Naboichenko

UDC 621.039.531

To construct economic fast-neutron reactors, it is necessary to develop fuel elements capable of withstanding deep burnup without disintegrating. The efficiency of a fuel element is determined by the change in its dimensions owing to core swelling. Therefore, the plasticity of the fuel during the interaction of the core and the fuel-element container is the determining factor on which the reliability of the fuel element depends.

Much attention is devoted to the study of fuel creep under conditions as close as possible to the operating conditions. Analytic models are being developed for irradiation creep to make it possible to justifiably extrapolate experimental data and to use generalized relations in programs for designing different fuel elements.

Many researchers link irradiation creep with the formation of point defects. For the low-temperature range, Brucklacher and Dienst [1] propose a model based on the Nabarro mechanism [2]. Solomon [3] gives a satisfactory explanation of the experimental data by means of a model taking account of the formation of dislocation loops as a result of vacancy condensation. Another mechanism is based on the climb of dislocations because of accelerated vacancy diffusion [4]. An attempt to create a unified model [5] led to a complex dependence of irradiation creep on the stress and neutron flux.

Translated from *Atomnaya Énergiya*, Vol.42, No.1, pp.8-13, January, 1977. Original article submitted January 7, 1976.

This material is protected by copyright registered in the name of Plenum Publishing Corporation, 227 West 17th Street, New York, N.Y. 10011. No part of this publication may be reproduced, stored in a retrieval system, or transmitted, in any form or by any means, electronic, mechanical, photocopying, microfilming, recording or otherwise, without written permission of the publisher. A copy of this article is available from the publisher for \$7.50.

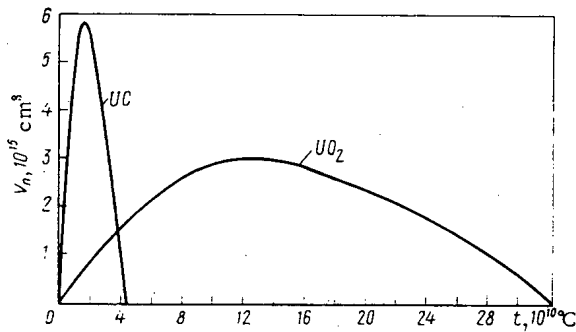


Fig. 1

Fig. 1. Volume of thermal spike vs time.

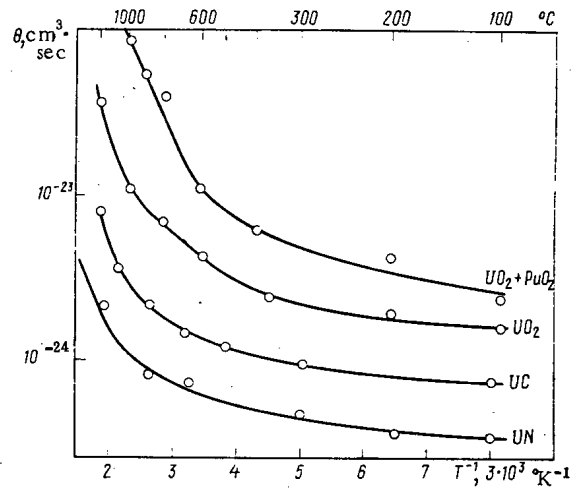


Fig. 2

Fig. 2. The dependence $\theta = \int_0^{t_0} v_n(t) dt$ on the temperature of the ambient material.

Some investigators explain radiation creep on the basis of the concept of thermal and displacement spikes. Irradiation creep is tied in with the relaxation of elastic stresses in the zone of a thermal spike [4] or with the annealing of the ceramic fuel within the volume of the thermal spike [6].

The present paper suggests a model describing the process of irradiation creep on the basis of measured nonstationary creep in out-pile tests.

Strain hardening, as is known, leads to a reduction in the creep rate under constant load up to the onset of steady-state creep characterized by a constant strain rate. Since strain hardening is exhausted during annealing of the material [7], and a renewed loading of such a sample leads to the reappearance of nonstationary creep.

Let us assume that a thermal spike from the fission of heavy atoms, produced by an elevated temperature in some portion of the sample, anneals this portion. As a result, the portion of the sample annealed by the spike is strained in the nonstationary creep stage.

Let us consider a sample of unit volume. Suppose that a constant fission density is established in the sample. The amount of material passing through the thermal spike state in the time t_0 is equal to the volume of the sample, i. e.,

$$t_0 = \beta / V_n \Phi, \tag{1}$$

where V_n is the volume of the spike; β is the coefficient of spike overlap and is equal to 1.6 according to [8]; Φ is the flux density in divisions/cm³·sec.

The time elapsed from the onset of the spike will be taken to be the spike age. Because the strain after annealing corresponds to the range of steady-state creep, the volume of the sample containing spikes of various ages are at different stages of the strain curve. Characteristic of ceramic fuel materials in the range of strains $\sigma \leq 4$ kgf/mm² is a linear dependence of the stationary creep rate on the stress [1, 3, 9, 10]. If the creep in the nonstationary and stationary regions is controlled by a single mechanism, the time dependence of the creep rate at constant temperature can be written as

$$\dot{\epsilon}(t) = A(t) \sigma. \tag{2}$$

All cross sections of the sample have the same creep rate, i. e., the material within the volume of spikes of various ages is strained at the same rate but has a differing creep resistance, determined by the spike age and the time dependence of the nonstationary creep rate.

An elementary cross section S_0 of the sample containing spikes of age 0- t_0 can be treated as a system of n parallel rods of differing rigidity, due to differing creep resistance $A_i = A(t_i)$, where t_i is the age of the i -th spike at a given instant.

For each elementary rod we can write

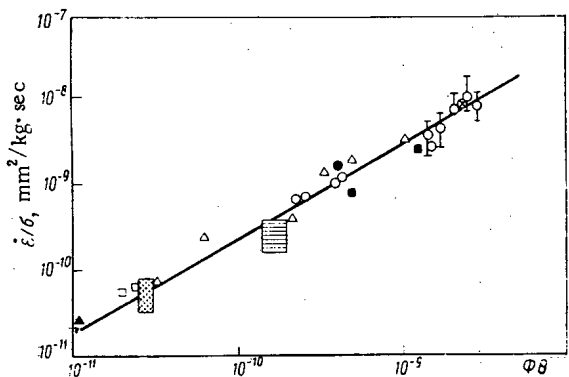


Fig. 3

Fig. 3. Dependence of creep rate on $\phi\theta$: $\circ, \Delta, \square, \blacksquare$) UO_2 [1,4,3,12], respectively; \odot) $\text{UO}_2 + 15\text{PuO}_2$ [12]; \bullet, \otimes) $\text{UO}_2 + 22\text{PuO}_2$ [9,12]; a, b) UN [1]; $\Phi = 3.5 \cdot 10^{13}; 2.5 \cdot 10^{14}$ fissions/cm³·sec; \blacktriangle) UC [17].

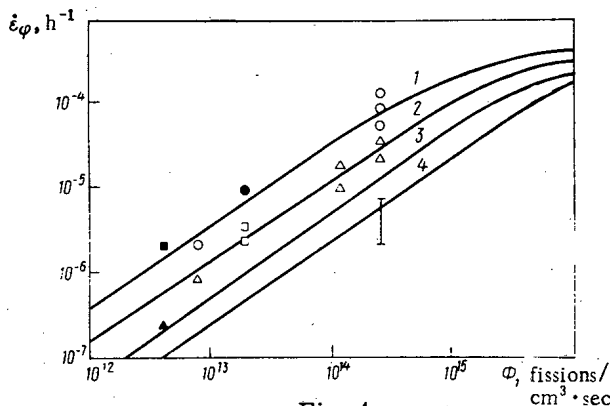


Fig. 4

Fig. 4. Irradiation creep rate vs fission density. Calculation data: 1,2,3,4) $\text{UO}_2 + \text{PuO}_2$; UO_2 ; UC; UN; experimental data: Δ, \square) UO_2 [1,3]; \bullet, \odot) $\text{UO}_2 + \text{PuO}_2$ [9,12]; I) UN [1]; $\blacksquare, \blacktriangle$) UC [13,17].

$$\begin{aligned} \dot{\epsilon}_\varphi &= A_i \sigma_i \quad i = 1, 2 \dots n; \\ \sigma_i &= \dot{\epsilon}_\varphi A_i. \end{aligned} \tag{3}$$

where σ_i is the stress in an individual rod and $\dot{\epsilon}_\varphi$ is the resultant creep rate.

If the time dependence of the creep rate is known for a stress $\sigma = F/S_0$, an expression can be obtained for the irradiation creep rate:

$$\dot{\epsilon}_\varphi = \left(\frac{1}{t_0} \int_0^{t_0} \frac{dt}{\dot{\epsilon}(t)} \right)^{-1}, \tag{4}$$

where $\dot{\epsilon}_\varphi$ is the irradiation creep rate and $\dot{\epsilon}(t)$ is the time dependence of the creep rate, determined outside the pile radiation field.

It follows from Eq. (4) that the model under consideration enables the irradiation creep rate to be determined if the laws of nonstationary creep in the absence of radiation are known.

In designing fuel elements it is of interest to describe the processes that occur in the fuel during transient reactor operating conditions.

The instantaneous increase in the fission density from 0 to Φ results in the following relation for irradiation creep:

$$\dot{\epsilon}_\varphi(t) = \frac{t_0}{\int_0^t \frac{dt}{\dot{\epsilon}(t)} \cdot \frac{t_0-t}{\dot{\epsilon}(\tau)}}, \tag{5}$$

where τ is the time after the sample loading and t is the time after the increase in the fission density.

When the fission density diminishes instantaneously from Φ to 0,

$$\dot{\epsilon}_\varphi(t) = \frac{t_0}{t+t_0} \cdot \int_0^t \frac{dt}{\dot{\epsilon}(t)}. \tag{6}$$

The proposed model permits the variation in the irradiation creep rate to be found for any law of time variation of the fission density.

The dependence of the strain creep on time is described well by a relation [15] in which

$$\epsilon(t) = \epsilon_0 + \frac{\dot{\epsilon}_{st}}{r} \ln \left\{ 1 + \frac{\dot{\epsilon}_{ini} - \dot{\epsilon}_{st}}{\dot{\epsilon}_{st}} [1 - \exp(-rt)] \right\} + \dot{\epsilon}_{st} t, \tag{7}$$

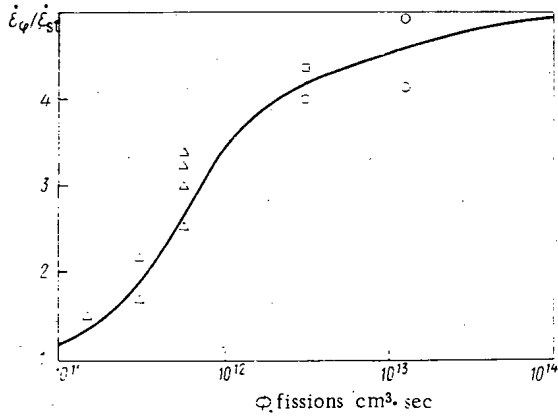


Fig. 5

Fig. 5. Irradiation creep rate vs fission density at a high temperature: ———) calculated curve for UO_2 ; ○) [10]; Δ, □) [14].

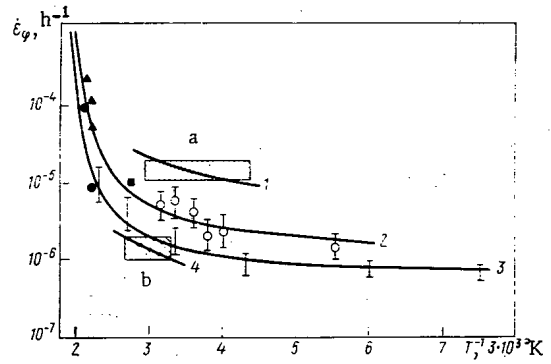


Fig. 6

Fig. 6. Irradiation creep rate vs temperature: ———) calculation data; 1, 3) UO_2 ; $\Phi = 2.5 \cdot 10^{14}$; $1.2 \cdot 10^{13}$; 2) $UO_2 + PuO_2$, $\Phi = 1.2 \cdot 10^{13}$; 4) UN, $\Phi = 2.5 \cdot 10^{14}$; experimental data: a, I, ●) UO_2 [1, 3, 10]; ○) $UO_2 + 15PuO_2$ [12]; ■, ▲) $UO_2 + 22PuO_2$ [9, 12]; b) UN [1].

where ϵ_0 is the instantaneous strain; $\dot{\epsilon}_{ini}$ is the initial creep rate, $\dot{\epsilon}_{st}$ is the steady creep rate, and r is a coefficient characterizing the rate of exhaustion of the nonstationary creep.

Differentiating Eq. (7) with respect to time and inserting the result in Eq. (4), we obtain the dependence of the irradiation creep rate on the fission density and the size of the thermal spike,

$$\dot{\epsilon}_\varphi = \frac{rK\dot{\epsilon}_{st}}{rK - V_n\Phi \left[1 - \exp\left(-\frac{r}{V_n\Phi}\right) \right]} (K-1), \tag{8}$$

where

$$K = \frac{\dot{\epsilon}_{ini}}{\dot{\epsilon}_{st}}.$$

Relation (8) implies that if $\Phi \rightarrow 0$, then the irradiation creep rate approaches the steady laboratory rate, and as $\Phi \rightarrow \infty$ the irradiation creep rate tends to $\dot{\epsilon}_{ini} = K\dot{\epsilon}_{st}$.

At a relatively low temperature, if $K \gg 0$ and $rt \ll 1$, relation (8) becomes

$$\dot{\epsilon}_\varphi = \frac{2\alpha V_n\Phi}{2V_n\Phi - \nu}, \tag{9}$$

where $\alpha = \dot{\epsilon}_{st}/r$ and $\nu = Kr$.

At a temperature of less than $(0.3-0.4)T_f$, it is recommended that nonstationary creep be described by the logarithmic equation [11]

$$\epsilon(t) = \epsilon_0 + \alpha \ln(1 + \nu t), \tag{10}$$

where ϵ_0 is the instantaneous strain, and α and ν are constants for the given testing conditions. This equation is a special case of the relation [15] and gives Eq. (9) for the irradiation creep rate; it follows from Eq. (9) that the irradiation creep rate tends to zero as $\Phi \rightarrow 0$ and tends to $\alpha\nu$ as $\Phi \rightarrow \infty$.

To find quantitative relations describing irradiation creep, it is necessary to make assumptions about the size of the thermal spike and the kinetics of its development.

If a spherical point heat source of output Q acts at the instant of a fission, then, solving the heat-conduction equation, we can find the volume of the thermal spike with a maximum temperature of T_s at its boundary and a lifetime of t_m .

Figure 1 shows the temporal variation in the size of the spike for UO_2 and UC for $T_s = 0.7T_f$ and $T_0 = 1100^\circ C$. The maximum size of the spike in UC is somewhat larger, but its lifetime at a given value of $T_s - T_0$ is significantly smaller than in UO_2 .

TABLE 1. Comparison of Irradiation Creep Rates of Columnar Crystals and Polycrystalline Uranium Dioxide

T, °C	Φ , fissions/cm ³ ·sec									
	1,2·10 ¹³		5,0·10 ¹³		1,0·10 ¹⁴		5,0·10 ¹⁴		1,0·10 ¹⁵	
	ρ 98%	columnar crystals	ρ 98%	columnar crystals	ρ 98%	columnar crystals	ρ 98%	columnar crystals	ρ 98%	columnar crystals
200	3,9·10 ⁻⁷	3,0·10 ⁻⁷	1,6·10 ⁻⁶	1,2·10 ⁻⁶	3,2·10 ⁻⁶	2,4·10 ⁻⁶	1,6·10 ⁻⁵	1,2·10 ⁻⁵	3,2·10 ⁻⁵	2,4·10 ⁻⁵
400	5,0·10 ⁻⁷	3,8·10 ⁻⁷	2,1·10 ⁻⁶	1,6·10 ⁻⁶	4,2·10 ⁻⁶	3,2·10 ⁻⁶	2,1·10 ⁻⁵	1,6·10 ⁻⁵	4,2·10 ⁻⁵	3,2·10 ⁻⁵
600	8,4·10 ⁻⁷	6,0·10 ⁻⁷	3,6·10 ⁻⁶	2,5·10 ⁻⁶	7,2·10 ⁻⁶	5,0·10 ⁻⁶	3,6·10 ⁻⁵	2,5·10 ⁻⁵	7,2·10 ⁻⁵	5,0·10 ⁻⁵
800	1,5·10 ⁻⁶	8,0·10 ⁻⁷	6,3·10 ⁻⁶	3,3·10 ⁻⁶	1,3·10 ⁻⁵	6,6·10 ⁻⁶	6,3·10 ⁻⁵	3,3·10 ⁻⁵	1,3·10 ⁻⁴	6,6·10 ⁻⁵
900	3,0·10 ⁻⁶	1,5·10 ⁻⁶	1,3·10 ⁻⁵	6,2·10 ⁻⁶	2,7·10 ⁻⁵	1,2·10 ⁻⁵	1,3·10 ⁻⁴	6,2·10 ⁻⁵	2,6·10 ⁻⁴	1,2·10 ⁻⁴
1000	—	—	—	—	5 ϵ_{st}	—	—	—	—	—
1200	—	—	—	—	5 ϵ_{st}	—	—	—	—	—

Intensive annealing in the materials is observed at a temperature above $(0.5-0.7)T_f$. Evidently, the depth of annealing is determined by the temperature and the time for which the given volume is at that temperature. Therefore, the following was chosen as a parameter characterizing the annealing of the material of the thermal spikes:

$$\theta = V_{s \text{ eff}} t_{\text{eff}} = \int_0^{t_m} V_s(t) dt, \quad (11)$$

where $V_{s \text{ eff}}$ is the effective spike parameter, t_{eff} is the effective time, and $V_s(t)$ is the dependence of the spike volume on time. Integration of the spike volume with respect to time yields an expression for θ in the form

$$\theta = \frac{8.2}{a} \left[\frac{Q}{(4\pi)^{3/2} C\rho(T_s - T_0)} \right]^{5/3}, \quad (12)$$

where a is the thermal diffusivity, ρ is the density, and C is the specific heat.

The plot of θ versus the reciprocal temperature for $\text{UO}_2 + 25\% \text{PuO}_2$, UO_2 , UC, and UN is shown in Fig. 2. It is seen from the figure that the effect of thermal spikes on the first and last of the materials listed differs by a factor of more than 10.

Let us consider Eq. (9) for irradiation creep at low temperature. If in this equation $\nu \gg V_s \Phi$, then the irradiation creep rate is a linear function of the fission density. Indeed, using relation (11) we obtain

$$\dot{\epsilon}_\varphi = 2\alpha \frac{V_{s \text{ eff}} t_{\text{eff}}}{t_{\text{eff}}} \Phi = \frac{2\alpha\theta}{t_{\text{eff}}} \Phi. \quad (13)$$

Figure 3 presents the dependence of $\dot{\epsilon}_\varphi/\sigma$ on the product for UO_2 , $\text{UO}_2 + \text{PuO}_2$, UC, UN approximating the data of [1,3,9,12,13,17]. All experimental results are reduced to a density equal to 96% of the theoretical value. The experiments were carried out at a temperature of 100–850°C and a density of $7 \cdot 10^{12} - 2.4 \cdot 10^{14}$ fissions/cm³·sec. The results of these investigations in the coordinates adopted are approximated by a straight line whose slope can be used to find the value of $2\alpha/t_{\text{eff}}$ in Eq. (13), equal to 2.7σ . Using Fig. 2 and Eq. (13), we can calculate the irradiation creep rate for various fuel materials.

The value of α in Eq. (13) must be determined in order to calculate the effective volume of a thermal spike. Typical values of α and ν in Eq. (10) were found at 800°C and a strain of 3 kgf/mm² for UO_2 samples with a grain size of 12–15 μ , obtained by cold pressing and subsequent sintering at 1920°K in an argon atmosphere. Under these conditions $\alpha \approx 10^{-5}$ and $\nu \approx 10^{-2} \text{sec}^{-1}$. Substituting this value in Eq. (13), we can find t_{eff} [14]. Then using Eq. [11], we find that $V_{\text{eff}} = 4.0 \cdot 10^5 \theta(T)$.

Thus, knowing the value of α , ν , and V_{eff} , we can write the equation for determining the irradiation creep rate in the low-temperature range.

Figure 4 gives the irradiation creep rate as a function of the fission density, calculated by Eq. (9) with the values found for $V_{s \text{ eff}}$, α , and ν . The calculated relation for UO_2 , $\text{UO}_2 + \text{PuO}_2$, UC, and UN is in satisfactory agreement with the experimental results of [1,3,9,12,13,17], reduced to 600°C.

To calculate the irradiation creep rate at temperatures in excess of 1000–1100°C under laboratory conditions, it is necessary to determine the quantities in Eq. (7). In laboratory experiments with UO_2 samples

it was found that the results obtained at 1150-1300°C and $\sigma = 1-4$ kgf/mm² are described well by Eq. (7) provided that $\dot{\epsilon}_{ini}/\dot{\epsilon}_{st} = 5$. The value of r depends on the temperature and stress; for $\sigma = 3$ kgf/mm², $T = 1150-1200^\circ\text{C}$, we find $r = 1.2 \cdot 10^{-5}$ sec⁻¹. The ratio $\dot{\epsilon}_{ini}/\dot{\epsilon}_{st}$ practically does not change in the given temperature interval. The experimental curves were processed on a computer by the least-squares technique. In Fig. 5 the calculated dependence of $\dot{\epsilon}_0/\dot{\epsilon}_{st}$ on the fission density is given along with data of [10, 14]. It is seen from Fig. 5 that the experimental results are in good agreement with the calculated curve.

To calculate the temperature dependence of the irradiation creep rate it is more convenient to use Eq. (14), consisting of thermal and athermal terms. In this case

$$\dot{\epsilon}_\varphi = A \frac{r\sigma K \exp(-H/RT)}{rA - V_{seff}\Phi [1 - \exp(-r/V_{seff}\Phi)](K-1)} + \frac{2\alpha\nu\sigma V_{seff}\Phi}{2V_{seff}\Phi + \nu} \quad (14)$$

where T is the absolute temperature, R is the gas constant, H is the activation energy, and A is a structure factor in the study of creep without irradiation. The use of Eq. (14) is related to the fact that at a low temperature it is easier experimentally to determine the parameters of Eq. (10).

The effective spike volume in Eq. (14) is determined by the method presented above whereas the other parameters are found from experiments on creep under laboratory conditions. At a high temperature the second term in Eq. (14) is small and at low temperatures, the first term can be neglected. At a temperature of 900-1000°C both terms of Eq. (14) must be taken into account.

Figure 6 presents the results of calculation of the irradiation creep rate by Eq. (14), which are in good agreement with experiment.

The model presented here was employed to calculate the irradiation creep rate of columnar crystals that are formed while the fuel elements are in use. The results of these calculations, with allowance for the differences in thermal diffusivity of the UO₂ polycrystal and single crystal [16], are given in Table 1.

The authors express their gratitude to Yu. N. Sokurskii for his assistance in preparing the paper and for his useful comments in discussing the results.

LITERATURE CITED

1. D. Brucklacher and W. Dienst, *J. Nucl. Mater.*, **42**, 285 (1972).
2. F. Nabarro, in: *Bristol Conference on Strength of Solids*, The Physical Society, London (1948), p. 75.
3. A. Soloman, *J. Am. Ceram. Soc.*, **56**, No. 3, 170 (1973).
4. J. Brinkman and H. Wiedersich, *American Society for Testing and Materials, Special Tech. Publ.*, N380, 3 (1965).
5. F. Nichols, *J. Nucl. Mater.*, **30**, 249 (1969).
6. E. P. Gilbert, *Irradiation Creep of Reactor Materials. Reactor Technology [in Russian]*, No. 3, TsNIIatominform, Moscow (1972).
7. R. W. Cahn (editor), *Physical Metallurgy*, Am. Elsevier (1971).
8. S. T. Konobeevskii, *Effect of Radiation on Materials [in Russian]*, Atomizdat, Moscow (1967).
9. J. Perrin, *J. Nucl. Mater.*, **42**, 101 (1972).
10. J. Perrin, *J. Nucl. Mater.*, **39**, 175 (1971).
11. F. Garofallo, *Laws of Creep and Long-Term Strength for Metals and Alloys [Russian translation]*, Metallurgiya, Moscow (1968).
12. D. Brucklacher and W. Dients, in: *Proceedings of the IAEA Symposium "Fuel and Fuel Elements for Fast Reactors"*, July 2-6, Brussels (1973), Rep. No. 31.
13. D. Glough, in: *Proceedings of the IAEA Symposium "Fast Reactor Fuel and Fuel Elements"*, Sept. 28-30, Karlsruhe (1970), Rep. No. 6.
14. Yu. V. Miloserdin et al., *At. Energ.*, **35**, No. 6, 371 (1973).
15. Jo Li, *Acta Metallurgica*, **11**, 1269 (1963).
16. J. Daniel, in: *Proceedings of the Conference "Thermal Conductivity of UO₂"*, HW-69945, Sept. (1962).
17. D. Glough, *J. Nucl. Mater.*, **56**, No. 3, 279 (1975).

TEMPERATURE DEPENDENCE OF EROSION OF ALLOYS
OF VANADIUM AND NIOBIUM DURING BOMBARDMENT
WITH HELIUM IONS

B. A. Kalin, N. M. Kirilin,
A. A. Pisarev, D. M. Skorov,
V. G. Tel'kovskii, and G. N. Shishkin

UDC 533.924:539.12.17

One of the principal processes leading to breakdown of the primary wall of thermonuclear installations is swelling of the material surface (blistering) owing to uniting of the gas cavities formed directly beneath the surface during ionic bombardment [1]. After thermonuclear installations have been in use for 20 years the coefficient of erosion induced by blistering should not exceed 10^{-2} atom·ion⁻¹ when the ion flux at the wall is $3 \cdot 10^{19}$ ion·m⁻²·sec⁻¹ [2]. It is therefore necessary to select materials stable under bombardment by light ions.

At present vanadium and molybdenum alloys [1] and stainless steel are promising materials for the primary wall, but insufficient work has been done on the behavior of these alloys under bombardment by helium ions and isotopes of hydrogen [3,4].

Our aim is to investigate the temperature dependence of the erosion coefficient of vanadium obtained by electron-beam melting, alloy V + 2.5% Zr + C, and niobium alloys Nb + 4.2% Mo + 0.8% Zr, and Nb + 1.1% Zr + C as a result of swelling during bombardment with 20-keV helium ions at 300-1400°K and doses in the range $(1-50) \cdot 10^{21}$ ion·m².

Experimental Procedure. The specimens for bombardment were obtained by electrolytic polishing of rolled foil $1 \cdot 10^{-4}$ m thick. The compositions of the test materials are listed in Table 1. Bombardment with helium ions was performed in a double-focusing mass monochromator under the conditions described in [3]. The character of the surface breakdown after bombardment was investigated in a UÉMV-100K electron microscope using single-stage carbon replicas. The erosion coefficient was determined from electron micrographs by measuring the geometric size of the broken blisters and calculating the number of atoms in the split-off domes, i.e.,

$$N = N_A \frac{\rho V}{A},$$

where N is the number of detached atoms of the alloy, N_A is the Avogadro number, ρ is the alloy density, V is the volume of the split-off domes, and A is the mean atomic mass of the alloy.

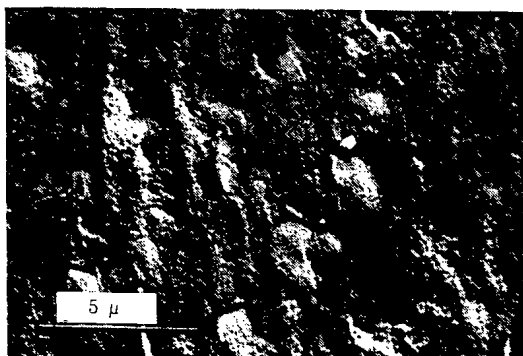
The overall error in the determination of the erosion coefficient was less than 50%.

TABLE 1. Composition of Materials Investigated

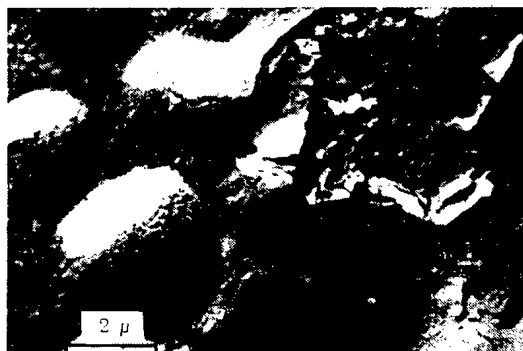
Alloy No.	Alloy composition	Element													
		Nb	Zr	Mo	V	Al	Fe	Ni	Y	Si	S	C	O ₂	N ₂	H ₂
1	V	—	—	—	99,90	0,01	0,05	0,01	—	0,01	0,005	0,02	—	—	—
2	V + 2.5% Zr + C	—	2,50	—	97,07	—	—	—	0,01	—	—	0,40	0,12	—	—
3	Nb + 4.2% Mo + 0.8% Zr	94,73	0,76	4,20	—	—	0,40	0,10	—	0,03	—	0,02	0,02	0,03	0,008
4	Nb + 1.1% Zr + C	98,80	1,10	—	—	—	—	0,011	—	—	—	0,12	0,01	—	0,001

Translated from Atomnaya Énergiya, Vol.42, No.1, pp.13-15, January, 1977. Original article submitted March 29, 1976.

This material is protected by copyright registered in the name of Plenum Publishing Corporation, 227 West 17th Street, New York, N.Y. 10011. No part of this publication may be reproduced, stored in a retrieval system, or transmitted, in any form or by any means, electronic, mechanical, photocopying, microfilming, recording or otherwise, without written permission of the publisher. A copy of this article is available from the publisher for \$7.50.



a



b

Fig.1

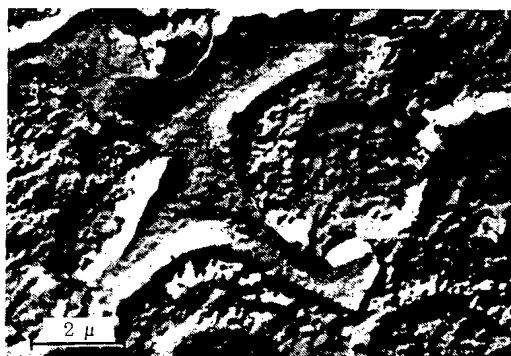


Fig.2

Fig.1. Swelling of alloy Nb + 1.1% Zr + C (a) and vanadium (b), bombarded with doses of helium ions $7.8 \cdot 10^{21}$ and $1 \cdot 10^{22}$ ion \cdot m $^{-2}$ at 800°K.

Fig.2. Erosion of vanadium subjected to a radiation dose of $3.0 \cdot 10^{22}$ ion \cdot m $^{-2}$ at 800°K.

Results and Discussion. An investigation of the character of breakdown of the specimens revealed that surface erosion depends on the radiation dose. When subjected to a radiation dose of up to $6 \cdot 10^{21}$ ion \cdot m $^{-2}$, all the alloys exhibit dome-like swelling of the surface without disintegration of the domes. As the radiation dose is increased to $1 \cdot 10^{22}$ ion \cdot m $^{-2}$ the blister density increases and we observe partial breakoff of the domes (Fig. 1a). When the dose is $1 \cdot 10^{22}$ ion \cdot m $^{-2}$ or more, second-generation blisters appear (Fig.2) and we observe disintegration and detachment of the domes, but the erosion coefficients of the materials scarcely increase, and coincide (within the measurement error) for different radiation doses.

The variation of erosion of the materials with the radiation temperature was revealed for all the alloys investigated (Fig.3); it will be seen that the curves have maxima, the maximal erosion coefficients of vanadium and niobium alloys being observed at 800 and 1000°K, respectively.

We found that 1000 and 1300°K are the temperatures for vanadium and niobium, respectively, above which the surface of the materials does not undergo breakdown by swelling (Fig.4). However, below this temperature (right down to room temperature) the material surface is intensely damaged; the coefficient of erosion due to blistering is several orders of magnitude higher than in the case of physical pulverization, data for which are given in [1].

The dependence of the erosion coefficient for vanadium alloys can be explained on the basis of experiments on evolution of helium from vanadium [5], and from the temperature dependence of the strength characteristics of vanadium alloys. In fact, as the radiation temperature is raised (other conditions being equal) the strength of the alloys decreases and the gas pressure in the blisters increases, promoting disintegration of the surface layer and erosion of the materials.

With a further increase in temperature (above 800°K) we observe stimulated helium diffusion by various vacancy mechanisms together with heightened probability of emergence of helium on the material surface, and also its diffusion to the grain boundaries and to dispersion particles of the second phase. The proportion of gas involved in bulge formation therefore decreases as the temperature is raised.

The temperature dependence of the erosion coefficient for niobium alloys can be explained in the same way. Two factors should be noted: firstly, diffusion processes (other conditions being equal) in these alloys

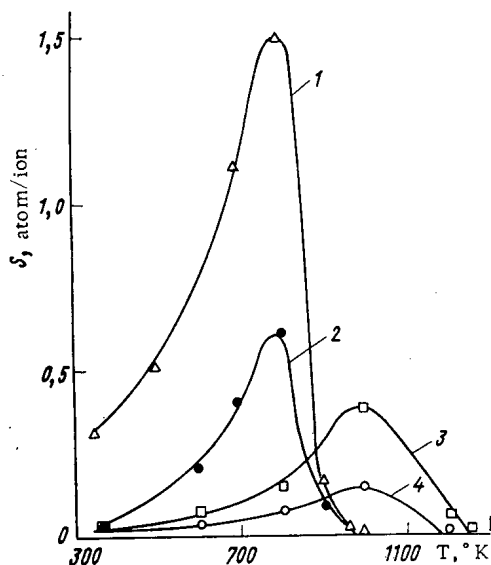


Fig. 3

Fig. 3. Erosion coefficients of niobium and vanadium alloys vs radiation temperature (the numbers near the curves are the alloy Nos. in Table 1).

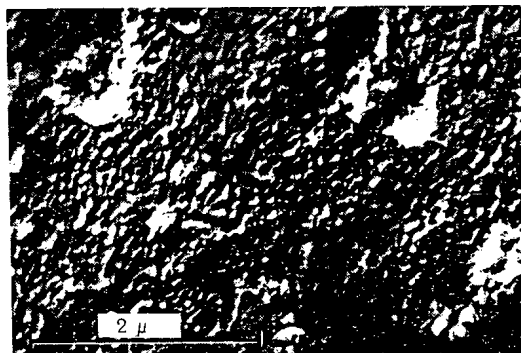


Fig. 4

Fig. 4. Surface of alloy Nb + 4.2% Mo + 0.8% Zr subjected to a dose of helium ions $1.6 \cdot 10^{22}$ ion·m⁻² at 1230°K.

take place at a higher temperature than in vanadium alloys [6]; secondly, a marked change in the strength properties of niobium alloys is observed at a higher temperature. Owing to these processes, the erosion maximum of niobium alloys is apparently shifted toward higher temperatures (~1000°K).

Thus, alloys of vanadium and niobium, alloyed with zirconium and carbon, exhibit high resistance to blister formation at 900–1100 and 1200–1400°K, respectively. In this range the alloys have a minimum SZ, where S is the erosion coefficient and Z is the atomic number of the element. The alloys can therefore minimize energy losses by the plasma, which are proportional to the square of the atomic number of the impurity present in it [7].

CONCLUSIONS

It has been established that maximal erosion of vanadium and its alloys is observed at 700–900°K, the corresponding range for niobium alloys being 900–1100°K. The maximal value of the erosion coefficients of alloys for vanadium and alloys V + 25% Zr + C, Nb + 4.2% Mo + Zr, and Nb + 1.1% Zr + C is 1.5 ± 0.7 , 0.6 ± 0.3 , 0.4 ± 0.2 , and 0.15 ± 0.07 , respectively.

LITERATURE CITED

1. G. Kulcinski and G. Emmert, *J. Nucl. Mater.*, **53**, No. 1, 31 (1974).
2. N. Lagreid and S. Dahlger, *J. Appl. Phys.*, **44**, No. 3, 2093 (1973).
3. B. A. Kanin et al., *At. Energ.*, **39**, No. 2, 126 (1975).
4. B. Kalin, *Proceedings of the Twelfth International Conference on Phenomena in Ionized Gases*, Pt. 1, North-Holland, Am. Elsevier (1975), p. 241.
5. W. Bauer and G. Thomas, *J. Nucl. Mater.*, **53**, No. 1, 127 (1974).
6. A. A. Pisarev and V. G. Tel'kovskii, *At. Energ.*, **38**, No. 3, 152 (1975).
7. D. Meade, *Nucl. Fusion*, **14**, No. 2, 289 (1974).

INVESTIGATION OF RADIATION SWELLING IN THE
ZIRCONIUM-HYDROGEN SYSTEM

P. G. Pinchuk, V. N. Bykov,
V. A. Karabash, Yu. V. Alekseev,
and A. G. Vakhtin

UDC 621.039.532

In order to study the effect of gaseous elements and structural nonuniformities on the vacancy swelling of injection phases, the varying properties and structure of the δ and ϵ phases of zirconium hydrides were investigated after irradiation in the VVRTs and BR-5 reactors at temperatures of 50 and 460-560°C with a fluence of up to $8 \cdot 10^{21}$ neutrons/cm². The hydrostatic density d , microhardness H_{μ} , electrical resistance ρ , crystal lattice periods a and c , phase composition, microstructure (with an increase of 10^2 - 10^5) and the hydrogen content (by the vacuum extraction method) were determined before and after irradiation. The results of the measurements of the properties are shown in Table 1 and also in Figs. 1 and 2.

ϵ Phase. The hydrogen content, type of crystal lattice (face-centered tetragonal), and also the "parquet" substructure (dislocation voids consisting of twins [1]) of ϵ ZrH_{1.9} were unchanged as a result of irradiation.

At an irradiation temperature of 50°C, there were no vacancy pores, but at an irradiation temperature of 500-560°C up to $3 \cdot 10^{16}$ pores are found per 1 cm³, with a diameter of up to 50 Å, whose total volume is equal to 0.2% of the volume of the sample, i.e., less by a factor of 11 than the macroswelling. It is not possible to explain the main part of the swelling by the accumulation of injected zirconium atoms, as there is no significant increase of the volume of an elementary cell, and also by the accumulation of hydrogen atoms displaced from the normal tetrahedral positions to octahedral positions, as the octahedrons are larger than the tetrahedrons. Consequently, the swelling can be explained almost entirely by the buildup of zirconium vacancies and their fine complexes, which are not revealed by means of the electron microscope (~ 10 Å). The absence of a significant increase of volume of an elementary cell does not agree with the concepts of [2], assuming that the cause of swelling of the ϵ phase of zirconium hydride can be only an increase of the volume of an elementary cell. The irradiation temperature of 50 and 470°C amounts to ~ 0.15 and $0.35T_m$ °K, respectively, if it is assumed that in this case the melting point of the metal (T_m) and of its hydride are close to one another, as in the uranium-hydrogen system [3].

In the hydride ZrH_{1.9} when $T_{irr} \sim 0.15 T_m$ it follows from estimates by the curve of increase of density in the divacancy (III) and vacancy (IV) stages of annealing (Fig. 2), that ~ 0.5 at. % of the zirconium vacancies has remained while the concentration of vacancies in metals, e.g., in molybdenum, found by extrapolation of the data of [4], should be less by a factor of ≈ 10 . Obviously, recombinations of the zirconium vacancies and injections in ϵ zirconium hydride prevent the numerous twin-boundaries forming its "parquet" substructure, and separated from one another in all by 500-1200 Å, as the electron microscope has shown. In metals, these boundaries are significantly less; it is well known, however, that they either contribute to an increase of the local concentration and dispersivity of the dislocation sinks of injections, or themselves serve as such sinks [5].

Prevention of recombinations of point defects of the metal sublattice in the hydride, obviously, is possible, and also their amalgamation with defects of the hydrogen sublattice. The presence of the latter is confirmed by the fact that the change of the periods a and c of the lattice of the hydrides ZrH_{1.78}-ZrH_{1.90} as a result of irradiation by a fluence of $1.8 \cdot 10^{21}$ - $8.0 \cdot 10^{21}$ neutrons/cm² corresponds to the release from hydrogen atoms of 4-7% of the tetrahedral positions during dehydrogenation, and a change of the periods a and c as a result of annealing the irradiated sample up to a temperature of 550°C corresponds to population of the tetrahedral positions during hydrogenation (see Figs. 1 and 2). In the case of the unchanged hydrogen content, this is

Translated from Atomnaya Énergiya, Vol. 42, No. 1, pp. 16-19, January, 1977. Original article submitted April 23, 1976.

This material is protected by copyright registered in the name of Plenum Publishing Corporation, 227 West 17th Street, New York, N.Y. 10011. No part of this publication may be reproduced, stored in a retrieval system, or transmitted, in any form or by any means, electronic, mechanical, photocopying, microfilming, recording or otherwise, without written permission of the publisher. A copy of this article is available from the publisher for \$7.50.

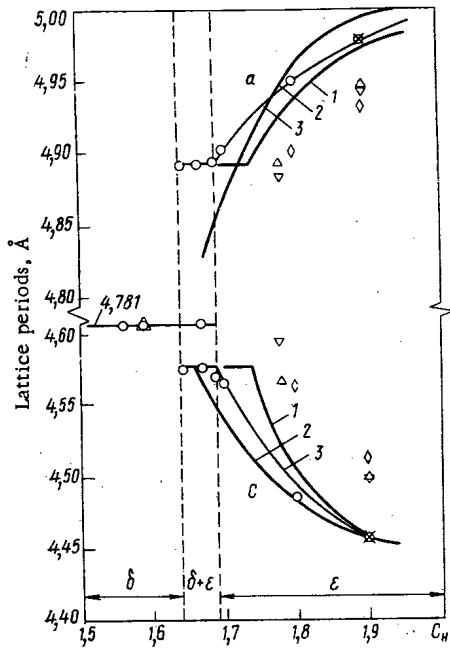


Fig. 1

Fig. 1. Crystal lattice periods of the original and irradiated zirconium hydrides. Before irradiation: 1) [11]; 2) [12]; 3) present paper, after irradiation at 50°C, with a fluence of 10^{21} neutrons/cm²; Δ) 1.8; ∇) 3.2; \diamond) 8; \times) 1.8 and annealing up to 550°C; \circ) experimental points before irradiation.

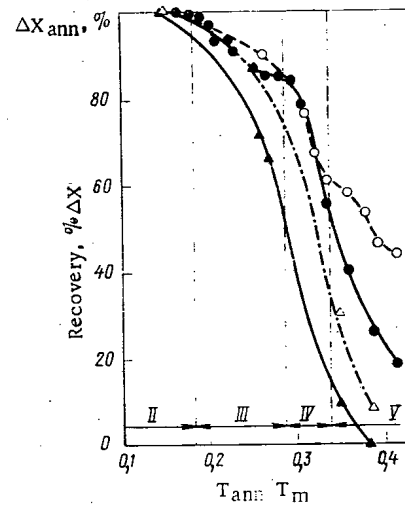


Fig. 2

Fig. 2. Stages of recovery of properties of the hydride $ZrH_{1.9}$, irradiated at 50°C with a fluence of $1.8 \cdot 10^{21}$ neutrons/cm² and with isochronal annealing for an exposure of 1 h. The melting temperature of the hydrides is assumed to be equal to the melting point of zirconium. The annealing stages and their temperature ranges are denoted according to the data of [13] for the face-centered metals: \circ) Δd ; \bullet) $\Delta \rho$; Δ) $\Delta \alpha$; \blacktriangle) Δc .

obviously explained by the buildup during irradiation and recombination during annealing, of approximately the same quantity of hydrogen vacancies and displaced atoms, which allows their number to be estimated.

In addition, the increase of electrical resistance in the ϵ region, initiated by irradiation at 50°C, increases rapidly with increase of the hydrogen content, which also affects the presence of radiation defects of the hydrogen sublattice. It is obvious that the considerable decrease of changes of the lattice periods and of the electrical resistance observed with increase of the irradiation temperature, and also the very considerable advance of the return of these characteristics by comparison with the return of the density in stage V (see Fig. 2), are associated with the annealing of these defects. The latter would be difficult to explain only the segregation of the zirconium vacancies, if we take into account the large degree of dispersion of the defects at an irradiation temperature of 500–560°C and the dependence [6] of the vacancy contribution to the electrical resistance on the size of the pile-up formed.

When $T_{irr} \sim 0.35T_m$, a pile-up of vacancies in the pores with a size, as a rule, of not less than 200 Å, is characteristic for metals. The thermal stability of the fine (~ 10 Å) defects of the vacancy type of the zirconium sublattice of the hydride, causing large swelling with a small total pore volume, is possibly due to the capture of hydrogen atoms by these defects.

Its condition in the voids with a radius of $r \sim 5$ Å is not known; it is easy to show, however, that the mechanism of stabilization does not lead to a counter effect of the hydrogen pressure in a pore p with a surface tension γ , as occurs, e.g., in the case of gas swelling, for which the condition of equilibrium in the cavity is the equation $p = 2\gamma/r$. Actually, at a temperature above 400°C, when the hydrogen in the hydride $ZrH_{1.9}$ is quite soluble and mobile, the pressure cannot be higher than the thermal equilibrium value, and during irradiation of the hydride of this composition [7], it is many times less than $2\gamma/r$ when $r = 5-50$ Å and $\gamma = 0.06 \text{ eV} \cdot \text{Å}^{-2}$, found by the formula

$$\gamma = U_f^v / 4\pi r^2 \quad [8],$$

where $U_{fZr}^v = 1.75 \text{ eV}$ [9].

TABLE 1. Properties of Zirconium Hydrides before Irradiation

Phase	C_H	Density, g/cm^3	Electrical resistance, $\mu\Omega \cdot cm$	Lattice period, \AA		Microhardness, kgf/mm^2
				a	c	
ϵ	1.9	5.610	35.6	4.975	4.454	145
	1.88	5.616	40.0	4.969	4.455	—
σ	1.56	5.647	64.0	4.780	—	265
Mean square error, %		0.1	1	—	—	—
Confidence interval for 90% probability		—	—	0.001	0.002	—

TABLE 2. Change of ΔX Properties of Zirconium Hydrides as a Result of Irradiation*

C_H	Irradiation, $^\circ C$	Fluence, 10^{21} neutrons/ cm^2		Δd	$\Delta \rho$	Δa	ΔC	ΔH_μ
		total	fast†					
1.9	50	1.8	0.1	-1.3	+111	-0.49	+0.99	+50
1.88	470±30	6.2	2.0	-2.4	+12	-0.04	+0.07	+72
1.91	500-560	6.7	2.2	-2.2	—	—	—	—
1.56	50	8.0	0.5	-1.2	+41	0	—	+34
1.56	470±30	4.3	1.4	-1.6	—	—	—	—

* $\Delta X = (X_{irr} - X_{orig}) \cdot 100 / X_{orig} \%$, where X is the property.

† $E > 1; 0.8$ MeV when $t_{irr} = 50; \geq 400^\circ C$, respectively.

The energy stimulus of the vacancy segregation, their emergence at the surface or recombinations with injections, is the reduction of the surface energy and therefore the stability of the vacancies and of their fine complexes will be the greater, the less is the coefficient of the surface tension. It is probable that the capture of hydrogen by zirconium vacancies and their fine pile-up strongly reduces the surface tension by comparison with the calculated value.

δ Phase. It can be seen from Table 1 that the δ phase swells only a little more weakly than the ϵ phase. The microhardness increment also is small, while its fcc lattice remained unchanged. The interpretation of the results is the same as for the ϵ phase. In [2], the dimensions of samples of δ phase irradiated at a temperature of 550-570°C with a fluence of $1.3 \cdot 10^{21}$ neutrons/ cm^2 ($E \geq 1$ MeV) were unchanged. However, the samples were obtained by the hydrogenation of zirconium, but in our case they were obtained by dehydrogenation of the ϵ hydride $ZrH_{1.9}$. Although in both cases there was no appearance in the δ phase of any substructure, an analysis of the facts cited shows that the system of preferential sinks of zirconium injections, originating during the conversion of δ to ϵ , disappears without trace during the reverse conversion, but continues to serve as sinks for the injected atoms. The density of samples of yttrium hydride $YH_{1.9}$, which do not have a substructure and were irradiated in the BR-5 reactor with a fluence of $6.2 \cdot 10^{21}$ neutrons/ cm^2 at a temperature of 460°C ($0.4T_m$), remained unchanged with an accuracy of 0.2%. Obviously, during swelling of the hydrides of the transition metals, the role of hydrogen with increase of temperature is less significant than the role of the structural characteristics. This allows us to suggest that in other alloys with a substructure similar to the substructure of the ϵ hydride of zirconium, the rate of recombination of vacancies and injections will be considerably less than in normal metals. To these alloys are related, e.g., the face-centered tetragonal phases of the systems indium-thallium, chromium-manganese, etc. formed as a result of transitions of the second species [10].

CONCLUSIONS

The radiation swelling of the hydrides $ZrH_{1.78}$ - $ZrH_{1.90}$ at a temperature of 50°C is due to the accumulation of zirconium vacancies and their fine pile-ups. At 430-560°C, swelling is determined by the accumulation of fine ($\sim 10 \text{\AA}$) vacancy complexes. In this case, micropores are also formed, with a diameter of 50 \AA , but their total volume does not exceed one-tenth of the macroswelling.

The considerable buildup of vacancies in the hydrides studied is related with the substructure of the ϵ hydride, formed by dislocation voids and the boundaries of twins, which promote an increase of concentration and dispersivity of the injection sinks or themselves serve as these sinks. In samples of the δ hydride obtained by dehydrogenation of the ϵ phase, the numerous dislocations remaining in the δ hydride after decay of the ϵ -phase substructure obviously fulfill this function. The weak tendency of the zirconium vacancies in the hydride to amalgamation in the pores during increased irradiation temperature (by comparison with the behavior of vacancies in metals) is explained by the reduction of their surface energy as a result of interaction with hydrogen atoms.

The displacement of hydrogen atoms from the tetrahedral positions during irradiation and their return during annealing changes the periods of the crystal lattice of ϵ zirconium hydride in the same way as the change of hydrogen content, which enables the number of defects of the hydrogen sublattice to be estimated.

The authors thank V. I. Shcherbaka and S. I. Porollo for assistance in the electron-microscope investigations, and also Yu. V. Konobeeva for discussions and valuable comments.

LITERATURE CITED

1. R. Chang, J. Nucl. Mater., 2, No.4, 355 (1960).
2. P. Paetz and K. Lucke, J. Nucl. Mater., 43, No.1, 13 (1972).
3. J. Lakner, Nucl. Sci. Abstr., 17, No.4, 579 (1962).
4. J. Brimhall, E. Simonen, and H. Kissinger, J. Nucl. Mater., 48, No.3, 339 (1973).
5. D. Norris, Radiat. Effects, 15, Nos.1-2, 1 (1972).
6. A. C. Damask and G. J. Dienes, Point Defects in Metals, Gordon (1964).
7. V. S. Karasev, V. G. Kovyrshin, and V. V. Yakovlev, At. Energ., 37, No.1, 65 (1974).
8. M. W. Thompson, Defects and Radiation Damage in Metals, Cambridge Univ. Press (1969).
9. Ya. A. Kraftmakher, in: Papers on Solid State Physics [in Russian], No.1, Nauka, Novosibirsk (1967).
10. L. Keys and J. Motteff, J. Nucl. Mater., 34, No.3, 260 (1970).
11. P. Paetz and K. Lucke, Z. Metallkunde, 62, No.9, 657 (1971).
12. R. Beck, Trans. ASME, 55, No.2, 542 (1962).
13. A. C. Damask and G. J. Dienes, Point Defects in Metals, Gordon (1964).

ESTIMATE OF PERTURBATIONS IN SOLVING NONUNIFORM
NEUTRON TRANSPORT PROBLEMS BY THE MONTE CARLO
METHOD

D. A. Usikov

UDC 621.039.51.12:539.125.52

As computers develop there is a steadily increasing interest in using the Monte Carlo method to model radiative transport processes. The present paper gives computational formulas for an important class of reactor physics problems, the calculation of nonlocal perturbations of linear functionals. We consider a group representation of the dependence of neutron cross sections on energy. We describe the case of finite perturbations resulting from a limiting transition when the perturbation parameter tends to zero, and we obtain formulas for the derivatives of linear functionals (the sensitivity coefficients). The dispersion of the computational scheme is studied in an example of a homogeneous one-velocity medium.

The paper presents typical accuracies in calculating the Doppler coefficients of reactivity and density reactivity effects by the Monte Carlo method in reactors and cores of various types.

Method of Correlated Trajectories. We assume that all the medium cross sections are functions of a certain parameter α . With $\alpha = 0$ we obtain a medium in which the particle motion is random. The "effective weight" of a particle belonging to a medium with $\alpha \neq 0$ but following a trajectory drawn by lot in a medium with $\alpha = 0$, we shall designate W . By X_n we denote the set of particle phase coordinates (r, E, Ω) at the n -th collision. The energy E and the flight angle Ω are taken at the moment of collision. The effective particle weight W_n at the n -th collision is determined as follows:

$$W_n = \frac{S(X_0, \alpha)}{S(X_0, 0)} \prod_{i=1}^{n-1} \exp(-\Delta\tau_i) \frac{\Sigma_s(X_i, \alpha) w_s(E_i, \Omega_i - E_{i+1}, \Omega_{i+1}, r_i, \alpha)}{\Sigma_s(X_i, 0) w_s(E_i, \Omega_i - E_{i+1}, \Omega_{i+1}, r_i, 0)} \exp(-\Delta\tau_n) \frac{\Sigma(X_n, \alpha)}{\Sigma(X_n, 0)}, \quad (1)$$

i. e., from the definition $\prod_{i=1}^0 f_i = 1$. In Eq. (1) $\frac{S(X_0, \alpha)}{S(X_0, 0)}$ is the source ratio; $\Delta\tau_i = \int_{l_{i-1}}^{l_i} [\Sigma(r, \alpha) - \Sigma(r, 0)] dl$ is the perturbation of optical depth between the points of collisions $i-1$ and i ; $\Sigma(X, \alpha)$ is the total cross section

Translated from Atomnaya Energiya, Vol.42, No.1, pp.19-22, January, 1977. Original article submitted January 13, 1976.

This material is protected by copyright registered in the name of Plenum Publishing Corporation, 227 West 17th Street, New York, N.Y. 10011. No part of this publication may be reproduced, stored in a retrieval system, or transmitted, in any form or by any means, electronic, mechanical, photocopying, microfilming, recording or otherwise, without written permission of the publisher. A copy of this article is available from the publisher for \$7.50.

for the medium [if elastic scattering of the particle is chosen isotropically in the laboratory coordinate system, and the transport cross section is taken as $\Sigma(X, \alpha)$]; $\Sigma_S(X, \alpha)$ is the scattering cross section*; and $w_S(E_i, \Omega_i \rightarrow E_{i+1}, \Omega_{i+1}, r, \alpha)$ is the angular energy index corresponding to the type of scattering. The values of Σ_S and w_S in the numerator and denominator of Eq. (1) are chosen for the specific scattering process occurring in the medium, where the random process holds (a medium with $\alpha = 0$). The ratio $\frac{\Sigma_S(\alpha)w_S(\alpha)}{\Sigma_S(0)w_S(0)}$ must be finite (a medium with $\alpha = 0$ must not be "narrower" than a medium with $\alpha \neq 0$) in a multitude of possible values of the particle phase coordinates X [1].

We now turn to a detailed determination of the ratio $w = \frac{\Sigma_S(\alpha)w_S(\alpha)}{\Sigma_S(0)w_S(0)}$ in a group model for the dependence of cross section on energy [2]: $w = \frac{\Sigma_S(\alpha)\Gamma \rightarrow \Gamma}{\Sigma_S(0)\Gamma \rightarrow \Gamma}$, if the neutron remains in the same group Γ , where $\Sigma_S(\alpha)\Gamma \rightarrow \Gamma$ is the reaction cross section for "remains in the same group"; $w = \frac{\Sigma_{S(e)}(\alpha)}{\Sigma_{S(e)}(0)}$, if the neutron transfers to the next group $\Gamma + 1$, where $\Sigma_{S(e)}(\alpha)$ is the cross section for transition to the next group.

There is a continuous degradation of neutron energy: 1. The reactions are selected from the macroscopic medium constants. If the neutron transfers to the next energy group after being scattered, then

$w = \frac{\xi(\alpha)\Sigma_S(\alpha)}{\xi(0)\Sigma_S(0)}$, where ξ is the average loss of lethargy; and $\Sigma_S(\alpha)$ is the elastic scattering cross section. If the neutron remains in the same group, then $w = \frac{\Sigma_S(\alpha)[\Delta u - \xi(\alpha)]}{\Sigma_S(0)[\Delta u - \xi(0)]}$, where Δu is the group lethargy interval.

2. We determine the nuclide i in which the scattering occurs. $w = \frac{\Sigma_{Si}(\alpha)}{\Sigma_{Si}(0)}$; and $\Sigma_{Si}(\alpha)$ is the scattering cross section for the i -th nuclide.

For inelastic scattering and the $n-2n$ reaction $w = \frac{\Sigma_{in(n-2n)}(\alpha)_{i \rightarrow j}}{\Sigma_{in(n-2n)}(0)_{i \rightarrow j}}$; and $\Sigma_{in(n-2n)}$ is the cross section for an inelastic transition (or the $n-2n$ reaction) from group i to group j .

If there is an energy degradation on a continuous scale in the scheme of random motion, then $w = \frac{\Sigma_{sH}(\alpha)}{\Sigma_{sH}(0)}$ for hydrogen scattering (with cross section Σ_{sH}). In the group approach w is determined in the same way as for inelastic transitions, as a ratio of the corresponding matrix elements [3]. However, in this case, since the matrix elements are not perturbed, $w = \frac{\Sigma_{sH}(\alpha)}{\Sigma_{sH}(0)}$.

For fission events $w = \frac{\nu(\alpha)\Sigma_f(\alpha)\chi(E_0, \alpha)}{\nu(0)\Sigma_f(0)\chi(E_0, 0)}$, where $\chi(E, \alpha)$ is the spectrum of ejected particles.

The perturbation of the linear flux functional

$$\Delta I = \int [\Sigma_p(\alpha)\Phi(\alpha) - \Sigma_p(0)\Phi(0)] dx,$$

obtained by evaluating the collisions, can be calculated from the formula [1]

$$\Delta I = \frac{1}{H} \sum_{i=1}^H \sum_{n=1}^{l_i} \left[W_n \frac{\Sigma_p(X_n, \alpha)}{\Sigma(X_n, \alpha)} - \frac{\Sigma_p(X_n, 0)}{\Sigma(X_n, 0)} \right], \quad (2)$$

where Σ_p is a certain weight function, e.g., $\nu\Sigma_f$, if the multiplication coefficient is determined [3]; l_i is the number of collisions in the i -th history; Φ is the flux; and H is the number of histories considered.

The evaluation of Eq. (2) is unbiased, since the minuend and the subtrahend are not biased [4].

Evaluation of Derivatives of the Linear Functionals. We can obtain a formula for the derivatives $\frac{\partial I}{\partial \alpha} \Big|_{\alpha=0}$

directly, by going to the limit $\lim_{\Delta \alpha \rightarrow 0} \frac{\Delta I}{\Delta \alpha}$ in Eq. (2) [5,6]. The analog of the effective weight W is the "differential weight" D , obtained by differentiating Eq. (1) with respect to α :

$$D_n = \frac{S'(X_0)}{S(X_0)} + \sum_{i=1}^{n-1} \left[-\Delta \tau'_i + \frac{\Sigma'_s(X_i)}{\Sigma_s(X_i)} + \frac{w'_s(E_i, \Omega_i \rightarrow E_{i+1}, \Omega_{i+1}, r_i)}{w_s(E_i, \Omega_i \rightarrow E_{i+1}, \Omega_{i+1}, r_i)} \right] - \Delta \tau'_n + \frac{S'(X_n)}{S(X_n)}. \quad (3)$$

The primes denote derivatives with respect to α (for $\alpha = 0$).

* The following types of scattering (the number of particles need not be conserved) we usually selected in reactor calculations by the Monte Carlo method: elastic, inelastic, $n-2n$ reactions, hydrogen scattering, and fission of fuel nuclei with ejection of secondary neutrons.

The formula for determining the differential weight (3) is valid for the case where the system geometry is not perturbed (by perturbation of the geometry we understand deformation of the interface of media of different composition), when $\Sigma_S(X_i)$ and $w_S(X_i)$ are not equal to zero. The case of perturbation of geometry was considered in [4, 5]. Extension of the method to the case where no secondary condition is fulfilled requires nonsimilar modeling of trajectories to be performed without change of reaction probabilities.

The derivative of a linear functional $I = \int \Sigma_p \Phi dx$, obtained by evaluating the collisions, is given by the formula

$$I' = \frac{1}{H} \sum_{i=1}^H \sum_{n=1}^{l_i} D_n \frac{\Sigma_p(X_n)}{\Sigma(X_n)}. \quad (4)$$

Because Eq. (2) is unbiased, Eq. (4) is also unbiased.

Dispersion of the Estimate of Perturbations. Even for a homogeneous one-speed problem it is difficult to calculate the dispersion. Therefore, we omit the intermediate calculations, which can be found in [7]. For more complex problems (e.g., multigroup) the analogous analytical calculations are scarcely possible in the real geometry. However, even for such a simplified problem the limits of application of the method can be clearly identified. In particular, the following important observation can be made: the accuracy may be poor in calculating finite perturbations [2], and therefore direct methods of calculating the derivatives, such as Eq. (4), have advantages.

We now determine the dependence of cross section on the parameters in the model problem, as follows:

$$\Sigma(\alpha) = \Sigma_0(1 - \alpha); \quad \Sigma_s = \Sigma_{s0}(1 - \alpha). \quad (5)$$

Let $p = \Sigma_a/\Sigma$ be the probability of capture, where p does not depend on α . As the linear functional we consider the range of capture

$$I = \int p \Psi dx, \quad (6)$$

where Ψ is the density of collisions ($\Psi = \Sigma \Phi$). $P_N = p(1-p)^{N-1}$ is the probability of capture in the N -th collision. The estimate of the interval of Eq. (6), obtained from collisions (all the quantities are quoted per unit neutron source) is

$$\begin{aligned} \bar{I} &= \sum_{N=1}^{\infty} p N P_N = 1; \\ \sigma_I^2 &= \sum_{N=1}^{\infty} (1 - pN)^2 P_N = 1 - p. \end{aligned} \quad (7)$$

The speed of convergence of Eq. (6) is of the order $\sigma_I^2 = (1-p)/H$. A similar calculation for $\frac{\Delta I}{\alpha} = \frac{1}{\alpha} \int [p(\alpha) \Psi(\alpha) - p(0) \Psi(0)] dx$ was given in [7]:

$$\begin{aligned} \Delta I/\alpha &= 0; \\ \sigma_{\Delta I/\alpha}^2 &= (2-p)/[p(1+\alpha)^2 - \alpha^2]. \end{aligned} \quad (8)$$

By analyzing the convergence of the appropriate series and integrals in the derivation of Eq. (8) we obtain the following necessary condition for the existence of finite dispersion:

$$p > (\alpha/1 + \alpha)^2. \quad (9)$$

The allowable values of α fall in the range (α_{\min} , α_{\max}):

$$\alpha_{\min} = \sqrt{p}/(1 + \sqrt{p}); \quad \alpha_{\max} = \sqrt{p}/(1 - \sqrt{p}).$$

The minimum dispersion $\sigma_{\Delta I/\alpha}^2 = [(2-p)(1-p)]/p$ is obtained for $\alpha = p/(1-p)$.

A neutron in a reactor experiences several tens of collisions before absorption or loss, i.e., p is generally a small quantity. The limits of Eq. (9) substantially reduce the sphere of application for direct calculation of perturbations. To calculate large perturbations by the Monte Carlo method one must integrate with respect to a parameter [5], i.e., for each value of α one must calculate $\partial I/\partial \alpha$ (in one history), and then perform the integration

$$\Delta I = \int_0^1 \frac{\partial I}{\partial \alpha} d\alpha.$$

The parameter α is chosen so that the initial medium is obtained for $\alpha = 0$, and the final medium for $\alpha = 1$.

In calculating the derivatives one can evaluate the dispersion from Eq. (8) with $\alpha = 0$

$$\sigma_{I'}^2 = (2-p)/p.$$

For a draw of H histories the following order of convergence is obtained in estimating I' :

$$\sigma_{I'}^2 = (2-p)/Hp. \quad (10)$$

When the capture probability is small the factor for $1/H$ in Eq. (10) is on the order of hundreds. This means that a draw of neutron trajectories 100 times larger is required, to attain the same relative accuracy in estimating a derivative of the number captured, compared with an estimate of the number of captures. The estimate of dispersion of Eq. (10), obtained for a uniform one-velocity medium, can clearly be considered a lower boundary in estimating the method of dispersion. For complete calculations of reactors the dispersion only increases.

When the region of perturbation spans only part of the phase space of the system, the estimate of dispersion of Eq. (10) can be improved:

$$\sigma_{I'}^2 = (2-p)Hvp, \quad (11)$$

where v is the coefficient of variation of the dispersion, which can be considered, as a first approximation, to be equal to the ratio of the number of neutron collisions in the region of perturbation to the total number of collisions.

We must remember that there are methods of calculating perturbations, using modeling of the equations for the importance functions [8-12], which allow us, in particular, to determine local perturbations relating to problems concerning the control action of rods, which cannot be calculated in the scheme considered (the coefficient v in Eq. (11) is small). These promising methods have come into practical use only recently and no dispersion analysis has been done for these.

Accuracy of Calculating Sensitivity Coefficients in the Monte Carlo Method. The index of efficiency in calculating a functional by the Monte Carlo method is considered to be $\delta = \varepsilon^2 t$, where ε is the relative accuracy attained in evaluating a given functional, and t is the machine time required, in minutes. The values of efficiency quoted were obtained by solving typical unsimplified reactor problems. The calculations were made using the ARMONT group of programs [13] in the 26-group or subgroup representation of cross sections in the ARAMAKO catalogue [14] on the M-222 computer with a speed of 20,000 arithmetic operations per second. In R-Z geometry [15] the sensitivity coefficients were computed with respect to change of the material density in the reactor zones or cores and the Doppler reactivity coefficient.

To illustrate the efficiency of computing perturbations the following typical examples of neutron-physics computations were chosen.

1. A thermal reactor with beryllium moderator, made up of 13 zones. The efficiency of calculating the derivative K_{eff} with regard to change in material density, was $\delta = 7.02$ in the zones with fuel. The ratio of the volume of the perturbed region to the total reactor volume was 0.067. Calculation of the derivative K_{eff} with respect to change in reflector density for the same reactor gave the value $\delta = 11.02$. In the latter case the ratio of the volume of the perturbed region to the total reactor volume was 0.73. The efficiency of calculating K_{eff} for the same reactor was 0.033.

2. A thermal reactor with a hydrogenous moderator, consisting of 5 zones. The ratio of the volume of the fuel blocks to the total volume was 0.041. The efficiency of calculating the Doppler reactivity coefficient was $\delta = 1.21$. The efficiency of calculating K_{eff} for the same reactor was $\delta = 0.026$.

3. A core with a hydrogenous moderator, composed of 18 zones. The ratio of volumes of blocks with fuel to the total core volume was 0.049. The efficiency of calculating the Doppler reactivity coefficient was $\delta = 1.044$ (the entire core was subjected to heating). The efficiency of calculating K_{eff} was $\delta = 0.024$.

As can be seen from the results of the calculations, the efficiency of determining K_{eff} is 40-300 times better than in determining the perturbation. In other words, to achieve equal relative accuracy in calculating perturbations we require 40-300 more histories, as compared with calculating K_{eff} .

We note that in the calculations we assumed there were no perturbations of fission sources at the start of the neutron trajectory, i. e., the term $S'(X_0)/S(X_0)$ is zero in Eq. (3). It was shown in [16] that this approximation gives a bias in the estimates of some functionals. For example, in calculating neutron life-time in a reactor the bias may be considerable, reaching 100%. However, in calculating reactivity effects associated with variation of density, and particularly in calculating Doppler reactivity coefficients, the bias does not exceed a 1% effect. This is confirmed by special model calculations. The physical considerations here are simple. It is known that the effect of a perturbation is determined by the probability of avoiding resonance capture. In the process of deceleration to the resonance region, the neutron "forgets" a three-dimensional source perturbation. (We recall that the source interval does not change!) However, for some cases of perturbations of geometry or composition in small reactors with strong reflectors we cannot neglect perturbation of a fission source in calculating perturbations of reactivity.

The author thanks V. G. Zolotukhin for valuable scientific advice.

LITERATURE CITED

1. V. G. Zolotukhin, Preprint FÉI-72, Obninsk (1967).
2. L. P. Abagyan et al., Constant Groups in Nuclear Reactor Computations [in Russian], Atomizdat (1964).
3. A. D. Frank-Kamenetskii, in: The Monte Carlo Method in Radiative Transfer [in Russian], Atomizdat, Moscow (1967), p.212.
4. G. A. Mikhailov, Some Aspects of the Theory of Monte Carlo Methods [in Russian], Nauka, Novosibirsk (1974).
5. D. A. Usikov, Preprint FÉI-423, Obninsk (1973).
6. L. Miller and G. Milley, Nucl. Sci. Engng, 40, 438 (1970).
7. D. A. Usikov, Preprint FÉI-656, Obninsk (1976).
8. M. Kalos, Nucl. Sci. Eng., 37, 410 (1969).
9. L. Carter and N. McCormick, Nucl. Sci. Eng., 39, 296 (1970).
10. J. Spanier and E. M. Gelbard, Monte Carlo Principles and Neutron Transport Problems, Addison-Wesley (1969).
11. V. B. Polevoi, At. Energ., 34, No.4, 296 (1973).
12. A. M. Tsibulya, Preprint FÉI-464, Obninsk (1973).
13. V. V. Korobeinikov et al., in: Topics in Atomic Science and Technology, Nuclear Constants Series [in Russian], No.18, Izd. TsNIIatominform (1972), p. 85.
14. V. F. Khokhlov, M. M. Savos'kin, and M. N. Nikolaev, in: Nuclear Constants [in Russian], No.8, Pt.3, Izd. TsNIIatominform, Moscow (1972), p.3.
15. D. A. Usikov, Preprint FÉI-627, Obninsk (1975).
16. A. D. Frank-Kamenetskii and M. S. Yudkevich, Preprint IAÉ-2155, Moscow (1971).

MEASUREMENT OF AVERAGE ENERGIES OF ^{233}U ,
 ^{235}U , AND ^{239}Pu FISSION NEUTRON SPECTRA BY
 A RELATIVE METHOD

L. M. Andreichuk, B. G. Basova,
 V. A. Korostylev, V. N. Nefedov,
 and D. K. Ryazanov

UDC 539.173

The development of nuclear power has made increased demands on the accuracy of the determination of the energy spectra of fission neutrons of a number of nuclides. The differences in the average energies of fission neutron spectra obtained by various experimenters reach 10%, although the accuracy of the individual measurements is 2-3% [1]. We have measured the average energies of the thermal neutron induced fission neutron spectra of ^{233}U , ^{235}U , and ^{239}Pu relative to the spontaneous fission neutron spectrum of ^{252}Cf .

The method of relative measurements permits a rather accurate estimate of the difference between measured spectra, since in this case the experimental conditions can be maintained closely the same for the standard and unknown spectra. An example of such measurements with an error of 1-2% appears in [2]. The usefulness of relative measurements depends on how well the standard is known. The most accurate measurements have been performed for ^{235}U and ^{252}Cf . There is a trend toward using ^{252}Cf as a standard neutron source, and this stimulates the performing of measurements by various methods to refine the shape of its neutron spectrum. Thus the reliability and accuracy of data on the spectra of other fissionable nuclides are increased by relating them to the ^{252}Cf spontaneous fission neutron spectrum. We have compared the spectra over a neutron energy range of 0.6-10 MeV in which the shape of the neutron spectra is fairly well described by a Maxwellian distribution.

Measurement Procedure and Results. The energy of fission neutrons was measured by the time-of-flight method using a time-to-pulse-height converter constructed on the pulse overlap principle. The ^{252}Cf spontaneous fission neutron spectrum and the neutron spectrum of the nuclide under investigation were measured simultaneously to decrease systematic errors. In addition, the use of a common converter circuit made for the same differential and integral nonlinearities and time calibration in the spectra being compared. Fission fragments were recorded by scintillations of a mixture of gases Ar + 5% N_2 by using two FÉU-30 photomultipliers placed in such a way that each viewed the scintillations from the fragments from only one target. Targets with ^{252}Cf and with uranium or plutonium isotopes were put close together and placed in a beam of thermal neutrons from the SM-2 reactor. The beam was filtered by a 4-cm layer of bismuth and a 10-cm layer of crystalline quartz. The contribution from the fission of ^{252}Cf by thermal neutrons can be neglected.

Targets with the fissionable nuclides ^{252}Cf , ^{233}U , ^{235}U , and ^{239}Pu were made by using a capillary to deposit a solution of a nitrate of the nuclide on a 5-mg/cm² aluminum backing and then evaporating the solution. The amount of ^{252}Cf deposited yielded $5 \cdot 10^3$ divisions/sec. The number of fissions of ^{233}U , ^{235}U , and ^{239}Pu were chosen so as to ensure recording approximately the same number of neutrons from ^{252}Cf and the nuclide being measured in equal time intervals.

The neutron detector was a plastic scintillator 170 mm in diameter and 50 mm thick coupled to an FÉU-63. By using γ radiation from ^{241}Am it was established that the recording threshold is ~ 400 keV for neutrons. To lower the background level, the neutron detector was placed in a shield of lead and borated paraffin which was covered with a 15-mm-thick layer of lead on the side toward the thermal neutron beam. The measurements were performed on a 1-m flight path. The overall time resolution of the apparatus was 4 nsec.

Translated from Atomnaya Énergiya, Vol.42, No.1, pp.23-25, January, 1977. Original article submitted April 5, 1976.

This material is protected by copyright registered in the name of Plenum Publishing Corporation, 227 West 17th Street, New York, N.Y. 10011. No part of this publication may be reproduced, stored in a retrieval system, or transmitted, in any form or by any means, electronic, mechanical, photocopying, microfilming, recording or otherwise, without written permission of the publisher. A copy of this article is available from the publisher for \$7.50.

TABLE 1. Results of Relative Measurements of Fission Neutron Spectra

E, MeV	K ± ΔK	Measured nuclide								
		233U			235U			239Pu		
		T ± ΔT	δK ± ΔδK	K ± ΔK	T ± ΔT	δK ± ΔδK	K ± ΔK	T ± ΔT	δK ± ΔδK	K ± ΔK
0,6-10,0	0,0172± 0,0070	1,372± 0,028	0,0494± 0,0052	0,0461± 0,0040	1,320± 0,022	0,0440± 0,0120	0,0139± 0,0056	1,379± 0,026	0,0311± 0,0074	
0,6-8,5	0,0330± 0,0057	1,343± 0,025	0,0525± 0,0060	0,0589± 0,002	1,298± 0,018	0,0356± 0,0070	0,0188± 0,0072	1,369± 0,028	0,0323± 0,0080	
0,6-8,0	0,0396± 0,0067	1,331± 0,027	0,0535± 0,0069	0,0672± 0,0040	1,284± 0,021	0,0330± 0,0060	0,0198± 0,0063	1,367± 0,027	0,0295± 0,0059	
0,6-7,5	0,0441± 0,0062	1,323± 0,026	0,0559± 0,0073	0,0681± 0,0042	1,283± 0,022	0,0372± 0,0100	0,0182± 0,0061	1,370± 0,027	0,0303± 0,0059	
0,6-6,15	0,0413± 0,0077	1,328± 0,029	0,0645± 0,0084	0,0679± 0,0032	1,283± 0,020	0,0385± 0,0060	0,0159± 0,0062	1,375± 0,027	0,0400± 0,0091	
0,6-5,48	0,0412± 0,0119	1,329± 0,036	0,0676± 0,0081	0,0642± 0,0033	1,289± 0,020	0,0415± 0,0061	0,0210± 0,0074	1,365± 0,029	0,0455± 0,0084	

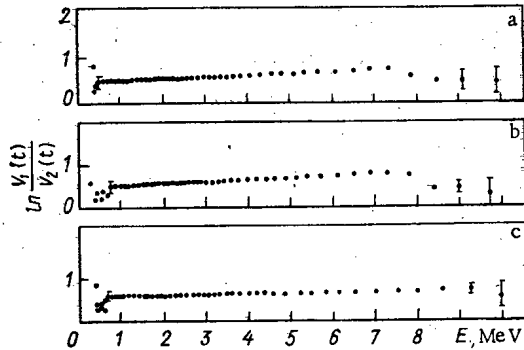


Fig. 1. Logarithm of ratio of two complete fission neutron spectra as a function of neutron energy for a) ^{233}U ; b) ^{235}U ; c) ^{239}Pu for $K = 0.0441 \pm 0.0280$, 0.0686 ± 0.0300 , and 0.0182 ± 0.0142 , respectively.

The time scale of the time-to-pulse-height converter was calibrated with segments of RK-3 cable inserted in the neutron channel. The integral nonlinearity of the time scale was 1%, and the differential 3%. The information was stored in two parts of the memory of an AI-2048 multichannel analyzer with 256 channels for each measured spectrum. Ten series of measurements were performed for each nuclide with the total number of recorded neutrons equal to 10^6 . The background of scattered neutrons was determined by using an iron cone 40 cm long covering the solid angle at the neutron detector.

Each of the two spectra being compared has the shape of a Maxwellian distribution

$$N_1(E) = C_1 \frac{2}{\sqrt{\pi}} T_1^{-3/2} \sqrt{E} \exp(-E/T_1); \quad (1)$$

$$N_2(E) = C_2 \frac{2}{\sqrt{\pi}} T_2^{-3/2} \sqrt{E} \exp(-E/T_2).$$

Here E is the neutron energy in MeV, and T_1 and T_2 are the temperatures of the spectra. Each spectrum can be expressed in terms of experimentally measurable quantities by the equation

$$N(E) dE = A \varepsilon(t) V(t) t^3 dE, \quad (2)$$

in which $\varepsilon(t)$ is the efficiency of the neutron detector, $V(t)$ is the measured distribution of time intervals between start and stop pulses, t is the time scale in nsec, and A is a normalization constant.

In Eq. (2) E and t are related by the familiar expression

$$t = 72.3l/\sqrt{E}, \quad (3)$$

where l is the neutron flight path.

The logarithm of the ratio of two spectra is

$$\ln \frac{N_1(E)}{N_2(E)} = \ln \frac{V_1(t)}{V_2(t)} + \ln \frac{A_1}{A_2} = \ln \frac{C_1}{C_2} + \frac{3}{2} \ln \frac{T_2}{T_1} + E \frac{T_1 - T_2}{T_1 T_2}. \quad (4)$$

It is assumed that $\varepsilon(t)$ has the same effect on both spectra being measured, which is admissible if the difference between the spectra is small. In the coordinates $\ln[V_1(t)/V_2(t)]$ and E Eq. (4) is the equation of a straight line with the slope $K = (T_1 - T_2)/T_1 T_2$. Taking account of the fact that $\ln(A_1/A_2)$, $\ln(C_1/C_2)$, and $(3/2) \ln(T_2/T_1)$, which is close to zero, produce a parallel displacement of the straight line, different for the various spectra being compared, but not affecting its slope, K can be used to find the temperature of the unknown spectrum T_2 from the known temperature T_1 . To do this the spontaneous fission spectrum of ^{252}Cf with $T_1 = 1.406 \pm 0.015$ is assumed known [3], and K is calculated by the least-squares method. The results of the data processing are shown in Table 1 and Fig. 1.

The values of K and ΔK were found by averaging 10 measurements for each nuclide. The error ΔK basically reflects the statistical error, and in the present case is small. The error δK is very much larger and reflects the accuracy with which the choice of experimental points of $\ln[V_1(t)/V_2(t)]$ is approximated by a straight line using the least-squares method (Fig. 1). This error includes all possible systematic and random errors. Taking account of the fact that the statistical errors are small and the systematic errors are appreciably decreased in the method of relative measurements, it is reasonable to assume that this error is the upper limit of the accuracy with which the real shape of the measured spectra follows a Maxwellian distribution in the neutron energy range considered. From this point of view, of the three measured spectra the ^{239}Pu spectrum is best described by a Maxwellian distribution, the ^{235}U spectrum is worse, and the ^{233}U spectrum is still worse, if the ^{252}Cf spectrum is assumed purely Maxwellian. The spectra of the uranium isotopes show a small predominance of neutrons with energies $E > 7.5$ MeV. This effect can easily be accounted for, for example, by the worsening of the time resolution of the apparatus. In the present case this is improbable since the spectra of the various nuclides were measured alternately, and in addition a control measurement of $^{252}\text{Cf}/^{233}\text{U}$ performed with better time resolution showed the same trend.

According to estimates in [4] the effect of time resolution ($\Delta t = 4$ nsec) on average values can be neglected. The values of ΔT were calculated on the basis of the error of the standard and the statistical error ΔK without taking account of δK . The average energies of the spectra can be found from the relation $\bar{E} = 3T/2$. In the 0.6-8-MeV energy range the values of \bar{E} found for ^{233}U , ^{235}U , and ^{239}Pu were, respectively, 1.996 ± 0.040 , 1.926 ± 0.030 , and 2.050 ± 0.040 MeV.

Our data are in good agreement with the results of [5] (1.950 ± 0.030 and 2.055 ± 0.030 MeV for ^{235}U and ^{239}Pu) which were obtained by the time-of-flight method, and with the data of [6] (1.950 ± 0.030 and 2.070 ± 0.030 MeV for ^{235}U and ^{239}Pu) determined by a single-crystal stilbene spectrometer. The value of the average energy $\bar{E} = 1.982 \pm 0.006$ MeV of the slow neutron induced ^{233}U fission neutron spectrum found in [7] by the time-of-flight method relative to the spectrum of ^{235}U neutrons with $\bar{E} = 1.935$ MeV was confirmed also.

LITERATURE CITED

1. A. Koster, in: Proceedings of the IAEA Symposium on Prompt Fission Neutron Spectra, Vienna, Aug. 25-27 (1971), p. 19.
2. A. Smith, Nucl. Sci. and Eng., 44, No. 3, 439 (1971).
3. L. Green, J. Mitchell, and N. Steen, Nucl. Sci. and Eng., 50, No. 3, 257 (1973).
4. N. V. Kornilov, Preprint FÉI-276, Obninsk (1971).
5. D. Abramson et al., in: Proceedings of the Conference on Neutron Physics [in Russian], Pt. 3, ONTI FÉI (1974), p. 46.
6. Z. Aleksandrova et al., At. Energ., 38, No. 2, 108 (1975).
7. L. Green, J. Mitchell, and N. Steen, Nucl. Sci. and Eng., 52, No. 3, 406 (1973).

SPECTRUM OF LOW-ENERGY NEUTRONS FROM
THE SPONTANEOUS FISSION OF ^{252}Cf

P. P. D'yachenko, E. A. Seregina,
L. S. Kutsaeva, V. M. Piksaikin,
N. N. Semenova, M. Z. Tarasco,
and A. Laitai*

UDC 539.173.84

A detailed study of the spectrum of prompt neutrons from the spontaneous fission of ^{252}Cf is of considerable interest both for nuclear physics and for a number of practical problems related to the use of californium as a standard neutron source. In spite of the large number of published papers the accuracy of the existing data is still inadequate for most of these problems. The region of low neutron energies has been least studied. According to the data of [1-4] an excessive number of neutrons is found in the $0 < E_n < 1$ -MeV range as compared with the number predicted by extrapolating the data from higher energies using the $\sqrt{E} \exp(-E/T)$ law. The nature of this excess is still not clear. All the measurements reported in [1-4] were made by the time-of-flight method. Thus there is a possibility that the observed effect is a consequence of systematic errors in this method related, for example, to inaccurate knowledge of the detector efficiency $\varepsilon(E_n)$ or, as noted in [5], to an inaccurate account of the background of scattered neutrons. In view of this it is expedient to perform the corresponding measurements with a ^6Li spectrometer using semiconductor counters. Although the ^6Li spectrometer has an energy resolution which is inferior to that of the time-of-flight method, it has a number of important advantages. Neutrons can be recorded in an appreciably larger solid angle (close to 2π) and this substantially decreases the uncertainty of the data on the background of scattered neutrons. By using a thin layer of ^6LiF the efficiency of the spectrometer can be taken as the cross section of the $^6\text{Li}(n, \alpha)^3\text{T}$ reaction without correcting for self-shielding and multiple scattering of neutrons as is necessary for scintillation detectors. In addition, the semiconductor detectors used in the ^6Li spectrometer are insensitive to γ rays.

Figure 1 shows a schematic diagram of the experiment. The products of the $^6\text{Li}(n, \alpha)^3\text{T}$ reaction were recorded by two silicon surface-barrier detectors 1 cm in diameter and 0.1 mm thick. The ^6Li target was a layer of ^6LiF $25 \mu\text{g}/\text{cm}^2$ in thickness and 1 cm in diameter on an aluminum oxide backing $30 \mu\text{g}/\text{cm}^2$ thick. The background from reactions occurring in the detector material and backing was measured by a special arrangement in which the target with the lithium layer could be replaced by a pure aluminum oxide backing. It was carefully constructed to ensure identical conditions in measuring background and effect, and to minimize the amount of scattering material. The backings with and without lithium were fastened to a rectangular frame of thin brass which under the action of its own weight could be shifted in a thin-walled cassette located halfway between the detectors which were 1.2 mm apart. The target was changed by rotating the vacuum chamber 180° around the longitudinal axis. The chamber was made of Duralumin with walls 0.5 mm thick. A sample of iron ~ 2.5 mm in diameter saturated with californium salts and enclosed in a stainless steel container with walls 0.3 mm thick served as a neutron source emitting $3.5 \cdot 10^7$ neutrons/sec. The container was fastened to the outer base of the chamber in such a way that the center of the source was on its axis. The distance between the source and target was 6 mm. After matching the amplification factors the pulses from the detectors were combined, amplified, and fed to the analyzer. The coincidence circuit operated through the analyzer to select counts of the $^6\text{Li}(n, \alpha)^3\text{T}$ reaction products from both detectors. The channel in which the combined pulses (amplifier and analyzer) were recorded was covered by automatic digital stabilization. The background and effect were measured alternately in 20-min cycles. Once per day the amplification in the channels of each detector was monitored and if necessary corrected by using a precision pulse generator. In addition, for energy calibration and to determine the resolution function a measurement was performed once per day for an hour

* Central Institute of Physics Research, Budapest.

Translated from *Atomnaya Énergiya*, Vol.42, No.1, pp.25-29, January, 1977. Original article submitted February 24, 1976.

This material is protected by copyright registered in the name of Plenum Publishing Corporation, 227 West 17th Street, New York, N.Y. 10011. No part of this publication may be reproduced, stored in a retrieval system, or transmitted, in any form or by any means, electronic, mechanical, photocopying, microfilming, recording or otherwise, without written permission of the publisher. A copy of this article is available from the publisher for \$7.50.

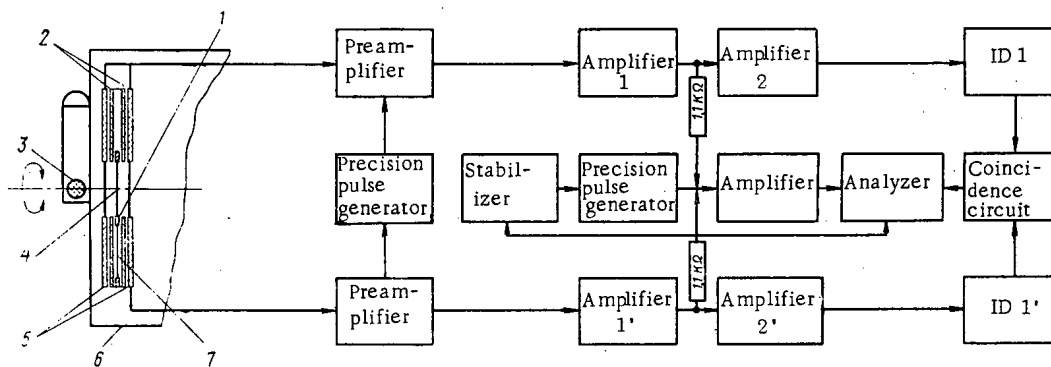


Fig. 1. Block diagram of experiment: 1) frame; 2) cassette; 3) ^{252}Cf source; 4) ^6LiF target; 5) semiconductor detectors; 6) vacuum chamber; 7) backing of pure aluminum oxide.

with thermal neutrons obtained by slowing down the fast neutrons in a 12-cm-thick polyethylene block. The experiment took 3.5 months.

The results of the measurements are shown in Fig. 2. There is good agreement between data corresponding to the measurement of background and effect plus background in the region below the thermal peak. This shows that the procedure for measuring the background is correct. The width of the thermal neutron peak at half maximum is 200 keV. This energy resolution is accounted for by the considerable spread in the energy lost by the reaction products in the dead layer (layer of ^6LiF , backing, and the entrance windows of the detectors), since the detectors were placed at a minimum distance from one another to minimize corrections due to the dependence of the angular distribution of the $^6\text{Li}(n, \alpha)^3\text{T}$ reaction products on E_n . It is obvious that in measurements with fast neutrons the resolution function obtained with thermal neutrons will be broadened by the superposition of effect and background pulses. Additional measurements performed with the precision pulse generator and a ^{234}U α particle source gave corresponding results and showed that the broadening function is Gaussian in form with a dispersion $\sigma^2 = 140 \pm 30 \text{ channel}^2$. Therefore, the real resolution function was assumed to be the thermal neutron peak N_i^T , broadened according to the law

$$R_k = \sum_{i=k-\Delta}^{i=k+\Delta} N_i^T (1/\sigma) \exp \left[-(i-k)^2 / 2\sigma^2 \right], \quad (1)$$

where $\sigma^2 = 140 \text{ channel}^2$, and i and k are analyzer channel numbers. The results of calculating the background from data corresponding to the measurement of effect plus background are shown in Fig. 3. The distribution obtained is the spectrum of neutrons from the spontaneous fission of ^{252}Cf , where $N(E)$ is measured with the resolution function R_k which can be written in the form

$$N_i = C \sum_{h=-\Delta}^{h=\Delta} \left| \frac{d\beta_i}{d_i} \right| \varepsilon(E_{i-h}) N(E_{i-h}) R_h, \quad (2)$$

where C is a constant, β is a quantity characterizing the dependence of the energy lost by the reaction products in penetrating the dead layer on neutron energy, and Δ is the domain of definition of the resolution function.

The data were processed on the assumption that the neutron spectrum is described by a Maxwellian distribution, and consisted in using Eq. (2) to find the parameter T by the method of least squares. Data estimated from the $^6\text{Li}(n, \alpha)^3\text{T}$ cross section [6] and corrected for the dependence of the angular distribution of reaction products on E_n reported in [7] were used to determine the efficiency $\varepsilon(E)$. Figure 4 shows the dependence of the correction δ and the $^6\text{Li}(n, \alpha)^3\text{T}$ cross section σ on neutron energy. The energy of neutrons corresponding to the i -th analyzer channel was calculated from the expression

$$E_i = \alpha_i - \beta_i, \quad (3)$$

where α is the value of the analyzer channel determined from the positions of the α particle, triton, and thermal neutron peaks, taking account of losses, and is equal to 0.0191 MeV/channel; β_i is the difference of the average energy losses of reaction products in penetrating the dead layer in measurements with thermal neutrons and neutrons of energy E_i . The function $\beta(E_n)$ is shown in Fig. 4. It was determined, as was $\delta(E_n)$, by using data from [7] on the angular distributions of products of the $^6\text{Li}(n, \alpha)^3\text{T}$ reaction.

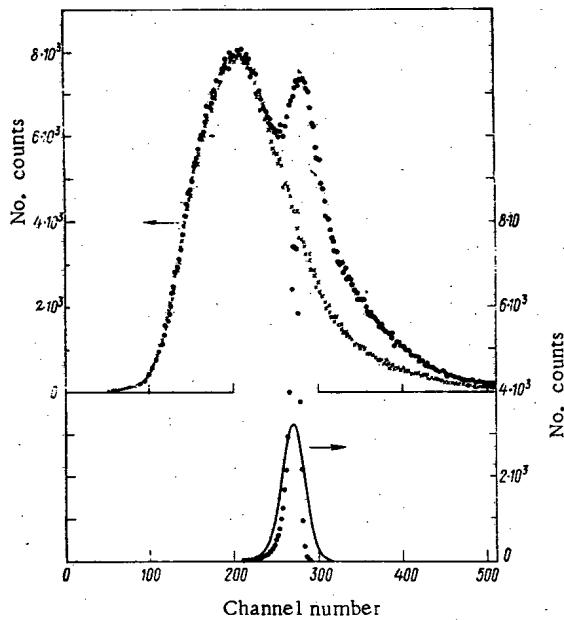


Fig. 2

Fig. 2. Results of measurements. Upper: ● effect plus background; ×) background. Lower: ● thermal neutron peak; —) actual resolution function.

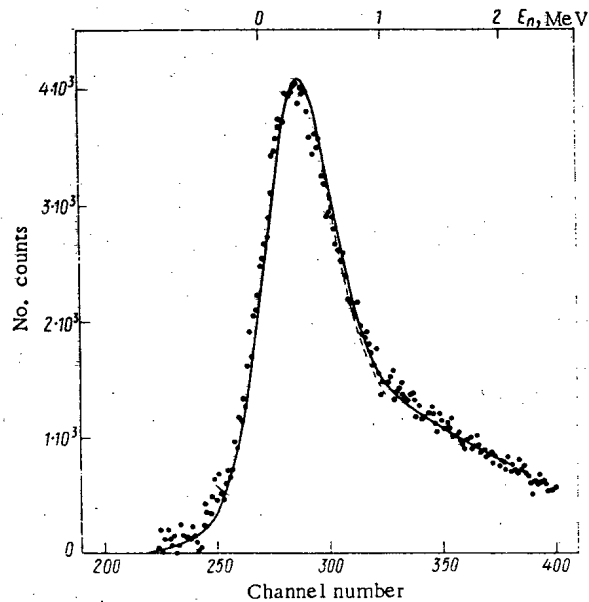


Fig. 3

Fig. 3. Results of data processing. ● Measured neutron spectrum; —, - - - -) results of parametrization of 170 and 115 points of the spectrum.

The results of the parametrization of 170 points of the experimental spectrum ($0 < E_n < 2\text{MeV}$) using Eq. (2) under the assumption that

$$N(E) = \sqrt{E} \exp(-E/T), \quad (4)$$

are shown by the solid curve of Fig. 3. The parameter $T = 1.18 \pm 0.05$, and $\chi^2 = 2.32$. The error in T was determined from the spread of the results of processing ten sets of measurements, and included the error in the determination of the dispersion of the resolution function. The open curve shows the results of processing 115 experimental points ($0 < E_n \leq 1\text{ MeV}$). In this case $T = 1.09 \pm 0.05\text{ MeV}$ and $\chi^2 = 3.06$.

It should be noted that the corrections δ and β used in the calculations are small, and their inclusion does not change the results significantly. This is shown by the data of the monitoring calculations in which $\varepsilon(E_n)$ was taken equal to $\sigma(n, \alpha)$ and Eq. (3) was replaced by the expression $E_i = \alpha_i$, and without taking account of losses α was found equal to 0.0175. In this case $T = 1.13 \pm 0.05\text{ MeV}$ and $\chi^2 = 2.51$.

In [8-11], devoted to the study of spectra and angular distributions of prompt fission neutrons in the energy range $E_n \geq 1\text{ MeV}$, the question of the presence of a neutron component with an isotropic angular distribution in the laboratory coordinate system was discussed. It was shown in [11] that the spectrum of the isotropic neutron component of the spontaneous fission of ^{252}Cf has the form of a Maxwellian distribution with $T = 1.01\text{ MeV}$, and these neutrons comprise about 20% of the total number of neutrons per fission. This effect must lead to a softening of the integral neutron spectrum, and may be the cause of the observed decrease in the parameter T with decreasing E_n . To test this hypothesis we performed a parametrization of the measured data using Eq. (2) under the assumption that

$$N(E) = C_1 \sqrt{E} \exp(-E/T_1) + C_2 \sqrt{E} \exp(-E/T_2). \quad (5)$$

In accord with [11] we took $C_1 = C_2 = 0.5$, and for T_2 we used the value $T = 1.43\text{ MeV}$ determined in the $E_n \geq 1\text{-MeV}$ energy range. For $\chi^2 = 2.28$, $T = 0.98 \pm 0.05\text{ MeV}$, which within the limits of error agrees with the value of this parameter for the isotropic component given in [11]. The corresponding curve of Fig. 3 coincides with the solid line.

To compare the data obtained with the results of the time-of-flight measurements it is of interest to process the latter in a similar way. To do this the numerical data from [3] for the $0 < E_n < 1\text{-MeV}$ range were transformed to an equivalent form and parameterized by using Eqs. (4) and (5). For $\chi^2 = 0.56$ and 0.54 ,

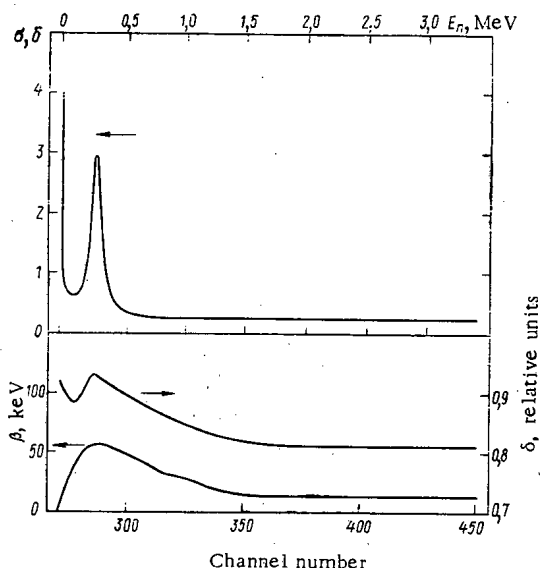


Fig. 4. Dependence of σ , δ , and β on neutron energy and analyzer channel number.

$T = 1.15 \pm 0.03$ and $T_1 = 0.96 \pm 0.03$, respectively. It is clear that these data are in satisfactory agreement with the corresponding quantities we obtained with a ${}^6\text{Li}$ spectrometer.

Thus, the measurements of the ${}^{252}\text{Cf}$ spontaneous fission neutron spectrum by a ${}^6\text{Li}$ spectrometer with semiconductor counters confirm the time-of-flight measurements showing an excess number of low-energy neutrons as compared with the estimate obtained by extrapolating data from higher energies by using the $\sqrt{E} \exp(-E/T)$ law. One possible cause of the observed phenomenon may be the presence of an isotropic neutron component in the laboratory coordinate system.

The authors thank B. D. Kuz'minov and V. S. Stavinskii for a discussion of the results, A. I. Gonchar for help in setting up the experiment, and A. V. Lukashkin, I. A. Gorokhov, and L. V. Egorova for their part in the work.

LITERATURE CITED

1. J. Meadows, *Phys. Rev.*, **157**, 1076 (1967).
2. Yu. S. Zamyatnin et al., in: *Proceedings of the IAEA Symposium Nuclear Data for Reactors*, Helsinki, June 15-19 (1970), p.183.
3. L. Eeki et al., in: *Proceedings of the IAEA Symposium Prompt Fission Neutron Spectra*, Vienna, Aug. 25-27 (1971), p.81.
4. M. V. Blinov et al., in: *Proceedings of the Conference Neutron Physics [in Russian]*, Pt.4, Obninsk ONTI FÉI (1974), p.138.
5. O. I. Ivanov and V. A. Safonov, *At. Énerg.*, **36**, No. 5, 397 (1974).
6. E. A. Seregina and P. P. D'yachenko, in: *Problems of Atomic Science and Technology, Ser. Nucl. Constants [in Russian]*, No.19, Atomizdat, Moscow (1975), p.10.
7. J. Overley, R. Sealock, and D. Ehlers, *Nucl. Phys.*, **A221**, 573 (1974).
8. S. Kapoor, R. Ramanna, and P. Ramo Rao, *Phys. Rev.*, **131**, 283 (1963).
9. K. Skarsvag and K. Bergheim, *Nucl. Phys.*, **45**, 72 (1963).
10. H. Bowman et al., *Phys. Rev.*, **126**, 2120 (1962).
11. V. M. Piksaikin, P. P. D'yachenko, and L. S. Kutsaeva, *Program III All-Union Conference on Neutron Physics [in Russian]*, Kiev, June 9-13 (1975), p.35.

THEORY OF SEPARATION CASCADES CONSISTING OF
ELEMENTS WITH SEVERAL OUTLETS

B. Sh. Dzhandzhgava, V. A. Kaminskii,
N. I. Laguntsov, G. A. Sulaberidze,
and V. A. Chuzhinov

UDC 621.039.3

In this paper, a further development of the theory of separation cascades is undertaken consisting of elements with many outlets [1]; in particular, the separative power of elements with three outlets is investigated and a general procedure is proposed for calculating the optimum schemes of combination of similar elements.

The scheme of an element is shown in Fig. 1. The enrichment process is described by the relations:

$$\delta^+ = \varepsilon_0 c (1-c) \frac{E+B}{D} \ln \frac{L}{E-B}; \quad (1)$$

$$\delta^0 = \varepsilon_0 c (1-c) \left(\frac{B}{E} \ln \frac{L}{B} - \frac{E+B}{E} \ln \frac{L}{E+B} \right); \quad (2)$$

$$\delta^- = \varepsilon_0 c (1-c) \ln \frac{L}{B}. \quad (3)$$

where ε_0 is the equilibrium coefficient of enrichment, which defines the effect and is dependent on the operating cycle of the element and the specific method of separation.

We will assume that the specific worth of a mixture with concentration c is determined by a certain function $\Phi(c)$. Then, the separative power is found from the relation

$$\delta U = \kappa \theta L \Phi(c + \delta^+) + (1-\kappa) \theta L \Phi(c + \delta^0) + (1-\theta) L \Phi(c - \delta^-) - L \Phi(c). \quad (4)$$

With regard to the separation of isotopes, the quantities δ^+ , δ^0 , and δ^- are small, the functions $\Phi(c + \delta^+)$, $\Phi(c + \delta^0)$, and $\Phi(c - \delta^-)$ can be expanded in series in the vicinity of c . Retaining second-order terms, we rewrite Eq. (4) in the form

$$\delta U = \frac{1}{2} [\kappa \theta L \delta^{+2} + (1-\kappa) \theta L \delta^{02} + (1-\theta) L \delta^{-2}] \frac{d^2 \Phi}{dc^2}. \quad (5)$$

Substituting formulas (1)-(3) in expression (5) and isolating terms that are independent of concentration, the separative power for the two boundary cases — equipment with a constant input flow L and equipment with a constant flow of the light fraction $L' = E + D$ — is represented, respectively, as

$$\delta U = \frac{L \varepsilon_0^2}{2} \chi_1^L; \quad L = \text{const}, \quad (6)$$

where

$$\chi_1^L = \frac{1-\kappa\theta}{(1-\kappa)\theta} \left[\frac{1-\kappa\theta}{\kappa} \ln^2 \frac{1}{1-\kappa\theta} - 2(1-\theta) \ln \frac{1}{1-\kappa\theta} \ln \frac{1}{1-\theta} + (1-\theta) \ln^2 \frac{1}{1-\theta} \right], \quad (7)$$

and

$$\delta U = \frac{L' \varepsilon_0^2}{2} \chi_1^{L'}; \quad L' = \theta L = \text{const}, \quad (8)$$

whence

$$\chi_1^{L'} = \frac{1}{\theta} \chi_1^L, \quad (9)$$

Translated from *Atomnaya Énergiya*, Vol. 42, No. 1, pp. 29-33, January, 1977. Original article submitted February 3, 1976.

This material is protected by copyright registered in the name of Plenum Publishing Corporation, 227 West 17th Street, New York, N.Y. 10011. No part of this publication may be reproduced, stored in a retrieval system, or transmitted, in any form or by any means, electronic, mechanical, photocopying, microfilming, recording or otherwise, without written permission of the publisher. A copy of this article is available from the publisher for \$7.50.

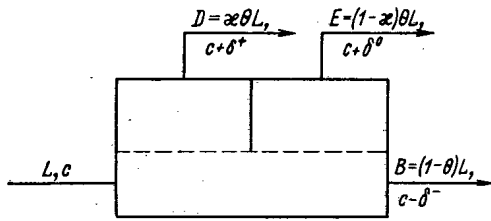


Fig. 1

Fig. 1. Separative element with three outlets.

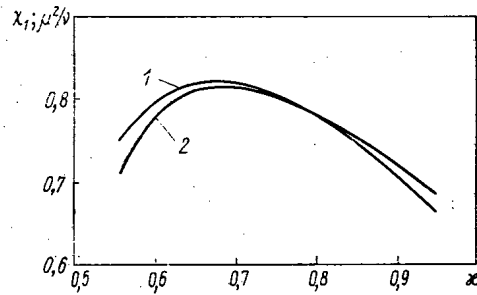


Fig. 2

Fig. 2. Dependence of χ_1 and μ^2/ν on the flow separation factor of the light fraction α [scheme (1, -1.4)].

and the numerical suffix with χ indicates the number of barriers for dividing the flow of the light fraction.

It should be noted that when $\alpha \rightarrow 0$ and $\alpha \rightarrow 1$, i. e., when the element with three outlets degenerates to a normal element, the expressions for χ convert to the well-known relations for elements with two outlets [2, 3].

We will consider an arbitrary scheme for combining the elements in cascade when the enriched flow D_S from the s element arrives at the inlet of the subsequent element $s + k$ and the depleted flow B_S reaches the inlet of the subsequent $s - (p - 1)$ element, where k and $(p - 1)$ are whole numbers greater than zero. The flow E_S is fed to the inlet of the $k + m$ element, where m is any whole number.

It is obvious that k , with respect to absolute value, should be less than m and $(p - 1)$. If the flow E_S is fed forward and in this case $m = k$, the element degenerates to a normal element. When $|m| > k$, into the section of the cascade with a large concentration of the important component is fed a flow with a lower content, which is disadvantageous. A similar pattern is observed when $|m| \geq (p - 1)$.

It can be assumed in isotopic approximation that the difference in concentrations between neighboring elements is a quantity that is small and equal to dc/ds [1]. Moreover, as the parameters of asymmetry are not very large numbers ($k \ll S$, $m \ll S$, and $(p - 1) \ll S$, where S is the number of elements in the cascade), it can be supposed that in the section of the cascade between the $(s - k)$ and the $s + (p - 1)$ elements, the quantity $c(1 - c)$ changes weakly for the isotopes, so that

$$\begin{aligned} \delta_{s-1}^+ &= \delta_{s-2}^+ = \dots \delta_{s-k}^+ = \delta^+; \\ \delta_{s\pm 1}^0 &= \delta_{s\pm 2}^0 = \dots \delta_{s+m}^0 = \delta^0; \\ \delta_{s+1}^- &= \delta_{s+2}^- = \dots \delta_{s-(p-1)}^- = \delta^-. \end{aligned}$$

Within the limits of the same section of the cascade, we will assume that the magnitude of the flows from element to element is changed slightly, and therefore

$$\begin{aligned} D_{s-1} &= D_{s-2} = \dots D_{s+k} = D; \\ E_{s\pm 1} &= E_{s\pm 2} = \dots E_{s+m} = E; \\ B_{s+1} &= B_{s+2} = \dots B_{s+(p-1)} = B. \end{aligned}$$

Then the balance equation of the total flows and of the flows of the light component can be written in the form

$$kD + mE - (p - 1)B = P; \quad (10)$$

$$kD\delta^+ + mE\delta^0 + (p - 1)E\delta^- - \frac{1}{2} \frac{dc}{ds} [k^2D + m^2E + (p - 1)^2E] = P(c_p - c). \quad (11)$$

Substituting in formula (10) the relations for the flows D , E , and B , in accordance with Fig. 1, and taking into account that $P \ll L$, we obtain

$$k\alpha\theta + m(1 - \alpha)\theta - (p - 1)(1 - \theta) = 0, \quad (12)$$

whence

$$\theta = (p - 1) / [(k - m)\alpha + m + p - 1]. \quad (13)$$

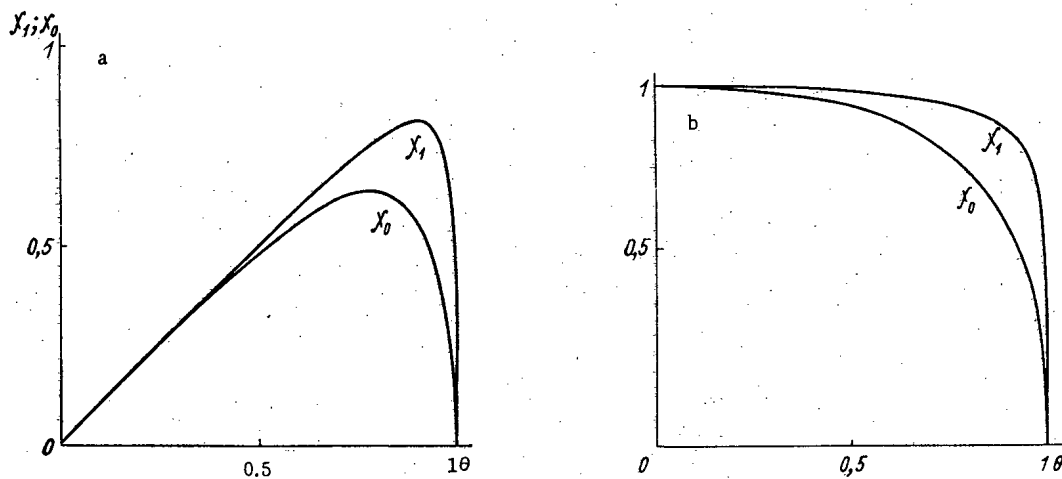


Fig. 3. Dependence of the coefficients χ_0 and χ_1 on θ for elements with two and three outlets, respectively, for a constant flow at the inlet of the element (a) and a constant flow of light fraction (b).

TABLE 1. Results of a Calculation of Cascade Schemes

(1, -2, 3)			(1, -2, 4)			(1, -1, 3)			(1, -1, 4)			(1, 0, 1)		
κ	θ	v/μ^2	κ	θ	v/μ^2	κ	θ	v/μ^2	κ	θ	v/μ^2	κ	θ	v/μ^2
0,700	0,968	0,704	0,700	0,976	0,664	0,550	0,968	0,695	0,550	0,967	0,677	0,100	0,909	0,914
0,733	0,938	0,677	0,733	0,952	0,630	0,600	0,937	0,630	0,600	0,952	0,611	0,200	0,833	0,789
0,767	0,909	0,668	0,767	0,930	0,620	0,650	0,909	0,609	0,650	0,930	0,590	0,300	0,769	0,760
0,800	0,882	0,669	0,800	0,909	0,622	0,700	0,882	0,608	0,700	0,919	0,588	0,400	0,714	0,767
0,833	0,857	0,676	0,833	0,889	0,632	0,750	0,857	0,617	0,750	0,889	0,597	0,500	0,667	0,791
0,867	0,833	0,687	0,867	0,870	0,647	0,800	0,833	0,634	0,800	0,870	0,614	0,600	0,625	0,823
0,900	0,811	0,700	0,900	0,851	0,666	0,850	0,811	0,656	0,850	0,815	0,637	0,700	0,588	0,862
0,933	0,789	0,715	0,933	0,833	0,689	0,900	0,789	0,683	0,900	0,833	0,666	0,800	0,556	0,905
0,967	0,769	0,732	0,967	0,816	0,714	0,950	0,769	0,715	0,950	0,816	0,701	0,900	0,526	0,951

We note that, as according to definition $0 < (\kappa, \theta) < 1$, Eq. (13) imposes one further limitation on the range of variation of the coefficient κ when $m < 0$:

$$\kappa > -m/(k-m). \tag{14}$$

Transformation of Eq. (11), taking account of expressions (1) and (2), gives the following equation for the transfer of the important component in the cascade:

$$v \frac{dc}{ds} = 2\mu\epsilon_0 c(1-c) - \frac{2P}{L}(c_T - c), \tag{15}$$

where

$$v = \frac{p-1}{(k-m)\kappa + m + p - 1} [(k-m)(k+m+p-1)\kappa + m(m+p-1)]; \tag{16}$$

$$\mu = (k-m) \frac{[k-(m+p-1)]\kappa + m + p - 1}{(k-m)\kappa + m + p - 1} \ln \frac{(k-m)\kappa + m + p - 1}{[k-(m+p-1)]\kappa + m + p - 1} + (m+p-1) \frac{(k-m)\kappa + m}{(k-m)\kappa + m + p - 1} \ln \frac{(k-m)\kappa + m + p - 1}{(k-m)\kappa + m}. \tag{17}$$

Equation (15) is valid for schemes with arbitrary values of the asymmetry parameters, i.e., it encompasses the entire class of cascades of elements with three outlets. As a special case, it includes the relations obtained in [1].

The efficiency of the cascade usually is estimated by the magnitude of the total flow. For a cascade enriching a mixture with the important component from the concentration c_F to the concentration c_P and operating with a power take-off P , the total flow is determined from the relation

$$\Sigma L = \int_{c_F}^{c_P} L ds = \int_{c_F}^{c_P} \frac{L}{dc/ds} dc. \tag{18}$$

Substituting dc/ds from Eq. (15) in relation (18), it is not difficult to derive the expression for the total flow in the form

$$\Sigma L = \frac{\nu}{\mu^2} \int_{c_F}^{c_P} \frac{dc}{\epsilon_0 c (1-c)} \frac{(\mu L)^2}{2\mu L - (\mu L)^*} \quad (19)$$

where we introduce the notation

$$(\mu L)^* = \frac{2P(c_F - c)}{\epsilon_0 c (1-c)} \quad (20)$$

It is obvious that the total flow of the cascade will have a minimum when the functional $(\mu L)^2 / [2\mu L - (\mu L)^*]$ for any value of μ is a minimum. Solving Euler's equation for this functional, we obtain the condition of minimality for the total flow in the form $\mu L = (\mu L)^*$. Substituting Eq. (20) in formula (16), we obtain the expression for the optimum concentration gradient through the cascade

$$\frac{dc}{ds} = \frac{\mu}{\nu} \epsilon_0 c (1-c) \quad (21)$$

Integration of expression (19), taking formulas (20) and (21) into consideration, gives the following relation for the total flow in the cascade:

$$\Sigma L = 2 \frac{\nu}{\mu^2} \frac{1}{\epsilon_0^2} P \Phi(c_P, c_F) \quad (22)$$

where $\Phi(c_P, c_F)$ is a known value function [4].

Thus, the choice of the optimum scheme of a cascade operating on specified external conditions is equivalent to finding the minimum of the function ν/μ^2 . At the same time, it should be noted that the function μ^2/ν can serve as a measure of the achievable separative power of an element, operating in the cascade, i.e.,

$$\delta U = (\mu^2/\nu) (L\epsilon_0^2/2) \quad (23)$$

The function ν/μ^2 for specified asymmetry parameters k , m , and $(p-1)$ depends on the coefficient of flow separation of the light fraction κ . We emphasize that the function χ is the characteristic of the element and ν/μ^2 is the characteristic of the cascade.

Losses of separative work in the cascade are caused by losses of the internal mixing in the element and mixing of flows with different concentrations at the inlet to the element. Separation of the flow of the light element fraction by means of impermeable barriers leads to a reduction of the loss by internal mixing. With increase of the number of barriers, the quantity χ increases and, as calculations show, its maximum tends to unity. This possibility of eliminating the logarithmic effect is considered in [5]. However, the achievement of elements with the number of emergent flows greater than three obviously is disadvantageous, as in this case the construction of the element becomes complicated and the number of communications of the actual cascade is increased, but the main advantage is achieved by the introduction of a further barrier: $\chi_1^{\max}/\chi_0^{\max} = 1.260$ and $\chi_2^{\max}/\chi_1^{\max} = 1.057$. The quantity χ determines which part of the separative power of the element, originated by the process at the barrier, can be used for attaining specified values of κ and θ . Then the losses by internal and external mixing will be determined, respectively, by the differences

$$\xi_{\text{int}} = 1 - \chi; \quad (24)$$

$$\xi_{\text{ext}} = \chi - (\mu^2/\nu) \quad (25)$$

The total losses of separative work are determined by the sum of the internal and external losses:

$$\xi = \xi_{\text{int}} + \xi_{\text{ext}} = 1 - (\mu^2/\nu) \quad (26)$$

Hence, it follows that the condition for a minimum of the coefficient ξ (minimality of the total loss by mixing) coincides with the condition for minimality of the total flow.

For cascades constructed of elements with two outlets, in which the internal mixing is constant, the condition for minimum of the total flow coincides with the condition for absence of external mixing. For cascades consisting of elements with three or more outlets, the condition of minimality of the total flow coincides with the condition of minimality of the total losses by mixing. As these conditions are more general, it is advantageous to use the definition of an ideal cascade as a cascade with minimum total flow.

We will show that, although in the case considered it is possible to construct a scheme of cascades without mixing at the inlet of the elements, these cascades are not ideal. This is due to the competitive effect of the internal and external mixing on the separation process. Actually, with a condition of nonmixing at the inlet to an element, we have in isotopic approximation

$$\begin{aligned}\delta^+ &= k (dc/ds); \\ \delta^0 &= m (dc/ds); \\ \delta^- &= (p-1) (dc/ds).\end{aligned}\tag{27}$$

The use of system (27) and the expressions for the enrichment functions (1)-(3) in the coefficient μ^2/ν shows that, as would be expected, it is identically equal to χ .

It should be emphasized that the condition of absence of external mixing is achieved only in those schemes of combined elements, for which the equation

$$\{[k-(m+p-1)]\kappa+m+p-1\} \ln \frac{(k-m)\kappa+m+p-1}{[k-(m+p-1)]\kappa+m+p-1} = k\chi \ln \frac{(k-m)\kappa+m+p-1}{(k-m)\kappa+m}$$

obtained from expression (27), has a solution different from 0 and 1.

It can be seen from Fig. 2 that μ^2/ν in the whole interval of change of κ is less than χ , except for a single value κ_0 for which there is no external mixing in the cascade. However, the cascade in this case is not optimal with respect to the total flow. This physically means that the minimum of the total losses by mixing do not coincide with the case when there is no external mixing.

Table 1 shows the results of the calculations carried out on a computer. All values of the function ν/μ^2 refer to its value corresponding to the symmetry of a cascade of simple elements. The calculations have been carried out for the following values of the asymmetry parameters: $k = 1, 2, 3, 4$; $m = -2, -1, 0, 1, 2$; $(p-1) = 1, 2, 3, 4$. Of the 80 variants of the scheme of cascades, five are given in Table 1.

The schemes are arbitrarily denoted by the values of the parameters and of the asymmetry $(k, m, p-1)$. The results of the calculations show that the greatest effect of reducing the total flow in the case of cascades constructed of elements with three outlets is observed for elements with a constant inlet flow. Of all the variants considered, the best for this type of element was found to be the scheme (1, -1.4). In this case, the reduction of the total flow by comparison with a symmetrical cascade of simple elements amounted to $\sim 70\%$. For elements with a constant flow at the outlet, the reduction of the total flow is insignificant and for the schemes considered amounts to a few percent. This is explained by the nature of the dependence of the separative power of the elements of the first and second type on the gas flow separation factor [2,3]. Figure 3 shows the dependence of χ_1 and χ_0 on θ for elements with $L = \text{const}$ (a) and $L' = \text{const}$ (b) when $\kappa = 0.6$, respectively. The relative increase of the separative power of elements with three outlets, by comparison with the separative power of simple elements is displaced to the region of large values of θ , and the achievement of larger values of θ is preferable for elements with $L = \text{const}$.

The results obtained can be used for the construction of more efficient elements and for the design of cascades having flow profiles that approximate to the profile of an ideal cascade. This can be achieved by choosing the appropriate magnitudes of the effective flow νL in the section, by varying the asymmetry parameters along the cascade.

The authors thank B. I. Nikolaev for discussion of the paper.

LITERATURE CITED

1. N. A. Kolokol'tsov, *At. Energ.*, 37, No.1, 32 (1974).
2. N. A. Kolokol'tsov, *At. Energ.*, 27, No.1, 9 (1969).
3. V. A. Chuzhinov et al., *At. Energ.*, 40, No.6, 471 (1976).
4. A. M. Rozen, *Theory of Isotope Separation in Columns* [in Russian], Atomizdat, Moscow (1960).
5. G. Bouligand, CEA Report 2622, UKAEA Prod. Group, Inform. Ser.16 (1965).

REVIEWS

DETECTION OF FLAWS IN METAL OF ATOMIC POWER
PLANT EQUIPMENT DURING OPERATION

B. R. Brodskii and É. F. Monina

UDC 620.179.14.15.16:620.192

According to the existing regulations, the equipment and piping of the primary circuit, the principal steam lines, and the equipment on feed lines should be inspected periodically. This inspection envisages:

- a. testing by nondestructive methods of the state of the metal in the equipment and piping during their use;
- b. checking the state of the metal according to reference samples placed in the working medium and zone, where a neutron flux exists;
- c. testing the soundness of the metal of equipment and piping of the primary circuit when small radioactive flows occur.

The principal nondestructive testing methods are: visual inspection (including optical and television means); capillary flaw detection (color and luminescence); magnetic, electric, and other surface methods; volumetric defectoscopy (ultrasonic, radiographic); and continuous inspection — vibroacoustic, diagnostics, acoustic emission (emission of stress waves).

The presence of radioactive background in atomic power plants and the very poor accessibility of some important elements of the equipment hinder the application of nondestructive methods of manually inspecting the condition of the metal. This makes it necessary to develop remote-controlled mechanized systems and devices for detecting flaws in metal in atomic power plants under operating conditions. The present paper give the descriptions and analysis of some devices developed in the USSR and elsewhere.

Means Used in the USSR for Operational Nondestructive Metal Testing

A number of devices have been developed at the Beloyarsk Atomic Power Plant for remote-controlled inspection of the condition of the metal in equipment and piping. ✓]

Unit for Inspecting Circular Welded Seams in Piping. This unit, for inspecting main steam line and the feed line, consists of a control panel, equipped with an ultrasonic flaw detector, and a scanner. The control panel is installed inside a box and may be up to 35 m from the scanner. The scanner device is mounted on the piping with a spring-loaded snap-lock. This consists of two mechanisms placed on diametrically opposite sides of the piping to provide rotation around the pipe along the seam and to-and-fro motion of two fault-finder heads on spring suspensions. This arrangement makes counterweights unnecessary. The mechanisms are connected to each other by hinged sections with guide rollers. The rigid hinged sections ensure that the device moves with comparatively high accuracy around the pipe even on vertical segments where the displacement of the device from the initial position after a complete turn does not exceed 5 mm. Heads positioned on either side of the welded seam are used to inspect the seam from both sides at the same time by the echo method. A welded seam can be inspected by manual remote control and automatic search for defects.

Device for Monitoring the State of the Metal Housing of Drum Separators. This is intended for remote inspection of drum wells, inspection of cladding for peeling, and detection of cracks on the internal and external surfaces of the housing and in welded seams. The unit consists of a control panel, an ultrasonic flaw detector and a scanner. The housing surface is scanned by a self-propelled mechanism, consisting of a walking device with electromagnetic suction feet, which can move over the surface of a ferromagnetic material in any

Translated from *Atomnaya Énergiya*, Vol.42, No.1, pp.34-40, January, 1977. Original article submitted April 12, 1976.

This material is protected by copyright registered in the name of Plenum Publishing Corporation, 227 West 17th Street, New York, N.Y. 10011. No part of this publication may be reproduced, stored in a retrieval system, or transmitted, in any form or by any means, electronic, mechanical, photocopying, microfilming, recording or otherwise, without written permission of the publisher. A copy of this article is available from the publisher for \$7.50.

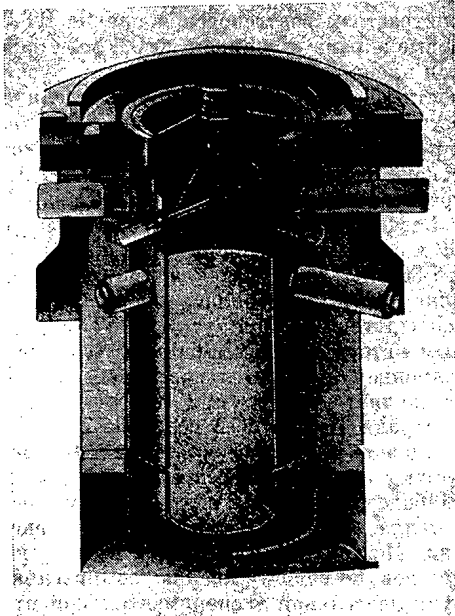


Fig. 1. The Dyatel-1 unit for inspection of welded joints of inlets and outlets of VVÉR-440 water-moderated water-cooled reactor.

TABLE 1. Characteristics of Radiographic Inspection

Thickness at welded seams inspected, mm	Focal distance, mm	Exposure dose rate at 1 m, R/sec	Sensitivity of radiography, rel. units		Exposure time	
			calc.	expt.	calc.	expt.
92	340	$1,25 \cdot 10^{-2}$	1,2	0,7-1,0	19	20
32	280	$1,5 \cdot 10^{-2}$	1,2	1-1,5	3	18

position in space, carrying the fault-finder head on it. The path of the motion is controlled manually or automatically.

Unit for Checking the Condition of Metal in Pipe Openings. This is designed to detect cracks on the outer surface of pipe openings. The inspection is carried out by an ultrasonic method from outside the drum housing. The scanning mechanism is a yoke with snap lock and three rubber guide rollers. One of the rollers is movable and swivels aside together with the catch. The scanning mechanism is driven by a 27-V dc electric motor. To carry out the inspection the scanning mechanism is mounted on a pipe connection. The motor of the scanning mechanism is switched on from the control panel and the fault finders move in a circle around the pipe connection. The unit inspects condition of pipe apertures of 25-mm diameter or more.

A system has been developed for remote inspection of the condition of the metal (the base metal and welded joints) of the housing of a water-moderated water-cooled reactor, incorporating ultrasonic and television devices. The inspection is carried out from the outside of the reactor vessel. In the space near the reactor a platform is set up with a vertical rod bearing the scanning device with a set of ultrasonic transducers or with a TV camera. Because the platform travels along the circular space between the reactor vessel and the biological shield and the scanner moves vertically along the rod, the entire surface of the reactor can be inspected. A computer is used to control the inspection and to record the results. The coordinates of defects are determined, typically, to within 20 mm.

The Dyatel-1 γ -Ray Flaw Detection Unit. Trials have been carried out at Novovoronezh atomic plant with a γ -ray flaw detection unit [1] for radiographic inspection of the welded joints of the vessel of a water-moderated water-cooled reactor and the main circulation tubing (Fig. 1).

With the reactor shut down and the in-pile devices removed, the welded seams were inspected, as was the austenitic metal deposit, by using a panoramic beam from ^{60}Co and ^{192}Ir radioactive sources with an activity of 50 g-eq radium each (see Table 1). The heads were aimed at the branch pipes and seams tested by remote control. A flexible cassette holder was set up manually on the external side of the branch pipes. The x-ray film used was high-contrast PT-5, with lead shields on either side and wire sensitivity standards [2]. The exposure time was found by calculation and from monograms and made more exact during inspection process. All told, six welded seams (about 12 m) on three "hot" lines of the pipe were inspected.

The calculated sensitivity of the radiographic inspection under conditions with a radiation background (up to $300 \mu\text{R}/\text{sec}$) was established by the well-known method [3] and verified experimentally in accordance with the GOST mentioned [2]. According to the authors cited, for the radiography conditions selected the reference sensitivity of the working diagrams is 1-2% as compared to requirements of no more than 2.5% in the inspection regulations PK 1514-72 [1].

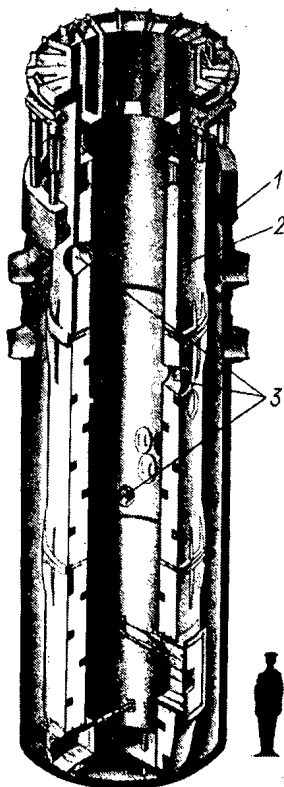


Fig. 2

Fig. 2. Shielded container for inspecting and repairing water-moderated water-cooled reactors: 1) reactor vessel; 2) shielded container; 3) viewing ports.

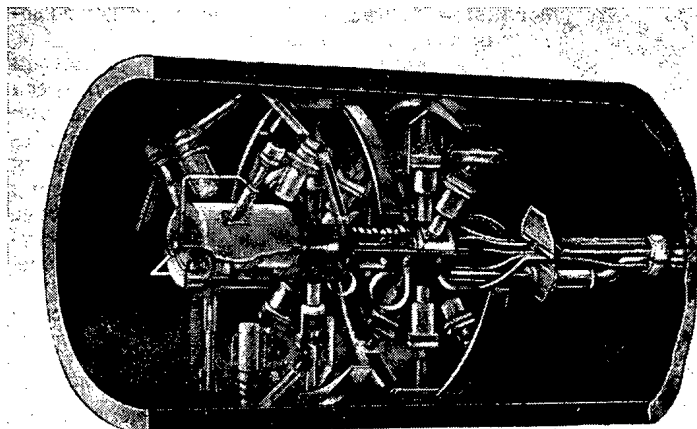


Fig. 3

Fig. 3. Self-propelled mechanisms for checking the condition of the metal of pipes.

Radiographic methods do not, however, guarantee detection of cracks [2,4], which are the most dangerous and the only metal defects that arise in the course of operation. Therefore, the effectiveness of these methods is, in our opinion, questionable and requires careful experimental verification. A similar point of view on this question has been expressed in the foreign literature as well [5,6]. The most promising methods as applied to nuclear reactor vessels are those of acoustic emission, ultrasonic holography, and ordinary ultrasonic flaw detection [7]. Solution of the problem of ultrasonic inspection of the condition of the metal in austenitic welded seams is facilitated by the use of fault finders which focus longitudinal and transverse ultrasonic waves [8].

For remote inspection of the reactor-vessel fittings at atomic power plants, the All-Union Heat Engineering Institute (Ural Branch of the Heat-Engineering Institute) has developed a self-propelled unit capable of moving in any position in space along a surface made of ferromagnetic materials; its purpose is to carry out periodic inspections of equipment in accessible places with the atomic power plant in operation and with it shut down. The unit consists of a mechanical self-propelled carriage, scanners for nondestructive testing, defect marker, TV camera, and control panel. The self-propelled unit is manually set up, taken down, and initially oriented. The unit moves, turns, and shuts down in response to remote control from a control panel which is installed in a safe place some 40 m outside the inspection zone. The unit weighs under 25 kg and its speed is 8 to 20 m/h. The construction is demountable, facilitating decontamination and replacement of individual components.

Scanners have been developed for ultrasonic and ferromagnetic-probe inspection. They can be fastened to the self-propelled carriage together or separately. The results of the inspection are presented as a record on paper tape from multichannel recorders installed on the control panel. The self-propelled carriage has provision for a small TV camera for visual observation. The position of the self-propelled unit on the object under inspection is established by TV survey cameras installed in boxes.

A shielded container has been developed in the Heat Engineering Institute for inspecting and repairing water-moderated water-cooled reactors (Fig. 2). It enables the vessel-type surface of a nuclear reactor to

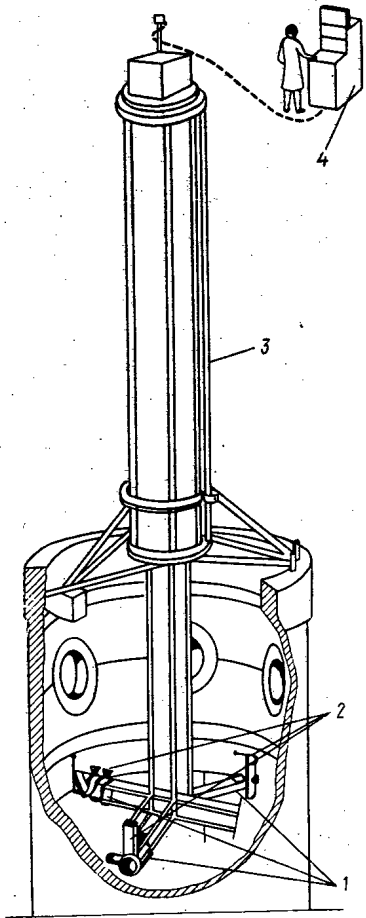


Fig. 4

Fig. 4. General view of manipulator with central mast (TEK-TRAN): 1) ultrasonic sensors; 2) TV cameras; 3) mast; 4) control panel.

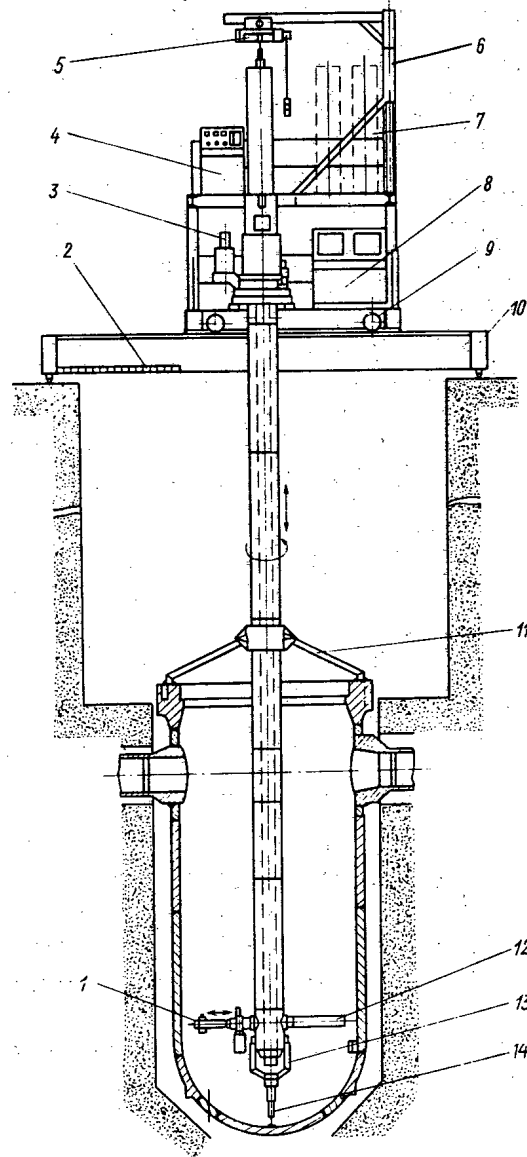


Fig. 5

Fig. 5. Diagram of manipulator with central mast: 1) system of sensors for inspection of cylindrical walls and branch pipes of reactor; 2) platform for servicing; 3) mast support; 4) control panel; 5) monorail hoist; 6) rotating crane; 7) mast structures; 8) electronic panel; 9) transverse bridge; 10) manipulator bridge; 11) star-shaped support; 12) telescopic tube; 13) articulated "arm"; 14) system of sensors for inspecting bottom.

be inspected and repaired under conditions of high radioactivity; enables personnel to remain inside a reactor safely for a long time; reduces the time required to inspect the internal surfaces of reactors by a factor of 18-20; and can be set up by the reactor-room crane (weight assembled contained, 120 tons) [9]. Special mechanisms move the shielded container up and down and turn it about its axis. The construction of the shielded container has been patented in a number of capitalist countries.

For visual inspection of the branch pipes of a reactor, piping, and other elements of the equipment, use is made of RPB periscopes measuring 15 mm in diameter or more, produced commercially by Soviet industry. With the periscopes it is possible to inspect reactors and piping over straight segments from a distance of up to 20 m. At high radiation levels the optic system of the periscope darkens quickly. Glass with a cerium additive is used in order to overcome this disadvantage.

An apparatus based on the PTU-26 unit manufactured by the Soviet television industry has been built by the High-Temperature Institute of the Academy of Sciences and has been tested on the Rheinsburg atomic power plant.

For access to the space between the pit and the vessel as well as to inspect 500-mm branch pipes, three holes 500 mm in diameter were cut opposite the "cold" branch pipes. A monorail bent to the radius of the shielding was installed in the space between the pit and the vessel and a carriage, with a small transmitting TV camera or a movie camera, moved along the monorail.

The carriage serves to move the TV camera along the monorail as well as to raise and lower it. A TV camera of the same kind but mounted on a platform, was used to track the moving TV camera. The platform was installed on the carriage. A panel, installed in the reactor room together with video monitoring equipment, permitted remote control of the travel along the monorail, and the aiming, raising and lowering, as well as focusing of the camera.

After the radiation situation, the water level was 1000-1500 mm above the upper end of the screen. The apparatus was hermetically sealed and the inspection was carried out in water. A periscope with its first elbow bent at 90° was provided for keeping track of the platform with the TV cameras in the event it became jammed.

For inspection of 500-mm pipes, a self-centering mechanism was constructed on a caterpillar drive unit to hold TV cameras, movie cameras, and a video recorder. Such units are now in use in atomic power plants. The TV units have poorer resolution than their purely optical counterparts. Television cameras can withstand irradiation of up to 10^{10} R. Optical or electrooptical methods are effective if the surface to be inspected does not have any deposits which could conceal possible cracks.

The Heat-Engineering Institute has developed a new construction of a self-propelled scanning mechanism for checking the condition of metal on the internal surface of 500-mm pipes of the primary circuit along the entire length (Fig. 3). The unit consists of a self-propelled mechanism, a guidance devices, a receiving-relaying device, a system for automatic control of the self-propelled mechanism can be introduced into the loop circuit in the segments: steam generator-main shutoff valve on the "hot" line, steam generator-main circulating pump on the "cold" line, and main circulating pump-main shutoff valve. The self-propelled mechanism is into the completely assembled loop through the internal cavity of the reactor vessel, the manhole of the steam generator, and the housing of the main circulating pump after removal of the rotor and dismantling of the control apparatus of the pump. The mechanism is transported to any spot in the pipe and fixed in place by clamping shoes mounted on piston rods of direct-action pneumatic cylinders.

The automatic control system of the self-propelled mechanism is provided with reversible step counters to measure the linear coordinate of the position of the mechanism in the pipe and a system to measure the polar coordinate of the position of the mechanism in the pipe in straight and inclined segments. The readings are fed to digital readout indicators mounted on the control panel. The entire apparatus for the automatic control of the self-propelled mechanism is contained in portable modules and the control panel.

The unit is characterized by a high degree of penetrability (pipe diameter and ovality of 400-500 mm in the absence of branches of up to 200 mm in diameter). It weighs 10 kg, its axial speed is 0.01-0.3 m/min, and its scanning speed along the circumference is 0.5-3 rpm.

Using the experience gained in developing the mechanism described, the Heat-Engineering Institute designed an improved version of a wheeled transport mechanism with better technicoeconomic indices: mass < 10 kg, pipe diameter 400-500 mm, reduced requirements as to precision in part fabrication, and higher rate of inspection.

Means Used Abroad for Operational Nondestructive

Metal Testing

Mechanisms of the mast or manipulator type (Figs.4-6) are used in the United States and other countries. One such manipulator, developed by MAN, is described in [10]. A manipulator should be easily assembled and dismantled, have a minimum of manual control, accurately reproduce its previous positions, and be easy to decontaminate. A manipulator consists of a stationary bridge, supporting the rotating mast consisting of individual moving sections which is placed in the center of the reactor. Mounted on the end of the mast are articulated devices for inspecting the bottom and a telescopic "arm" with a system of detecting heads for inspecting the walls of the reactor and branch pipes. The mast manipulator performs five motions which are controlled from the control panel: translational, rotational, rotation of the devices for bottom inspection, and radial motion and rotation of the telescopic arm.

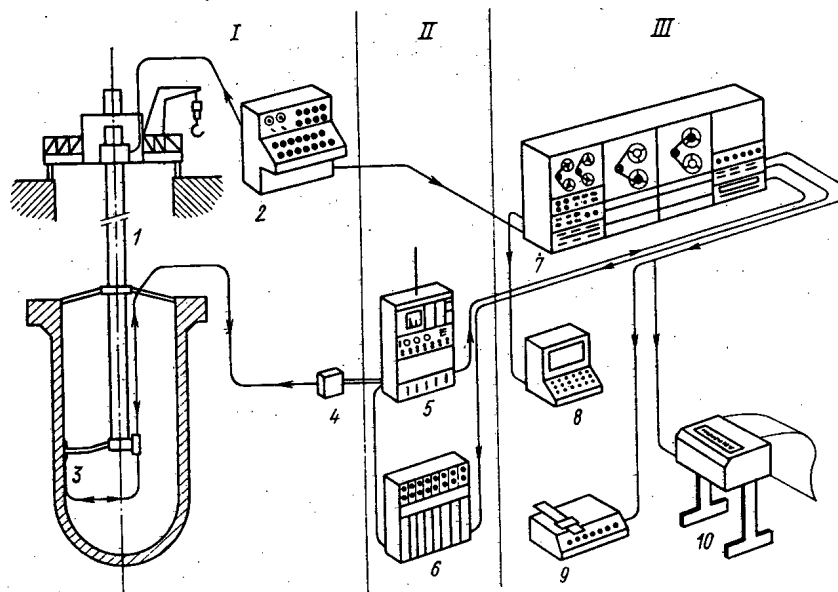


Fig. 6. Structural diagram of unit for ultrasonic inspection of reactor vessel: I) manipulator and module section; II) ultrasonic section; III) data analysis section; 1) manipulator with central mast (mfg. by MAN); 2) control panel; module for inspection of bolts, branch pipes, welded joints of cover and places for insertion of control rods (mfg. by KWU); 3) blocks of sensors; 4) channel distribution box; 5) 32-channel Sonolog-73 and 16-channel Sonolog-7 (mfg. by RTD); 6) 24-channel recorder; 7) computer; 8) display; 9) XY recorder; 10) teletype [11].

The automatic system sets the manipulator at the desired inspection point. Indicator lamps show the position of the manipulator. The order of the operations is controlled manually or automatically according to a predetermined program. The accuracy with which the detecting heads are set up on the vessel at a desired point fluctuates from 1 to 3 mm. This manipulator can be used to inspect a reactor vessel, branch pipes, and welded seams of branch pipes and piping. A TV camera can be used in addition to the ultrasonic system of detecting heads. The inspection is carried out under water to a depth of 25 m below the level of filling. The mast has a total length of 32 m and the manipulator weighs 15 tons.

Investigations in Saclay, France, have made it possible to employ sensors that focus longitudinal and transverse ultrasonic waves in some industrial units for automatic inspection. These sensors were used to inspect the fillet welds of the cover of the French reactor Phoenix as well as the fillet welds of T-shaped joints of sheets of 60-mm stainless steel. Use of these sensors greatly expands the capabilities of ultrasonic inspection in determining small defects and obtaining information about the size of defects. With them, it is easy to inspect materials, such as stainless steel, which do not lend themselves to ultrasonic inspection with ordinary sensors. The sensor used in the inspection, with a focal spot of 2.5-mm diameter, makes it possible to detect inclusions measuring up to 0.5 mm, regardless of the noise background. Ultrasonic inspection was successfully carried out on welded joints of pipes with tube sheet (thickness of tube sheet 40 mm, pipe wall 10-50 mm), arc-welded butt joints (maximum thickness inspected 120 mm for sensor with a 2.5-mm focal spot) [8].

Japanese-manufactured endoscopes based on fiber optics are used extensively in France to inspect the internal surfaces of tubes, rotors, and other parts. The endoscope probe is inserted inside the tube, inspection of channels in various directions being possible. The minimum diameter of the tube inspected is 9 mm. The endoscope comes with a set of flexible tubes with which channels up to 2 m long can be viewed.

In addition to work on nondestructive inspection of a shut-down reactor, it is desirable to inspect an operating installation after major repairs. This is especially important for detecting emergency situations. Accordingly, acoustic emission method is under development in many laboratories. The companies ENEL and CIZE are developing new apparatus for continuous observation of the operation of equipment in the primary circuit. This apparatus consists of standard instruments as well as TV cameras and microphones installed at different places in the primary circuit. The new remote-control apparatus is based on sound signals transmitted by standard transducers placed on the outside of various elements of the primary-circuit equipment.

In this way information can be obtained about, for example, the state of devices inside the reactor vessel, without disturbing the operation of the plant. The first results obtained with this apparatus are encouraging, but it is desirable to carry out more extensive experimental tests before it is introduced into atomic power plants [6].

LITERATURE CITED

1. V. P. Kalinin et al., *Energ. Stroit.*, No.8, 21 (1975).
2. GOST 7512-69. Seams of Welded Joints. Methods of Inspection by Radioscopy with Penetrating Radiation [in Russian], Moscow (1969).
3. A. I. Maiorov, *Defektoskopiya*, No.5, 61 (1970).
4. OST 5.9095-72. Seams of Welded Joints of Marine Constructions and Products. Techniques of Radiographic Inspection [in Russian], Moscow (1972).
5. H. Meyer, *Kerntechnik, Isotopentechnik und Chemie*, No. 2, 56 (1971).
6. F. Gioli, G. Anna, and I. Velona, Fourth International Conference, Geneva (1971), p.12.
7. "Research project on reactor vessel testing and inspection near completion," *Edison Elec. Inst. Bull.*, No.2, 41 (1973).
8. *Svarka, Ekspress-Informatsiya*, No.45, All-Union Institute of Scientific and Technical Information (VINITI), Moscow (1974).
9. A. M. Bukrinski et al., *Byul. Izobret.*, No.36 (1972).
10. H. Meyer and A. Walter, Contribution to the Special Conference during the "Nuclex" Exhibition, N 9, Basel (1972).
11. C. Honeycutt et al., *Materials Evaluation*, 32, No.9 (1974).

DEPOSITED PAPERS

OPTIMIZATION OF THE COST OF THE STRUCTURAL
DESIGN OF THE RADIATION SHIELDING AND THE
SANITARY-SAFETY ZONE OF CHARGE-PARTICLE
ACCELERATORS

Yu. A. Bolchek and A. Ya. Yakovlev

UDC 621.039.58:621.384.6

In designating the protective measures for high-energy accelerators, taking account of direct and scattered radiation that enters the territory as well as the discharge of radioactive air into the atmosphere, it is advisable, at the stage of the pre-project studies of the shielding parameters, to optimize the costs C_{tot}^{opt} (x, y, r, h), where x and y are the thicknesses of the side and top shielding, respectively, r is the radius of the sanitary-safety zone, and h is the height of the ventilation pipe.

The interrelation among these parameters, given in a paper by Yu. A. Bolchek and A. Ya. Yakovlev [At. Energ., 39, No.4, p.281 (1975)], makes it possible to obtain their cost-optimal values as applied to point radiation sources (ring accelerators up to 4-5 GeV, as well as targets of ring and linear accelerators).

The present paper gives the results of calculations that enable an evaluation to be made of the effect that a number of factors characterizing a constructive design of shielding, some natural conditions of the territory, and the cost indices of protective measures have on the optimal costs C_{tot}^{opt} . The calculations were performed for a cyclic accelerator with $E_p = 1$ GeV, $I = 10^{12}-10^{15}$ protons/sec; a study was made of the effect of c_0, s, b , and α on the optimal values of x, y, r , and h and the corresponding values of C_{tot}^{opt} at beam intensities ranging from 10^{12} to 10^{15} protons/sec, where c_0 is the cost of appropriating the land dispossessed for establishing a sanitary-safety zone ($c_0 = 0.1, 1.0, 10.0$ rubles/m²); s is the turbulence factor that depends on the relief of the locality and the character of the landscape and the site development ($s = 0.027, 0.08, 0.1, 0.2$); b is the cost of 1 m of top shielding ($b = 8.8 \cdot 10^4, 1.76 \cdot 10^5, 6.6 \cdot 10^5, 10^6$ rubles/m); α is the communication cost per unit length of the radius of the sanitary-safety zone ($\alpha = 108, 200, 300, 400$ rubles/m).

The calculations have shown that the cost factors affect the size of the sanitary-safety zone, the effect being most pronounced at $I = 10^{12}-10^{13}$ protons/sec, i.e., as the activation of the air increases, the influence of c_0 on r decreases and at $I \sim 10^{15}$ protons/sec r practically does not depend on c_0 . Therefore, at high intensities ($I = 10^{14}-10^{15}$ protons/sec) c_0 strongly affects C_{tot}^{opt} .

Two practical recommendations follow from this: it is inadvisable to locate high-current facilities in regions of high cost factors; for facilities of relatively low intensity ($I \sim 10^{11}-10^{12}$ protons/sec) the cost coefficients are not as important, although they do affect C_{tot}^{opt} (up to 20%).

It is recommended that the sanitary-safety zone be landscaped with shrubbery and trees to increase the turbulence factor. A smooth land surface is unallowable since this leads to a sharp increase in the zone size and cost C_{tot}^{opt} .

In the case of optimization of protective measures, the material and construction of the housing prove to have little effect on the radius of the sanitary-safety zone; this effect is large at $I \sim 10^{12}-10^{13}$ protons/sec and decreases as the beam intensity increases; when $I \geq 10^{15}$ protons/sec, r practically does not depend on b .

(No. 886/8632. Original article submitted Jan. 21, 1976;
abstract submitted July 7, 1976. Complete text 0.5
author's folios, 10 figs., 1 table, 2 references.)

Translated from *Atomnaya Energiya*, Vol.42, No.1, pp.41-43, January, 1976.

This material is protected by copyright registered in the name of Plenum Publishing Corporation, 227 West 17th Street, New York, N.Y. 10011. No part of this publication may be reproduced, stored in a retrieval system, or transmitted, in any form or by any means, electronic, mechanical, photocopying, microfilming, recording or otherwise, without written permission of the publisher. A copy of this article is available from the publisher for \$7.50.

THEORY OF UNSTEADY γ TRANSPORT IN THE
SMALL-ANGLE SCATTERING APPROXIMATION

V. S. Galishev and G. Ya. Trukhanov

UDC 539.12.04

Within the framework of the Zaitsev and Kaplan method [1] the problem of the unsteady transport of γ radiation from a plane monodirectional monoenergetic pulsed source is solved analytically in the small-angle scattering approximation.

Based on this solution the main characteristics of the space-time and energy distributions of γ radiation from a 1-MeV source in a homogeneous air medium are studied.

The solid lines in Fig. 1 show the results of numerical calculations of the energy dependence of the energy flux of scattered γ radiation $\lambda N_0^S(s, \lambda, t)$, where λ is the wavelength of the radiation in Compton units, z is the distance from the source, and t is the time, for penetrations $\mu_0 z = 1, 2, 4, 10$, and times $t_i = t_0(1 + i\Delta)$, where μ_0 is the attenuation coefficient of air at the source energy, t_0 is the delay time, $i = 0, 1, 2, \dots$, and Δ is the integration step. The open curves represent the cutoff of the spectrum of γ radiation passing through the given point for times $t \geq t_0(1 + i\Delta)$, and the vertical dashed lines separate the region of allowed energies $E \gg m_0 c^2 / (\lambda_0 + 2)$, in which the small-angle approximation can be used, from the region of forbidden energies $E \ll m_0 c^2 / (\lambda_0 + 2)$ where this approximation is invalid. An analysis of the allowed parts of the curves (Fig. 1) shows that as time increases the soft multiply scattered γ radiation begins to predominate in the γ spectrum. This agrees with time-energy spectra of scattered γ radiation calculated by the Monte Carlo method [2] for a different source geometry.

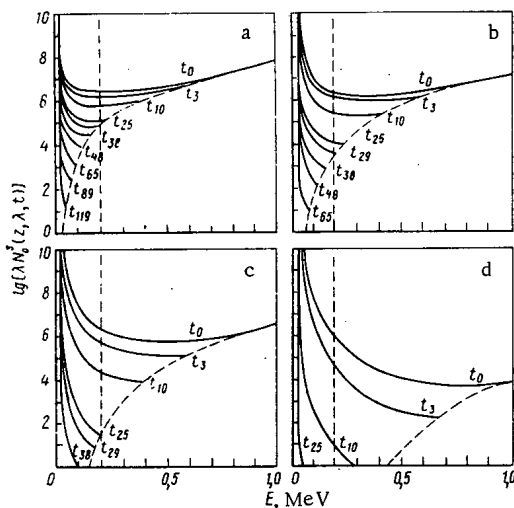


Fig. 1. Energy flux of scattered radiation as a function of energy for a plane monodirectional 1-MeV γ source in air for $\mu_0 z = 1, 2, 4, 10$ and $t_0 = 0.4, 0.8, 1.6, 4.05 \mu\text{sec}$ (a, b, c, d), respectively.

LITERATURE CITED

1. V. V. Zaitsev and S. A. Kaplan, *At. Energ.*, 16, No. 2, 149 (1964).
2. O. I. Leipunskii et al., *At. Energ.*, 10, No. 5, 493 (1961).

(No. 887/8637. Original article submitted Jan. 27, 1976.
Complete text 0.3 author's folios, 2 figs., 4 references.)

INTENSITY OF γ RADIATION FROM AN ACTIVATED CYLINDER

G. S. Vozzhenikov and A. L. Zagoryuev

UDC 550.835

An expression is obtained for the intensity of the primary γ radiation along the axis of an activated cylinder of finite diameter and length.

We consider a cylindrical body in an infinite quasihomogeneous strongly moderating medium, and assume that the properties determining the transport of neutrons and γ radiation are the same for the cylinder and the medium. The cylinder, but not the surrounding medium, contains a uniformly distributed chemical element — an indicator — which is activated as a result of its interaction with thermal neutrons from a point source. It is assumed that the slowing down length of fast neutrons in the medium is much longer than the diffusion length of thermal neutrons.

The expression obtained is used as the starting point for calculating the dependence of the normalized induced γ activity on the parameters of the cylinder. The results may turn out to be useful in processing data on neutron activation measurements of a core material if the properties of the moderator and the body being investigated are identical with respect to the transport of neutrons and γ radiation.

(No. 888/8717. Original article submitted Mar. 29, 1976.
Complete article 0.3 author's folio, 3 figs., 3 references.)

ANALYSIS OF THE PROCEDURE FOR MEASURING FAST MONOENERGETIC NEUTRON FLUXES WITH PROTON RECOIL PROPORTIONAL COUNTERS

A. N. Davletshin and V. A. Tolstikov

UDC 621.039.556

All the stages of the procedure for using proportional hydrogen H counters to measure fast neutron fluxes or the neutron source strength Q at electrostatic accelerators are analyzed (calculation and measurement of proton recoil spectra (PRS), methods of processing results). Particular attention is paid to the sources of systematic errors in experiment and calculation, to means of eliminating them, and to an estimate of their magnitudes.

To determine the value of Q it is necessary to determine the number of interactions N_{in} in the volume of the H counter:

$$Q = N_{in}/G_c n_{nc} V_c \sigma_{ps} t;$$

$$N_{in} = \epsilon_e(x)/K_N \epsilon_c(x) \text{ or } N_{in} = \rho_e(x)/K_N \rho_c(x) \Delta x,$$

where V_c is the geometrically sensitive volume of the H counter, n_{nc} is the number of hydrogen nuclei per cm^3 , G_c is the geometrical factor, σ_{ps} is the cross section for the scattering of neutrons by hydrogen, t is the time, $x = E_s/E_p$ is the relative energy of recoil protons, $\epsilon_e(x)$ and $\epsilon_c(x)$ are the experimental and calculated integral PRS, $\rho_e(x)$ and $\rho_c(x)$ are the experimental and calculated differential PRS, Δx is the channel width, and K_N is a factor taking account of the recording in the experimental PRS of events occurring outside the geometric volume of the counter.

Analysis showed that the main source of systematic errors is the quantity N_{in} , and therefore particular attention was paid to the expression for N_{in} . The procedure for calculating the PRS by the Monte Carlo method was discussed earlier [1,2].

The statistical errors of the calculation and the errors due to mistakes in the parameters of the design model are described. Relations and graphs are presented for determining the calculational errors resulting from errors in the parameters of the model.

Background corrections for scattered neutrons were determined. It was shown that the proper introduction of the background correction is possible only in the form of corresponding background PRS.

The methods of determining N_{in} for the same and different forms of $\rho_e(x)$ and $\rho_c(x)$ were analyzed. The causes of systematic errors were investigated and methods were proposed for eliminating them or estimating their possible values.

It was shown by specific examples that by using our counters and the methods of measurement and analysis of the PRS presented it is possible to determine the neutron source strength (flux) for $\epsilon_n = 350$ and 1200 keV to within ± 1.4 and $\pm 2\%$, respectively. An estimate of the systematic errors is presented.

The requirements necessary for increasing the reliability of the value of Q are formulated, and a research program for further increasing the reliability and accuracy of the measurement of fast neutron fluxes with gas hydrogen counters is proposed.

LITERATURE CITED

1. A. N. Davletshin and V. A. Tolstikov, Bull. of Inform. Center on Nucl. Data [in Russian], No. 7, Atomizdat, Moscow (1970), p. 277.
2. A. N. Davletshin, V. A. Tolstikov, and V. P. Platonov, in: Nuclear Constants [in Russian], No. 9, Atomizdat, Moscow (1972), p. 107.

(No. 889/8889. Original article submitted July 30, 1976.
Complete text 1.1 author's folios, 6 figs, 3 tables,
16 references.)

LETTERS TO THE EDITOR

APPLICATION OF DIRECT-CHARGE DETECTORS
FOR POWER MONITORING IN WATER-COOLED
WATER-MODERATED POWER REACTORS

L. I. Golubev, V. A. Zagadkin,
M. G. Mitel'man, A. B. Morev,
N. D. Rozenblyum, and V. V. Fursov

YDC 621.039.524.4:621.039.517

Direct-charge detectors (DCD) are widely used in power monitoring systems of fuel channels in channel-type reactors [1]. The application of such detectors in intrareactor measurements in water-cooled water-moderated reactors of the Novovoronezh Atomic Power Plant has been mentioned in [2], but no data are available on their application in power distribution monitoring systems in reactors. The experience gained with channel-type reactors is not relevant in our instance because of the specific construction features and operating conditions of water-cooled water-moderated power reactors, in particular with boron control [3].

Here we discuss the metrological characteristics of an intrareactor power monitoring system using direct-charge detectors as transducers.

Five neutron measurement channels (NMC) have been inserted into the reactor of the fourth unit of the Novovoronezh Power Plant; each channel consisted of five DPZ-1p direct-charge detectors with 250-mm-long emitters, the coordinates of the sensitive region centers of the detectors being located at 250, 750, 1250, 1750, and 2250 mm along the core height. The coordinates and parameters of the fuel holders in which the detectors were mounted are listed in Table 1. The detector currents were measured periodically with an M-135, class 1 microammeter. The coupling line current was taken into account by measuring the current in the background conductor provided in each detector [4].

All detectors remained useful after 12 months of operation. The average detector current was proportional to the integral neutron flux in the reactor and thus, to its power. Figure 1 indicates that the current is a linear function of reactor power. The spread of experimental points ($\pm 4\%$) is within the experimental error depending on the accuracy of measurement of reactor thermal power. The dependence of the detector system sensitivity i_{av}/W (where i_{av} is the average detector current and W is reactor power) on the number of reactor operation days is shown in Fig. 2. The detector system sensitivity remains unchanged after 320 effective operation days, which is apparently due to the fact that detector burnup is compensated by the reduction of boron content in the coolant and by fuel burnup. The spread of experimental points ($\pm 6\%$) is within the limits of accuracy of reactor power determination by the operational staff.

The determination of the sensitivity of the neutron measuring channel (NMC) as a transducer of the holder power is complicated by two factors: the impossibility of measuring the holder power by heat-engineering methods and by the probable dependence of the NMC sensitivity on uranium enrichment and burnup. For these reasons for the thermal power of the holder we have taken the value obtained from the average heating of the coolant in adjacent fuel holders.

Interpolation of the magnitude of coolant heating on fuel holders surrounding the NMC holders and fitted with heat monitors proved that the difference between the measured and interpolated values is less than 10% when averaged over three-four holders. Figure 3 shows the ratio of the average detector current to coolant heating in the holder, which is proportional to its power, as a function of effective reactor operating time.

Figure 3 shows that the neutron measuring channel sensitivity remains constant for the entire reactor run. The spread of experimental points is $\pm 12\%$ (for different NMC and the same measuring time the spread does not exceed $\pm 5\%$) and lies within the measuring error limits. The total spread in readings can be assumed to be associated with random measuring errors and with possible fluctuations of coolant flow rate in the holders.

Translated from *Atomnaya Énergiya*, Vol. 42, No. 1, pp. 44-45, January, 1977. Original article submitted December 17, 1975.

This material is protected by copyright registered in the name of Plenum Publishing Corporation, 227 West 17th Street, New York, N.Y. 10011. No part of this publication may be reproduced, stored in a retrieval system, or transmitted, in any form or by any means, electronic, mechanical, photocopying, microfilming, recording or otherwise, without written permission of the publisher. A copy of this article is available from the publisher for \$7.50.

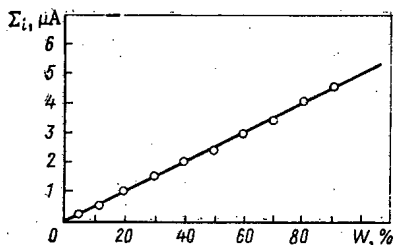


Fig. 1. Average detector current as a function of reactor thermal power.

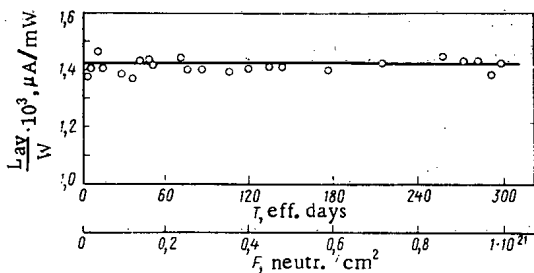


Fig. 2

Fig. 2. Dependence of detector system sensitivity i_{av}/W as a reactor power transducer on the effective reactor operating time and on neutron fluence.

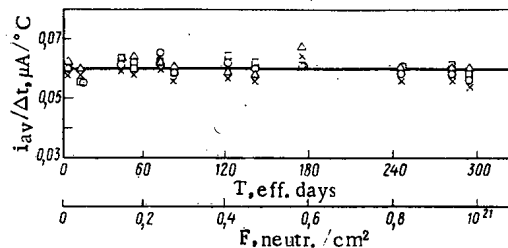


Fig. 3

Fig. 3. Ratio of average detector current to coolant heating in the holder as a function of effective reactor operating days and of neutron fluence. ○) NMC A; ×) B; △) C; □) A.

The average value of $i_{av}/\Delta t$, where Δt is the average coolant heating in the holders in all cells, agrees to within $\pm 0.6\%$, which suggests that the NMC sensitivity as a holder power transducer is independent of uranium enrichment (within the range 2.4–3.6%) and burnup (the amount of slag was 8.2–13.3 kg). This is apparently due to the fact that the neutron-measuring channel is practically outside the region of the external block effect of the fuel element.

Thus, an intrareactor power monitoring system makes it possible to measure the overall reactor power and its distribution in the core.

The measuring accuracy of absolute reactor power is determined by the accuracy of system calibration, which in turn depends mainly by the accuracy of thermal power measurement and amounts to $\pm 4\%$. The accuracy of relative power measurements depends on the accuracy of direct-charge detector current measurement and on errors associated with detector background currents, and can be reduced to $\pm 1-1.5\%$. In all cases the maximum permissible measuring error is considered.

Any possible variations of absolute sensitivity of the system during a run can be easily accounted for by periodically carrying out a reactor heat balance.

The error in relative power measurements consists of the error in detector current measurement (allowing for background currents), the errors due to detector differences and to their different arrangement in the neutron-measuring channels and to differences in holders, and it amounts to 2–3%.

LITERATURE CITED

1. B. G. Dubovskii, A. Ya. Evseev, and V. V. Ezhov, *At. Energ.*, **36**, No. 3, 171 (1974).
2. V. V. Fursov and A. M. Berezovets, in: *Ten Years of Experience in the Novovoronezh Atomic Power Plant* [in Russian], Novovoronezh (1974), p.144.
3. F. Ya. Ovchinnikov, L. M. Voroniv, and S. N. Samailov, *Operation of Reactor Plants of the Novovoronezh Atomic Power Plant* [in Russian], Atomizdat, Moscow (1972).
4. *Direct Charge Detectors. Technical Specifications* [in Russian], TU 16-538, 243-74.

TABLE 1

Name of NMC	Coordinates of NMC holder	Initial conc. of holder, %	Amount of slags, kg
A	09-48	2,4	10,7
B	05-48	3,6	11,8
C	20-49	2,4	12,3
D	14-39	3,6	8,2
E	18-39	2,4	11,7

HEAT PRODUCTION AND FRAGMENT CAPTURE CROSS SECTION IN THERMAL REACTORS

P. É. Nemirovskii and V. A. Chepurnov

UDC 621.039.517

Here we consider the concentration of ^{235}U and Pu fission fragments in a thermal reactor. An OSA program has been written for this purpose, which besides the fission fragment concentration also computes the heat produced by them as well as their absorption cross section.

The concentration of uranium and plutonium is described by

$$\frac{dN_5}{dt} = -\Phi_0 \langle \sigma_a^5 \rangle N_5(t);$$

$$\frac{dN_9}{dt} = -\Phi_0 \langle \sigma_a^9 \rangle N_9(t) - \Phi_0 \langle \sigma_a^8 \rangle N_8(t) + (1-\varphi) \Phi_0 \sum_{\tau} \nu \bar{\sigma}_a^{\tau} N_{\tau}(t),$$

where the subscripts 5, 8, and 9 refer to ^{235}U , ^{238}U , and ^{239}Pu , respectively. For other nuclides we have

$$\frac{dN_i}{dt} = -\Phi_0 \langle \sigma_a^i \rangle N_i(t) - \Phi_0 \langle \sigma_a^{i-1} \rangle N_{i-1}(t) - \lambda_i N_i(t),$$

where Φ_0 is the thermal neutron flux, λ is the radioactive decay constant, $\langle \sigma_{\mu}^i \rangle = \bar{\sigma}_{\mu}^i + R_{\mu}^i$ is the effective cross section allowing for processes in the epithermal energy region, μ is the process index, φ is the probability of avoiding resonance capture in ^{238}U , and ν^{τ} is the number of secondary neutrons per one absorption by a splitting nuclide τ .

The concentration of fragments is given by

$$\frac{dN_j(t)}{dt} = \sum_{\tau} \gamma_{\tau}^j \langle \sigma_f^{\tau} \rangle \Phi_0 N_{\tau}(t) + \lambda_{j\mu} N_j(t) + \langle \sigma_{\mu}^j \rangle \Phi_0 N_j(t) - [\langle \sigma_a^j \rangle \Phi_0 + \lambda_j] N_j(t),$$

where γ_{τ}^j is the yield of the j -th nuclide in fission of the nuclide τ , $\langle \sigma_{\mu}^j \rangle = \bar{\sigma}_{\mu}^j + \alpha I_{\mu}^j$, α is the hardness factor, I_{μ}^j is the total resonance integral, and $\lambda_{j\mu}$ is the radioactive decay constant of the j -th nuclide in which a j nuclide is formed. Resonance fragment absorption was allowed for under the condition $I_j \gg \bar{\sigma}_j$ (see Table 1). Thermal cross sections have been adopted from [1].

The OSA program includes fragments from ^{78}Se to ^{158}Gd , except ^{135}Xe , which is always treated separately. Nuclides with a yield less than 0.01% in ^{235}U and Pu fission were neglected. Radioactive fragments with $T_{1/2} \leq 8$ days are considered only in their fission products. The program computes the total macroscopic absorption cross section of neutrons:

$$\Sigma_a = \sum_j \rho_j(t) \langle \sigma_a^j \rangle,$$

necessary in calculating the thermal utilization factor. Figure 1 shows Σ_a as a function of total fragment concentration in a natural-uranium reactor with a neutron temperature of 0.053 eV. For a pair of fragments $\sigma_a \approx 46$ b, which conforms to the $1/v$ law.

The program also computes the energy liberated in β decay of fission fragments as a function of "cooling" time after irradiation ceases. Since short-lived isotopes are not considered, this time exceeds 2-3 weeks. The characteristics of radioactive fragments have been adopted from [2]. The isomeric states of ^{95}Nb , ^{125}Te , and ^{127}Te have been taken into account in three chains. In ^{129}Te the decay of the normal state (69 min) was regraded as instantaneous. The α and β decay energies were allowed for in calculating energy release in plutonium isotopes.

Translated from *Atomnaya Énergiya*, Vol. 42, No. 1, pp. 45-46, January, 1977. Original article submitted December 19, 1975.

This material is protected by copyright registered in the name of Plenum Publishing Corporation, 227 West 17th Street, New York, N.Y. 10011. No part of this publication may be reproduced, stored in a retrieval system, or transmitted, in any form or by any means, electronic, mechanical, photocopying, microfilming, recording or otherwise, without written permission of the publisher. A copy of this article is available from the publisher for \$7.50.

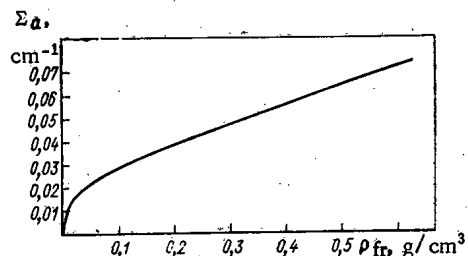


Fig. 1. Total fragments cross section as a function of their overall concentration.

TABLE 1. Total Resonance Fragments Integrals

Nuclide	I, b	Nuclide	I, b	Nuclide	I, b	Nuclide	I, b
⁹⁵ Mt	106	¹²⁹ I	55	¹⁴⁵ Nd	140	¹⁵² Sm	3100
¹⁰³ Rh	656	¹³³ Cs	370	¹⁴⁷ Pm	3270	¹⁵³ Sm	1420
¹⁰⁹ Ag	1910	¹⁴³ Nd	140	¹⁴⁷ Sm	570		

It is usually assumed that the average kinetic energy $\bar{\epsilon}$ of β electrons is equal to $1/3$ of their maximum energy ϵ_0 . This assumption is wrong. The energy spectrum of electrons for allowed β decays has the well-known form

$$W(E) dE \approx E^2 (E_0 - E)^2 dE \text{ for } E_0 \gg 1;$$

$$W(E) dE \approx \sqrt{E-1} (E_0 - E)^2 dE \text{ for } E_0 - 1 < 1.$$

where E_0 is the total maximum electron energy. For $E_0 = 1.2, 2.0, 3.0,$ and 5.0 m.e., $\bar{\epsilon}/\epsilon_0 = 0.343, 0.373, 0.397,$ and 0.427 , respectively. Hence, $\epsilon = 1/3 \epsilon_0$ is only the lower limit for allowed β decays, whereas β electrons of fission fragments contain many with $E_0 \geq 2$.

Fragment decays include many β decays of the first hindrance [3]. An analysis of electron spectra of these transitions indicates that for them $\bar{\epsilon}/\epsilon_0$ is nearly independent of E_0 and is close to 0.435, i.e., 30% greater than the accepted value of 0.333. It has been also taken into account that β decay takes place along different allowed and forbidden branches. The electron energy was thus averaged over the specific spectrum of each β -active fragment. The total heat production due to β and γ emission of fragments was computed from the average energy.

The following results have been obtained in calculating the heat production of fission fragments in the "Dresden" reactor. The fuel elements have been extracted from the reactor after 300 days of operation. After 60 days of cooling, the β and γ activities were about 0.4 cal/sec·g each. If all β decays were allowed with low-energy decays, then their activity would be 0.3 cal/sec·g.

LITERATURE CITED

1. Neutron Cross Sections, Vol.1, BNL-325, New York (1973).
2. C. Leederer, J. Holander, and I. Perlman, Tables of Isotopes, New York (1967).
3. L. N. Zyryanova, Unique Beta Transitions [in Russian], Izd. Akad. Nauk SSSR (1960).

EFFECT OF APPROXIMATING THE SCATTERING
INDICATRIX AND REPRESENTATION OF THE CONSTANTS
ON THE RESULTS OF CALCULATING THE FIELD
CHARACTERISTICS BEYOND AN IRON BARRIER

G. Sh. Pekarskii, Yu. Ya. Katsman,
and G. A. Kucher

UDC 539.125.523.348

The transport equation for neutrons through a one-dimensional barrier was solved by a Monte Carlo method on a model M-222 computer for an exactly monodirectional ($\theta_0 = 0$) source fission spectrum. The differential energy characteristics were calculated for the radiation field passing through an area of radius R in the plane $Z = H$

$$\Phi(\Delta E) = \int_{\Delta E} F(E, x, y, Z=H) dE; \quad (1)$$

$$N_R(\Delta E) = 2\pi \int_0^R \Phi(\Delta E) \rho d\rho. \quad (2)$$

Calculations were carried out for barriers of thickness $H = 5, 10, 20, 40,$ and 60 cm and for $R = 2.5, 10,$ and 100 cm. The neutrons passing through the barrier were distributed over the nine energy intervals (10.5-6.5; 6.5-4.0; 4.0-3.0; 3.0-2.0; 2.0-1.5; 1.5-1.0; 1.0-0.5; 0.5-0.25; 0.25-0.1 MeV). Absorption and escape of neutrons beyond the barrier were taken into account by the appropriate change in the statistical weight when modeling the history of a neutron. The neutron spectrum beyond the barrier was determined by the method of expected quantities. The problem was solved by using correlation sampling. Positive correlation was achieved as follows. Events with the same numbers began from the same random number, which, in its turn, ensured that the same sequences of random numbers were used during the entire history of the event for calculations with different constants. In order to investigate the effect of accuracy in approximating the elastic scattering indicatrix, the latter was represented in the transport and P_7 approximations. In order to analyze the effect of the constants, the calculations were carried out both omitting and taking into account resonance blocking of the cross sections, as well as for constants in the subgroup representation [2]. Data on the energy dependence of the angular moments of the elastic scattering cross section for neutrons was taken from [3]. Inelastic scattering was assumed to be isotropic in the laboratory frame. The transition matrix for inelastic scattering taken from [1] was used in the calculations.

Results of the Calculations. Integral field characteristics for transmitted neutrons are given in Fig. 1a, and b, in the transport and P_7 approximations for the three types of constants, N_{res} for calculations taking resonance blocking of the cross sections into account, N_{subgr} for calculations with the constants in the subgroup representation, and N_{gr} for calculations without allowing for blocking

$$N = \int_{0.1}^{10.5} N_R(\Delta E) dE. \quad (3)$$

The results are represented in relative units and divided by the data obtained by using the subgroup constants in the corresponding approximation.

The effect of approximating the elastic scattering indicatrix on the integral characteristics of the neutron field beyond an iron barrier is shown in Fig. 2. The effect of representation of the constants on the

Translated from *Atomnaya Énergiya*, Vol.42, No.1, pp.47-48, January, 1977. Original article submitted January 7, 1976.

This material is protected by copyright registered in the name of Plenum Publishing Corporation, 227 West 17th Street, New York, N.Y. 10011. No part of this publication may be reproduced, stored in a retrieval system, or transmitted, in any form or by any means, electronic, mechanical, photocopying, microfilming, recording or otherwise, without written permission of the publisher. A copy of this article is available from the publisher for \$7.50.

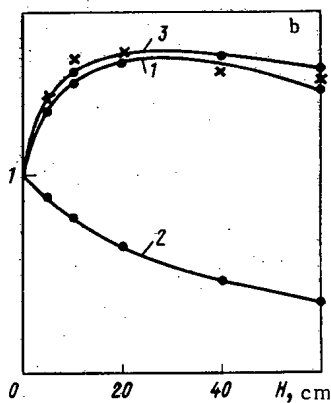
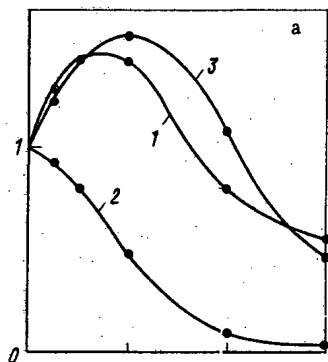


Fig. 1

Fig. 1. Effect of representation of the constants on the neutron flux beyond an iron barrier for (a) $R = 2$ and (b) $R = 100$ cm (in all the figures the ratios of the corresponding fluxes in relative units are given on the ordinates): 1) $N_{\text{res}}(P_7)/N_{\text{subgr}}(P_7)$; 2) $N_{\text{gr}}(P_7)/N_{\text{subgr}}(P_7)$; 3) $N_{\text{res}}(\text{tr})/N_{\text{subgr}}(\text{tr})$.

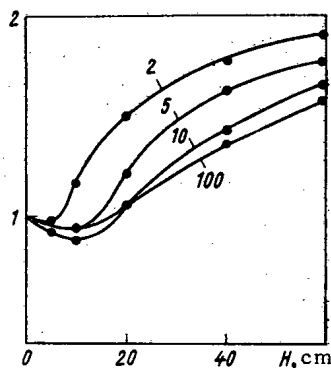


Fig. 2

Fig. 2. Effect of approximating the scattering indicatrix on the integral field characteristics of neutrons beyond an iron barrier $N_{\text{subgr}}(\text{tr})/N_{\text{subgr}}(P_7)$ (the numbers on the curves correspond to the radius of integration).

differential characteristics of the transmitted neutron field is shown in Fig. 3 in relative units. Results obtained with constants in the subgroup representation are shown in Fig. 4 for two forms of scattering indicatrix approximation.

Thus (see Fig. 1), using constants that omit and allow for [1] resonances leads to a reduction and an increase of the results, respectively, compared with data obtained using constants in the subgroup representation. The results for an exact monodirectional source with $R = 100$ cm, equivalent to the data for a plane monodirectional source, agree well with the results of [4], which were obtained by a multigroup calculation in the $2D_5P_1$ approximation (marked by crosses in Fig. 1b). The nature of the effect exerted by the representation of the constants has a marked dependence on the relative contribution from the unscattered component of the radiation (detection radius for an exact monodirectional source). In both the P_7 as well as the transport approximations for elastic scattering, the effect of representation of the constants is the same with regard to results in the subgroup representation (curves 1 and 3, Fig. 1).

The effect of approximating the elastic scattering indicatrix in the P_7 and transport approximations, using constants in the subgroup approximation, shows that the results in the transport approximation are overestimated (see Fig. 2). The overestimate of results increases with the barrier thickness, and is more important for small detection radii. It can be seen from Fig. 3 that the representation of the constants has an ambiguous effect on the different energy groups of the spectrum beyond the barrier for a relatively constant overestimate of the total flux (see Fig. 1b). The data shown in Fig. 4 show that for neutrons with $E > 1$ MeV, application of the transport approximation for the indicatrix of elastic scattering by iron introduces an error

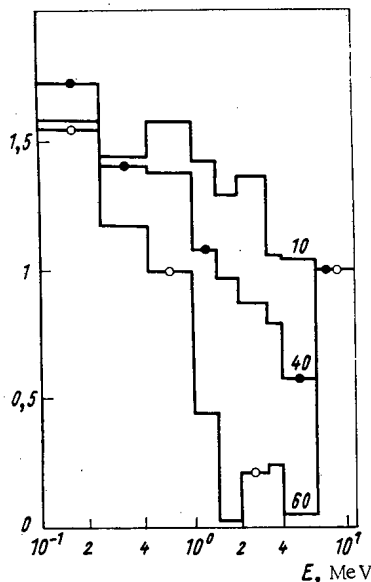


Fig. 3

Fig. 3. Effect of representation of the constants on the differential characteristics of the field in the R approximation $\Phi_{\text{res}}(\Delta E_i)/\Phi_{\text{subgr}}(\Delta E_i)$ for $R = 100$ cm (the numbers of the curves give the barrier thickness in cm).

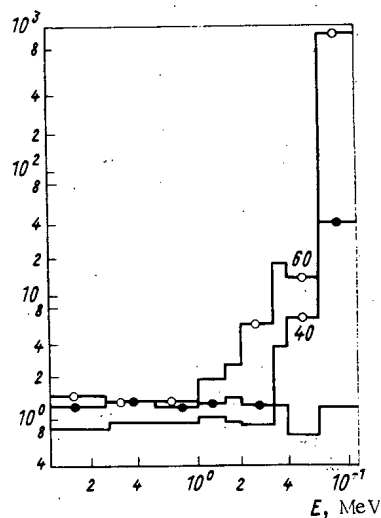


Fig. 4

Fig. 4. Effect of approximating the scattering indicatrix on the differential field characteristics $\Phi_{\text{tr}}(\Delta E_i)/\Phi_{P_7}(\Delta E_i)$ for $R = 100$ cm (numbers of the curves give the barrier thickness in cm).

such that for barriers of thickness 60 cm the overestimate in the high-energy component of the transmitted radiation is observed to be of the order of ten or a hundred, although the integral overestimate of the flux compared with the P_7 approximation is less than 1.7 (see Fig. 2).

LITERATURE CITED

1. L. P. Abagyan et al., Group Constants for Nuclear Reactor Calculations [in Russian], Atomizdat, Moscow (1964).
2. V. F. Khokhlov et al., in: Nuclear Constants [in Russian], Central Scientific-Research Institute for Atomic Data (TsNIIatominform), No. 8, Sec. 3, Moscow (1972), p. 3.
3. N. O. Bazazyants et al., in: Nuclear Constants [in Russian], Central Scientific-Research Institute for Atomic Data (TsNIIatominform), No. 8, Sec. 1, Moscow (1972), p. 61.
4. V. F. Khokhlov et al., in: Nuclear Constants [in Russian], Central Scientific-Research Institute for Atomic Data (TsNIIatominform), No. 8, Sec. 4, Moscow (1972), p. 154.

FLOW RATE MEASUREMENT BY MEANS OF CORRELATING
THE RANDOM SIGNALS OF THERMOCOUPLES IN CIRCUITS
WITH A NATURAL CIRCULATION OF COOLANT

V. M. Selivanov, A. D. Martynov,
Yu. A. Sergeev, V. S. Sever'yanov,
A. P. Solopov, V. I. Sharypin,*
D. Pallagi, S. Horanyi,
T. Hargitai, and S. Työgyer†

UDC 642.039.564

Control of coolant flow rate is a complex problem if the natural circulation of a single-phase liquid is used to remove heat from the active zone [1], since in this case the available useful pressure head is measured in tens of millimeters of water.

With regard to natural circulation, it is worth considering those methods that use flowmeters in which there is no restriction of the flow (tachometric and correlation methods). Practical experience with turbine-type flowmeters shows that they are not reliable enough, and do not have a long enough life. Correlation methods for measuring the flow rate apparently hold more promise [2-5]. Particularly attractive is a method for detecting temperature fluctuations of the coolant using ordinary thermocouples as detectors. An indisputable advantage of correlation flowmeters is their reliability (as a result of the absence of moving parts), a minimum of pressure loss, and the possibility of obtaining information from the noise of the technological process itself.

The present paper considers questions connected with practical processing in the method of correlating random thermocouple signals for measuring the flow rate of water in circuits with natural circulation (reactors, test stands). The effect of the following factors on the results of correlation measurements were studied experimentally, the time lag of the thermocouples (with insulation of the hot junction and without insulation), the base distance between thermocouples (in the range of velocity variation from 0.1 to 1.3 m/sec), and the positioning of the hot thermocouple junctions in the coolant flow. The investigations were carried out by Soviet (FÉI) and Hungarian (TsIFI) specialists. A dynamic model UKM test stand [6], a loop channel [7] of the First Atomic Electric Station with fuel-element assembly from an ABV-1.5 reactor, and special measuring apparatus (TsIFI) were used for the experiments.

Experimental Apparatus. The UKM test stand (Fig.1) is a model of a two-circuit nuclear steam-generating device with natural circulation of single-phase and two-phase coolants in the primary and secondary circuits, respectively. The active region of the test stand is simulated by four electrically heated units. The inputs to these units are made in the form of branch pipes inside of which are set turbine flow-rate sensors with shaped electrodes. The steam-generator is incorporated into the body of the primary circuit and is collected from Field tubes. The flow rate of water in the second circuit is controlled by Venturi tubes mounted in the fall pipes.

The experimental measuring sections of the secondary circuit were situated in front of the inputs to the cassette units, and consisted of sections of pipes inside of which were set thermocouples. Cable thermocouples were used with an external sheath diameter of 0.5 and 1.0 mm. The part of the thermocouples with an external diameter 0.5 mm had an insulated hot junction. The thermocouples were set at a distance of 2.5-5.0 tube diameters from the entrance to the tube section. The relative distance of the thermocouple junctions from the walls y/R was 0.35, 0.5, and 1.0. Different combinations of thermocouples enabled us to investigate

* USSR.

† Hungarian People's Republic.

Translated from Atomnaya Énergiya, Vol.42, No.1, pp.49-52, January, 1977. Original article submitted February 3, 1976.

This material is protected by copyright registered in the name of Plenum Publishing Corporation, 227 West 17th Street, New York, N.Y. 10011. No part of this publication may be reproduced, stored in a retrieval system, or transmitted, in any form or by any means, electronic, mechanical, photocopying, microfilming, recording or otherwise, without written permission of the publisher. A copy of this article is available from the publisher for \$7.50.

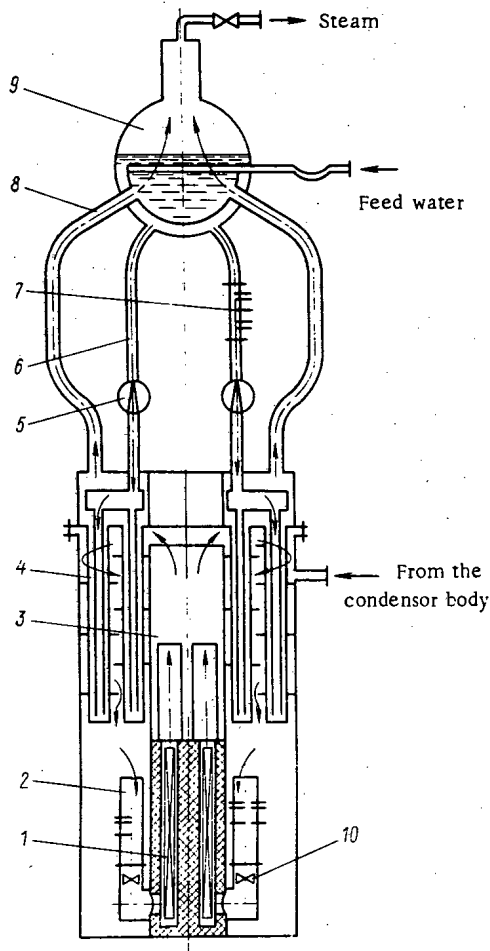


Fig. 1

Fig. 1. Schematic diagram of the steam generator part of the UKM test stand: 1) active zone; 2) experimental measuring sections of the first circuit; 3) rise column; 4) steam generator; 5) Venturi tubes; 6) fall pipes; 7) experimental measuring section of the second circuit; 8) rise pipes; 9) separator drum; 10) turbine flowmeters.

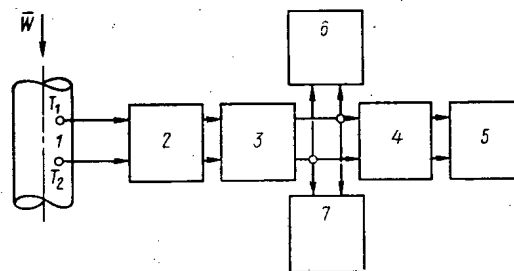


Fig. 2

Fig. 2. Block diagram of the measuring apparatus: 1) correlation sensor; 2) preamplifier (TsIFI); 3) amplifier (TsIFI); 4) correlator (Hewlett Packard); 5) two-channel recorder (Hewlett Packard); 6) MAS-54 tape recorder; 7) two-beam oscillograph C1-18 (FÉI); T_1 and T_2 are thermocouples.

base separations of 10, 20, 30, 80, and 100 mm. The measuring section of the secondary circuit was equipped with three sets of moveable thermocouples, and was fitted in one of the fall pipes. The distances between thermocouples in this section were 10, 20, 30, and 40 mm, which defined nine variants of base separation from 10 to 100 mm. Each set was made up of five identical thermocouples with a hot junction not insulated from the housing. The diameters on the thermocouple sheaths in the sets were 0.5, 1.0, and 1.5 mm.

The loop channel [7] was set in a regular cell of the active zone of a First Atomic Electric Power Station Reactor (First AES reactor) and was intended for testing fuel elements of an ABV-1.5 reactor. Two Chromel-Alumel thermocouples with sheath diameter 0.5 mm and base separation of 20 mm were used for correlation measurements of the flow rate of natural circulation in the channel. The hot thermocouple junctions were not insulated from the housing and were set at a distance of 2 mm from the inner wall of an annular channel of cross-sectional width 8 mm, distant 200 mm from the outlet from the assembly.

Method of Measurement. The essence of statistical methods for measuring velocities consists in the fact that any random or periodic signals propagating in a moving medium can, theoretically, be analyzed in order to determine the time characteristics of the flow. In our case these signals were the temperature fluctuations of the coolant.

The measuring apparatus consisted (Fig. 2) of a preamplifier, a basic amplifier with a filter, a universal correlator, a two-channel automatic recorder, and a tape recorder for recording the thermocouple signals.

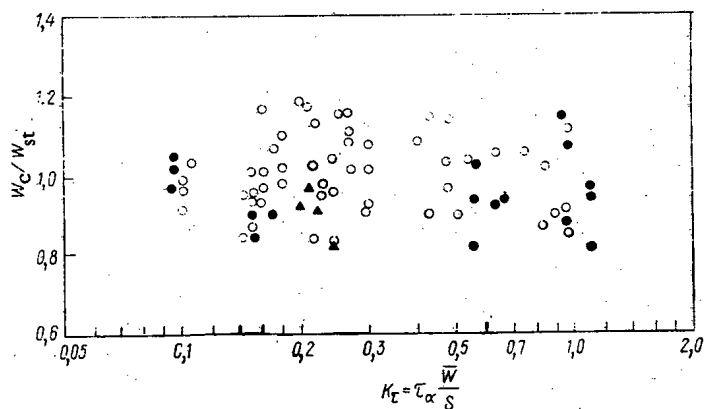


Fig. 3

Fig. 3. Results of the measurements as a generalized function of the dimensionless quantity $K_T = \tau_\alpha (\bar{W}/S)$: \circ , \bullet) measurements in the primary and secondary circuits of the UKM test stand, respectively; \blacktriangle) measurements at the output of the loop channel assembly.

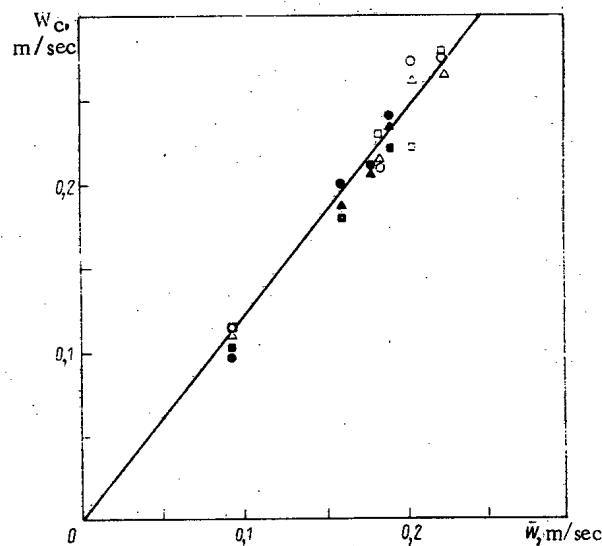


Fig. 4

Fig. 4. Results of velocity measurements on the flow axis in the first circuit of the UKM test stand: \blacksquare , \bullet , \blacktriangle) TsIFI section; \square , \circ , \triangle) FÉI section; —) theoretical value of the velocity with $y/R = 1.0$ for stabilized flow. Base separations S , mm: \blacksquare and \square) 10; \bullet and \circ) 20; \triangle and \blacktriangle) 30.

Over a specified time interval in the steady-state regime, the signals from two thermocouples separated by a distance S in the flow were fed, after amplification and filtering, to the universal correlator, which reproduced the autocorrelation function (ACF)

$$C_{1-2}(\tau) = \lim_{T \rightarrow \infty} \frac{1}{2T} \int_{-T}^{+T} U_1(t) U_2(t + \tau) dt. \quad (1)$$

The "flight" time $\tau_0(c)$ (time for the random signals to traverse the distance S between the thermocouples) and coolant velocity W_k (m/sec) were determined from the position of the ACF maximum, Eq. (1). The results of these measurements were compared with the theoretical value of the velocity over a section of stabilized flow, and also compared with the mean flow velocity obtained in the primary circuit of the UKM test stand from turbine flowmeters, in the secondary circuit from Venturi tube data, and in the loop channel of the First AES reactor from heat balance data. The turbine flowmeters and Venturi tube were calibrated in the flow test stand. The error in the calibration data was less than $\pm 3\%$.

Discussion of Results. It is well known [3-5] that the form and amplitude of the ACF maximum, which reflect the nature of the correlations between the sensor signals, depend on the placing of these sensors, their base separation, their time lag, and the level of electromagnetic noise.

To allow for the complex interrelations between correlation stability of the thermocouple signals and these factors the following dimensionless quantity was adopted in order to generalize the experimental data

$$K_T = \tau_\alpha (\bar{W}/S), \quad (2)$$

which is the ratio of the thermocouple time constant τ_α to the flight time τ_0 corresponding to the mean velocity of the flow. Thanks to this quantity it was possible to represent all the results obtained in the range of parameters (mean velocity $0.1 \leq \bar{W} \leq 1.35$ m/sec, base separation $0.1 \leq S \leq 0.1$ m, sheath diameters of thermocouple cables $0.5 \leq d_0 \leq 1.5$ mm) in the form of a single generalized function

$$W_c/W_{st} = f[\tau_\alpha (\bar{W}/S)], \quad (3)$$

where W_c/W_{st} is the ratio of the velocity measured by the correlation method to the theoretical velocity of stabilized flow in the place of measurement, τ_α is the time lag of the thermocouples (without and with insulation of the hot junction from the housing) calculated according to the recommendations of [8].

Results of the measurements are given in Fig. 3 in the form of the function Eq. (3). It was established that a stable correlation exists between the thermocouple signals in the range of variation of the dimensionless quantity $0.1 \leq K_T \leq 1.1$, which means that velocity measurements by the statistical method are possible. In our tests we were unable to obtain ACF's for $0.1 > K_T > 1.1$. A knowledge of the region of correlation stability enables the sensor characteristics to be chosen in the range of parameters under investigation.

Accumulated experience and the data of [4] show that when there is a low level of useful signal the results of the measurements can depend strongly on the electrical noise caused by the feed circuit ($f = 50$ Hz). The effect of this noise was so great for measurements in the primary circuit of the UKM test stand that the resulting information was sometimes insufficient to determine the velocity. Installation of additional filters at the inputs to the measuring channels enabled the effect of the background noise to be compensated. As a rule, such compensation was not needed for measurements using thermocouples with insulated junctions. The problem of combatting electromagnetic noise did not arise for measurements in the loop channel. Thus, it should be stressed that when making correlation measurements of velocity under the conditions of strong electromagnetic fields in electrically heated test stands thermocouples with junctions insulated from the housing should be used. Thermocouples without insulation of the hot junction can also be used under reactor conditions.

Statistical methods make possible direct measurements of the local flow velocity between the points where the sensor elements are located. In this case there is no problem in determining the flow rate if the relation between the velocity in the place of measurement and the mean flow velocity is known. These relations can be calculated accurately enough over a section of stabilized coolant flow, where the velocity distribution over the radius has been well studied.

In practice it usually turns out that the flow rate sensors are installed where the velocity profile is not stabilized. For measurements in active zones of the cassette unit type (for example, in an ABV-1.5 reactor) the entrances to the cassette units are convenient for installing the flowmeters.

The hydrodynamic features of flow in the initial section of a smooth pipe have been investigated in [9], in particular, and results indicate that in this section the development of velocity profiles is determined by the conditions at the inlet and has a complicated nature. For pipes with sharp edges (or with a spoiler) the maximum velocity change registered on the flow axis over the whole length of the stabilization region was less than $\pm 10\%$.

In our case axial velocity measurements over the nonstabilized section of coolant flow agree well with these data (Fig. 4). It follows from the figure that the velocity on the flow axis, as measured by the correlation method, differs from the maximum velocity of the stabilized profiles by less than $\pm 10\%$, and exceeds the value of the mean velocity by roughly 20%. On comparing results of measurements for $y/R = 0.2$ and 0.35 with the corresponding velocity of the stabilized flow, a wider scatter was obtained (up to $\pm 20\%$), which evidently indicates that the correlation is impaired in the region close to the wall as a result of the effect of the wall [3]. Similar results were obtained for measurements in the second circuit. Velocity measurement data in the loop channel agree satisfactorily with calculations.

Results of the tests show that it is possible, in principle, to measure the rate of flow by setting sensors in a region of nonstabilized coolant flow, and that the sensor elements of the thermocouples should be set a distance apart which, relative to the tube radius, is in the range of values $0.25 \leq y/R \leq 1.0$.

It should be noted that an absolute error in the radial placement of the thermocouples of up to ± 3 mm has practically no effect on the results of the measurements, while large displacements can lead to a substantial deterioration of correlation and to a degeneration of the autocorrelation functions.

Finally the authors are grateful to G. A. Klochko, E. A. Nikonov, A. N. Solozhentsev, and E. A. Yashchenko for a great deal of assistance in preparing and conducting the experiments.

LITERATURE CITED

1. V. A. Zhil'tsov et al., *At. Energ.*, 26, No. 5, 403 (1969).
2. J. Boland, *Nuclear Reactor Instrumentation*, Gordon (1970).
3. C. Mika, K. Raes, and D. Stegemann, in: *IAEA Specialist Meeting on Analysis of Measurements to Diagnose Potential Failures*, Rome, April 10-12 (1972).
4. K. Termaat, *J. Phys.*, 3, No. 43, 589 (1970).
5. D. Pallagi, S. Horanyi, and T. Hargitai, *Ann. Nucl. Energ.*, 2, 333 (1975).

6. V. M. Selivanov et al., *At. Energ.*, 27, No.2, 101 (1969).
7. G. A. Klochko et al., *At. Energ.*, 34, No.1, 40 (1973).
8. S. I. Morozov and E. D. Naumov, *Inzh. Fiz. Zh.*, 15, No.6, 1100 (1968).
9. M. Kh. Ibragimov et al., *Teplofiz. Vys. Temp.*, 12, No.3, 542 (1974).

NEUTRON RESONANCE PARAMETERS OF ^{245}Cm FOR
NEUTRON ENERGIES IN THE 1-30-eV RANGE

T. S. Belanova, Yu. S. Zamyatnin,
A. G. Kolesov, V. M. Lebedev,
and V. A. Poruchikov

UDC 621.039.556

The total neutron cross sections and resonance parameters of ^{245}Cm have been inadequately investigated. In addition to [1], up to the present time two studies have been published. In 1972, Berreth et al. [2] used selector measurements to determine the resonance parameters of the levels of ^{245}Cm in the range 1-30 eV. Similar data were obtained in an atomic explosion [3] from fission cross-section measurements in the range 20-60 eV. A common disadvantage of selector measurements [1,2] is the multiple isotopicity of the curium samples as well as the presence of plutonium and americium isotopes in the samples. In [1], e.g., the admixtures of ^{240}Pu and ^{243}Am amounted to 1.6% and 2.2%, respectively; in [2], there was not only ^{240}Pu (0.6-1.3%) and ^{243}Am (0.2-0.3%) present, but also ^{243}Cm (1.5%).

In this work, measurements were made of the resonance parameters of ^{245}Cm using a purer sample of curium. The total content of admixtures amounted to 3.5%, including 2% platinum, 0.23% ^{240}Pu , and $< 0.05\%$ ^{243}Am . The sample was prepared from a specially treated [1] dehydrated powder of stable curium oxide with a known oxygen content (Cm_2O_3). An aluminum plate holder with 1-mm-thick walls was filled with 206.9 ± 0.2 mg of powder within a space of dimensions $0.8 \times 8.0 \times 9.0$ mm. The percent isotopic composition of the curium sample and the number of nuclei of each isotope for a "thick" sample (10^{20} atoms/cm²) are as follows:

^{243}Cm	< 0.09	—
^{244}Cm	86.68;	56.8
^{245}Cm	9.34;	6.1
^{246}Cm	3.79;	2.45
^{247}Cm	0.19;	0.12
^{248}Cm	< 0.09	—

Using a time-of-flight method, the transmission within the 1-30-eV region of neutron energies was measured for two values of sample thickness ($2.6 \cdot 10^{20}$ and $6.1 \cdot 10^{20}$ atoms/cm²) at an SM-2 reactor. The neutron burst was prepared by a selector with synchronized rotors suspended in a magnetic field [4]. A bank of helium counters was used to detect the neutrons. The best energy resolution obtained with the spectrometer was 70 nsec/m. The statistical uncertainty in the measurements was 1-2%, with the neutron background varying between 0.5 and 2.0%. The transmission data were corrected for the scattering of the neutrons in the oxygen.

A BESM-4M electronic computer was used to calculate the resonance parameters by the method of areas and the one-level Breit-Wigner formula. The calculation resulted in the values of the level positions E_0 , the neutron width $2g\Gamma_n$, and the radiative width $\Gamma_\gamma = 40$ meV (see Table 1). Table 1 also lists previously obtained [2,3] values of the resonance parameters. A comparison revealed discrepancies between our data and those of [2]. Resonances in ^{245}Cm were found for the first time, with the following energies (in eV): 1.24, 2.45, 3.21, 9.40, 10.10, 13.60, and 18.60. The identification of the level at 1.24 eV is uncertain; it is possible that it belongs to ^{247}Cm . It is still difficult to say definitely whether there are resonances at 9.40 and 18.60 eV. Measurements with a thicker sample need to be made in order to establish their existence. Levels at 25.9 and 26.9 eV were also obtained; these were not given in [2] either, but were first discovered in fission cross section measurements [3].

Translated from *Atomnaya Énergiya*, Vol.42, No.1, pp.52-53, January, 1977. Original article submitted April 8, 1976; resubmitted July 25, 1976.

This material is protected by copyright registered in the name of Plenum Publishing Corporation, 227 West 17th Street, New York, N.Y. 10011. No part of this publication may be reproduced, stored in a retrieval system, or transmitted, in any form or by any means, electronic, mechanical, photocopying, microfilming, recording or otherwise, without written permission of the publisher. A copy of this article is available from the publisher for \$7.50.

TABLE 1. Resonance Parameters of ^{245}Cm

E_0 , eV	$2g\Gamma_n$, meV	$2g\Gamma_n$, meV [2]	$2g\Gamma_n$, meV [3]
$1,240 \pm 0,008$ *	—	—	—
$1,980 \pm 0,005$	$0,18 \pm 0,02$	$0,313 \pm 0,035$	—
$2,450 \pm 0,006$	$0,08 \pm 0,02$	—	—
$3,207 \pm 0,009$	$0,010 \pm 0,003$	—	—
$4,69 \pm 0,01$	$2,0 \pm 0,2$	$2,08 \pm 0,03$	—
$9,25 \pm 0,02$	$0,30 \pm 0,04$	$0,67 \pm 0,12$	—
$9,40 \pm 0,02$ †	$0,02 \pm 0,01$	—	—
$10,10 \pm 0,03$	$0,29 \pm 0,04$	—	—
$11,40 \pm 0,05$	$0,58 \pm 0,05$	$0,71 \pm 0,10$	—
$13,60 \pm 0,06$	$0,12 \pm 0,01$	—	—
$13,90 \pm 0,06$	$0,26 \pm 0,03$	$0,335 \pm 0,075$	—
$15,70 \pm 0,07$	$0,25 \pm 0,02$	$1,2 \pm 0,4$	—
$18,60 \pm 0,07$ †	$0,12 \pm 0,05$	—	—
$21,60 \pm 0,08$	$1,7 \pm 0,2$	$3,24 \pm 0,93$	2,11
$24,9 \pm 0,1$	$2,4 \pm 0,3$	$3,98 \pm 0,99$	2,6
$25,9 \pm 0,1$	0,05	—	0,036
$26,9 \pm 0,1$	$1,2 \pm 0,2$	—	0,76
$27,8 \pm 0,1$	$0,7 \pm 0,1$	$0,89 \pm 0,30$	0,6
$29,6 \pm 0,1$	$3,5 \pm 0,4$	$3,78 \pm 1,15$	3,46

* Possibly a level of ^{247}Cm .

† Doubtful levels.

The values for the neutron width of the levels are in general agreement with nuclear explosion data [3], but differ considerably from the data of [2]. Our values of $2g\Gamma_n$ are smaller by a factor of two for a number of levels. These discrepancies evidently stem from the following causes. The spectrometer of Berreth et al. [2] had lower energy resolution (280 and 147 nsec/m for the energy ranges 1-7 eV and above 7 eV, respectively) than the spectrometer used in our measurements. The ^{245}Cm sample characteristics were not as good for the ones used in [2]. For each of three samples, the largest number of nuclei were those of ^{244}Cm (on the average, ~94%, or $187.3 \cdot 10^{20}$ atoms/cm²). The content of ^{243}Cm , ^{245}Cm , and ^{246}Cm in the various samples was at most 1.5-4.0%, while that of ^{243}Am was 0.3%. The maximum thickness of ^{245}Cm was $7.6 \cdot 10^{20}$ atoms/cm². The values of the $^{244}\text{Cm}/^{245}\text{Cm}$ ratio were 9.3 and 23.3 for the samples used in this work and [2], respectively. The samples studied in the present investigation thus had 2.5 times the relative content of ^{245}Cm and a lower content of admixtures of ^{243}Am and ^{240}Pu .

Using the data given in Table 1, we calculated the mean spacing between the levels, obtaining a value $\bar{D} = 1.45 \pm 0.15$ eV; our result for the neutron strength function was $S_0 = (0.8 \pm 0.3)10^{-4}$. These agree with the corresponding values of [2].

The authors thank S. I. Babich, S. N. Nikol'skii, V. A. Safonov, T. V. Denisov, V. M. Nikolaev, and G. V. Kuznetsov for the help they have given in this work at various stages.

LITERATURE CITED

1. T. S. Belanov et al., At. Energ., **39**, No. 5, 369 (1975).
2. J. Berreth, F. Simpson, and B. Rusche, Nucl. Sci. and Eng., **49**, 145 (1972).
3. M. Moore et al., Phys. Rev., **3**, No. 4 (1971).
4. S. M. Kalebin et al., in: Proceedings of the Conference on Neutron Physics [in Russian], Part II, Naukova Dumka, Kiev (1972), p. 267.

EFFECT OF PRESSURE IN LIGHT WATER AND BENZENE
VAPORS ON THE TOTAL INTERACTION CROSS SECTION
FOR SLOW NEUTRONS

V. E. Zhitarev and S. B. Stepanov

UDC 539.171.02:539.171.4.162.2:539.2

The scattering of slow neutrons by gases and the dependence of this scattering on gas density was discussed in [1-4]. Molecular motion in light water vapor superheated by the scattering of neutrons at a wavelength of 4 \AA is investigated in [1] for pressures of 4 and 60 atm, and at a temperature of 3000°C in both cases. It was established that, although the scattering spectrum in the vapor exhibits a strong dependence on angle and on temperature, change in pressure has no effect on the spectrum.

Calculations of the scattering of slow neutrons by real gases were made in [3] in the quasi-ideal approximation. It was shown that in this approximation the form of the neutron spectrum remains the same as for an ideal gas. However, the absolute value of the cross section varies as a result of intermolecular interactions in the scattering gas. In a real gas the microscopic cross section increases, compared with the cross section in an ideal gas, by ρ/ρ_0 which is the ratio of the real density to the density calculated from the equation of state for an ideal gas.

TABLE 1. Total Interaction Cross Section for Neutrons of Various Wavelengths with Superheated Vapors of Light Water at Different Pressures, b

P. bars	Wavelength, \AA						
	13	14	15	16	17	18	19
17,8	604 ± 18	608 ± 19	677 ± 21	718 ± 17	736 ± 20	774 ± 20	817 ± 17
13,8	580 ± 21	617 ± 19	659 ± 18	692 ± 18	724 ± 23	773 ± 20	799 ± 18
9,6	558 ± 31	601 ± 23	634 ± 22	693 ± 26	741 ± 19	739 ± 27	799 ± 24
5,1	624 ± 48	584 ± 28	648 ± 28	660 ± 35	665 ± 28	709 ± 36	754 ± 31

TABLE 2. Total Interaction Cross Sections for Neutrons of Various Wavelengths with Superheated Benzene Vapors at Different Pressures, b

P. bars	Wavelength, \AA						
	13	14	15	16	17	18	19
17,9	1418 ± 115	1591 ± 66	1609 ± 69	1750 ± 63	1861 ± 64	1857 ± 61	1987 ± 67
14,5	1460 ± 60	1484 ± 58	1492 ± 56	1610 ± 57	1704 ± 56	1798 ± 58	1873 ± 63
11,1	1331 ± 58	1337 ± 54	1444 ± 56	1452 ± 63	1571 ± 64	1634 ± 60	1703 ± 64
4,9	—	1264 ± 103	1439 ± 106	1457 ± 113	1575 ± 113	1713 ± 108	1757 ± 102

Translated from Atomnaya Énergiya, Vol.42, No.1, pp.53-55, January, 1977. Original article submitted April 30, 1976.

This material is protected by copyright registered in the name of Plenum Publishing Corporation, 227 West 17th Street, New York, N.Y. 10011. No part of this publication may be reproduced, stored in a retrieval system, or transmitted, in any form or by any means, electronic, mechanical, photocopying, microfilming, recording or otherwise, without written permission of the publisher. A copy of this article is available from the publisher for \$7.50.

TABLE 3. Comparison of Various Ratios of the Coefficients C and Total Cross Sections for Different Light Water Vapor Pressures

K	C_1/C_k	σ_1/σ_k	C_2/C_k	σ_2/σ_k	C_3/C_k	σ_3/σ_k
2	1,022	$1,020 \pm 0,006$	—	—	—	—
3	1,042	$1,030 \pm 0,011$	1,018	$1,018 \pm 0,009$	—	—
4	1,065	$1,076 \pm 0,010$	1,041	$1,042 \pm 0,019$	1,022	$1,027 \pm 0,025$

TABLE 4. Comparison of Various Ratios of the Coefficients C and Total Cross Sections for Different Benzene Vapor Pressures

K	C_1/C_k	σ_1/σ_k	C_2/C_k	σ_2/σ_k	C_3/C_k	σ_3/σ_k
2	1,028	$1,054 \pm 0,013$	—	—	—	—
3	1,096	$1,150 \pm 0,011$	1,067	$1,092 \pm 0,013$	—	—
4	1,168	$1,170 \pm 0,022$	1,137	$1,108 \pm 0,010$	1,065	$0,99 \pm 0,02$

The present set of investigations was undertaken in order to detect this effect. The investigations were carried out with superheated light water and benzene vapors at a temperature of 513°K, and for four values of the pressure in each case. The range of neutron wavelengths was 13–19 Å in each case. The experimental apparatus is described in [5]. Results for the cross sections of water and benzene vapors are given in Tables 1 and 2.

The experimental results were processed as follows in order to obtain a quantitative estimate of the effect under investigation. The vapor densities ρ_c were calculated from the equation of state for an ideal gas, and the coefficients

$$C_k = (\rho/\rho_0)_k$$

were calculated, where ρ is the density of the real gas. Further, the ratio of the coefficients C_i/C_k was compared with the ratio of the measured cross sections σ_i/σ_k . The results are given in Tables 3 and 4. Thus, the total neutron cross section was shown to be a function of the gas pressure, and increased as the pressure increased. In light water vapors, the ratios σ_i/σ_k were observed to be in good agreement with the theoretical prediction in the quasi-ideal approximation (with the ratio C_i/C_k) [3], i. e., light water vapor (in the pressure range up to 18 kgf/cm²) is a weakly nonideal gas. The form of the spectrum for neutrons scattered by light water vapor is independent of the pressure, a particular result established in [1]. Intermolecular interactions in light water vapor (in the pressure range up to 18 kgf/cm²) do not change the intramolecular degrees of freedom, and only affect translational motion. All coherent effects and dynamic correlation effects in light water vapor are negligible up to a pressure of 18 kgf/cm². For benzene vapor the ratios σ_i/σ_k and C_i/C_k agree somewhat less well than for water; however, the total cross section continues to depend in the same general way on the degree to which the gas departs from the ideal.

LITERATURE CITED

1. G. Olsson, Arkiv Fys., **37**, Nos. 1–2, 85 (1968).
2. F. Sefidvash, in: Proceedings of Conference on Nuclear Structure Study with Neutrons, Budapest (1972), p.4.
3. A. Fulinski and M. Zcierski, Acta Phys. Polon., **34**, No. 5, 867 (1968).
4. A. Fulinski and M. Zcierski, Acta Phys. Polon., **34**, No. 6, 1037 (1968).
5. S. D. Stepanov et al., in: Neutron Physics [in Russian], Vol. 4, Sec. 4, Izd. FÉI, Obninsk (1974), p. 257.

CERTAIN CHARACTERISTICS OF A PERSONAL FILM DOSIMETER WITH "K" EMULSION

M. G. Gelev, M. M. Komochkov,
I. T. Mishev, Yu. V. Mokrov,
and M. I. Salatskaya

UDC 539.12.08

Neutron detectors with a sensitivity obeying the $1/v$ law are now frequently used to measure personal doses of intermediate neutrons. Such detectors are located on the human body. They detect primarily thermal neutrons backscattered from the human body (phantom) when exposed to neutrons in a wide energy range, including intermediate neutrons. Such detectors are called albedo dosimeters and the method, the albedo method [1-6]. Its fundamental parameter is the thermal albedo (β_t) defined as the ratio of backscattered thermal neutrons to the fluence of incident neutrons.

At the Joint Institute of Nuclear Research, type "K" nuclear emulsion 20μ thick in a corrective package [7] is used for personal neutron dosimetry; the emulsion is placed in one of the IFK-2, 3 magazine cells. The emulsion contains nitrogen, which makes it possible to detect thermal neutrons from protons formed in the $^{14}\text{N}(n,p)^{14}\text{C}$ reaction.

Gelev et al. [8] calculated the dosimeter sensitivity for different incident neutron energies using the β_t values [2]. Since new data are now available on the thermal albedo [4], we have decided to recalculate the sensitivity curve and to check it experimentally for two incident neutron energies.

The values of β_t used in these calculations were those cited in [4]. The dependence of β_t on the energy of incident neutrons [4] is shown in Fig. 1.

Figure 2 shows the dependence of sensitivity η of type "K" emulsion used as an albedo dosimeter (curve 2) on incident neutron energy calculated from the above data. A comparison of the obtained results with the data of [8] (curve 1) shows significant sensitivity differences and indicates that the obtained results must be experimentally verified. The values of β_t and η were checked with thermal and intermediate neutrons with an energy of about 30 keV. The data on β_t (Fig. 1) agree with the results obtained in [4] to within the experimental error.

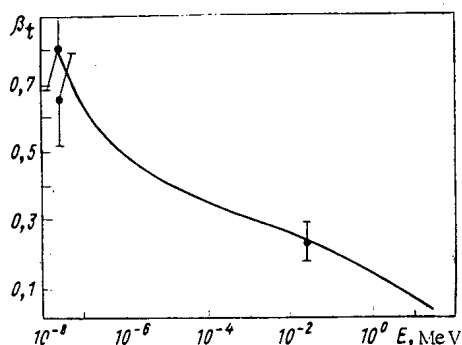


Fig. 1

Fig. 1. Thermal albedo as a function of incident neutron energy: \bullet) experimental values obtained in this work and in [4].

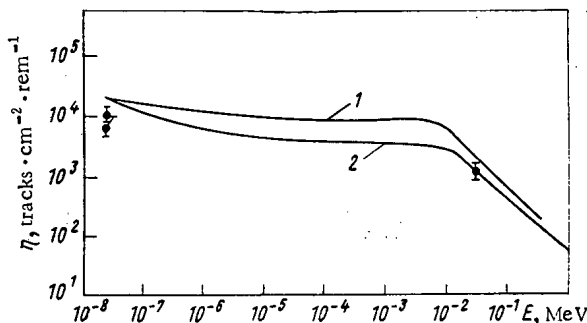


Fig. 2

Fig. 2. Sensitivity of type "K" emulsion used as an albedo dosimeter as a function of incident neutron energy: 1, 2) data of [8, 4]; \bullet) experimental results of this work.

Translated from *Atomnaya Énergiya*, Vol. 42, No. 1, pp. 55-56, January, 1977. Original article submitted May 10, 1976.

This material is protected by copyright registered in the name of Plenum Publishing Corporation, 227 West 17th Street, New York, N.Y. 10011. No part of this publication may be reproduced, stored in a retrieval system, or transmitted, in any form or by any means, electronic, mechanical, photocopying, microfilming, recording or otherwise, without written permission of the publisher. A copy of this article is available from the publisher for \$7.50.

The theoretical sensitivity of emulsion to thermal neutrons, which does not take into account the effect of the holder and the corrective package, is three times the experimental value obtained by exposing the holders to thermal neutrons on a phantom. It has been estimated that an IFK-2,3 holder with x-ray film and corrective package attenuates radiation by 50 to 60%. In addition, one has to take into account the survey efficiency (75 to 85%) and the loss of tracks in survey as a result of their small length and large angles (~10%). Taking into account these corrections indicates that the experimental and theoretical sensitivities of personal dosimeters to thermal neutrons are nearly equal. The value of η for neutrons with an energy of 30 keV has been obtained by irradiating the emulsion without the holder and corrective package, and to within the experimental error it agrees with the theoretical value. The experiments are described in detail in [9].

The calculations and obtained experimental results provided more accurate values of the sensitivity of personal dosimeters using "K" emulsion film as albedo dosimeters in the neutron energy range from 0.025 eV to 0.4 MeV. The dosimeter sensitivity has been found to be approximately one half of that formerly accepted in the 0.025 eV to 10 keV interval.

LITERATURE CITED

1. J. Harvey, Rep. CECB, RD/B-827 (1967).
2. J. Dennis, J. Smith, and S. Boot, in: Proceedings of the IAEA Symposium "Neutron Monitoring," Vienna (1967), p. 537.
3. P. Nagarajan and D. Krishnan, Health Phys., 17, 323 (1969).
4. J. Harvey, W. Hudd, and S. Townsend, in: Proceedings of the IAEA Symposium "Neutron Monitoring for Radiation Purposes," Vienna, 11, 199, Dec. 11-15 (1972).
5. D. Hankins, *ibid.*, p. 15.
6. E. Piesch and B. Burgkhard, *ibid.*, p. 31.
7. L. S. Zolin, V. N. Lebedev, and M. I. Salatskaya, At. Energ., 13, No. 5, 467 (1962).
8. M. G. Gelev et al., At. Energ., 34, No. 2, 118 (1973).
9. M. G. Gelev et al., Preprint JINR, R16-9749, Dubna (1976).

CROSS SECTIONS FOR THE FISSION OF ^{235}U AND
 ^{239}Pu BY 2-, 24-, 55-, and 144-keV NEUTRONS

K. D. Zhuravlev, N. I. Kroshkin,
 and L. V. Karin

UDC 539.173.4

The further development of contemporary ideas of nuclear structure, and the practical requirements of accurate nuclear physics constants for calculating fast reactors and the accumulation of nuclides require extensive research with monoenergetic neutrons. In addition to methods using accelerators and time-of-flight techniques, a method which has been widely used in recent years is based on the penetration of a continuous spectrum of reactor neutrons through filters of various elements whose total effective cross sections for the interaction of neutrons with nuclei show deep minima as a result of the interference of resonance and potential scattering.

Rather intense beams of monoenergetic neutrons with energies of 2, 24, 55, and 144 keV can be obtained with filters of scandium, iron, and silicon, respectively [1-3]. The monochromatism of the filtered beams was increased by using additional filters of Al, ^{10}B , S, and Ti which have little effect on the intensity of the main peak, but remove neutrons of other energies. The background of neutrons of other energies in a monochromatic beam was measured experimentally by adding to the filters other materials with appreciable cross sections at the energy corresponding to the minimum in the cross section of the filter. For a beam of 2-keV neutrons such a material is manganese with a strong resonance at 2.3 keV.

Translated from Atomnaya Énergiya, Vol. 42, No. 1, pp. 56-57, January, 1977. Original article submitted June 7, 1976.

This material is protected by copyright registered in the name of Plenum Publishing Corporation, 227 West 17th Street, New York, N.Y. 10011. No part of this publication may be reproduced, stored in a retrieval system, or transmitted, in any form or by any means, electronic, mechanical, photocopying, microfilming, recording or otherwise, without written permission of the publisher. A copy of this article is available from the publisher for \$7.50.

TABLE 1. Shaping and Characteristics of Filtered Beams*

E, keV	Flux density, neutrons/cm ² ·sec	Back- ground, %	Dimensions of filters, mm									
			main			auxiliary				for meas. of background		
			Sc	Fe	Si	¹⁰ B	Al	Ti	S	Mn	Ti	S
2	10 ⁷	9	900	—	—	—	—	10	—	30	—	—
24	1,6·10 ⁵	10	—	650	—	—	220	—	50	—	10	—
55	1,6·10 ⁶	15	—	—	800	5	—	—	230	—	40	—
144	10 ⁷	5	—	—	900	5	—	40	—	—	—	250

*Fraction of thermal neutrons 0.1%.

TABLE 2. Results of Measurements

Neutron energy, keV	$\sigma_f(^{235}\text{U}), \text{b}$	$\sigma_f(^{239}\text{Pu}), \text{b}$	$\sigma_f(^{239}\text{Pu})/\sigma_f(^{235}\text{U})$	
2	6,69±0,13	3,97±0,08	0,593±0,018	0,603±0,022
24	2,26±0,05	1,73±0,04	0,765±0,023	0,785±0,035
55	1,92±0,04	1,58±0,03	0,823±0,026	0,847±0,028
144	1,49±0,03	1,50±0,03	1,010±0,030	1,034±0,030
2,53·10 ⁻⁵	582,2±1,3*	742,5±3,0*[5]	1,275*	1,274±0,025

*Standard values.

The scandium (99.9%), iron (Armco), and silicon filters and the auxiliary filters 30 mm in diameter were placed in the shield of a horizontal reactor channel. At exit the neutron beam was shaped by a collimator made of a mixture of paraffin and boron carbide with an opening 20 mm in diameter and 1500 mm long for the extraction of the beam. The linear dimensions of the filters and the characteristics of the neutron beams are listed in Table 1. Neutrons with energies of 0.0253 eV were extracted by using a double-crystal neutron monochromator. By shuttering the beam of neutrons with 1 mm of cadmium the background of thermal neutrons was found to be 0.5%. The thermal neutron flux density was $2 \cdot 10^4$ neutrons/cm²·sec.

The cross sections for fission by neutrons of energy E were measured relative to the cross sections for the fission of ²³⁵U and ²³⁹Pu by neutrons of energy E₀ = 0.0253 eV, which are accurately known. Therefore, the number of fissions in the target and the number of thermal neutrons and neutrons of energy E incident on the target were recorded simultaneously. The ratio of the fluxes of neutrons of energy E and thermal energy E₀ was measured with a ¹⁰B neutron detector since the cross section for the ¹⁰B(n,α)⁷Li reaction is well known. Targets of ¹⁰B, ²³⁵U, and ²³⁹Pu 15 mm in diameter were deposited on 0.1-mm aluminum backings. The ¹⁰B target was made by vacuum deposition of a 0.3-mg/cm² film. A grid ionization chamber was used to record products of the ¹⁰B(n,α)⁷Li reaction, and a fission chamber of the type [4] to record fission fragments. The fission chamber and the grid ionization chamber were placed in the same working volume which was filled with argon to a pressure of 600 mm Hg. The chambers were constructed so that the targets of fissionable material and ¹⁰B were back to back and served as a common electrode of the chamber.

The measured fission cross sections of ²³⁵U and ²³⁹Pu are listed in Table 2. In determining the fission cross sections corrections were introduced for the isotopic composition of the targets and for the deviation of the ¹⁰B cross section from the 1/√E law [6,7]. Table 2 also lists the ratios $\sigma_f(^{239}\text{Pu})/\sigma_f(^{235}\text{U})$ calculated from the measured cross sections for the fission of ²³⁵U and ²³⁹Pu by neutrons with energies of 2, 24, 55, and 144 keV, and the values measured by direct comparison of the number of fissions in ²³⁵U and ²³⁹Pu targets and the number of nuclei in them, known to 1%. From this ratio the thermal fission cross section of ²³⁹Pu is $\sigma_{f_0} = 741.7 \pm 15.0$ b. The value obtained is in good agreement with that recommended in [5] and indicates the reliability of the present measurements. Table 2 shows that the cross section ratios obtained are in good agreement with one another. The measured fission cross sections agree rather well with published data [8-10].

LITERATURE CITED

- O. Simpson and L. Miller, Nucl. Instrum. and Methods, **61**, 245 (1968).
- E. N. Kuzin et al., At. Energ., **35**, No. 6, 391 (1973).
- R. Chrien et al., in: Proceedings of the Second International Symposium on Neutron Capture γ -Ray Spectroscopy and Related Topics, Petten, Sept. 2-6 (1974), p. 99.

4. F. Nasyrov and I. F. Pashkin, Prib. Tekh. Eksp., 2, 64 (1966).
5. Neutron Cross Sections, BNL-325, 3rd Ed. (1973).
6. M. Sowerby et al., J. Nucl. Energy, 24, 323 (1970).
7. R. La Bauve, Summary Documentation for B-10. LASL, 1971, in: ENDF/B Summary Documentation. BNL-17541 (ENDF-201) (1973).
8. I. Blons et al., in: Proceedings of the IAEA Symposium Nuclear Data for Reactors, Vol.1, Helsinki, June 15-19 (1970), p.469.
9. J. Blons, H. Derrien, and A. Michaudon, *ibid.*, p.513.
10. R. Perez et al., Nucl. Sci. and Eng., 55, 203 (1974).

POSSIBILITIES OF RECORDING THERMAL NEUTRONS WITH CADMIUM TELLURIDE DETECTORS

UDC 539.107.45

A. G. Vradii, M. I. Krapivin,
L. V. Maslova, O. A. Matveev,
A. Kh. Khusainov, and V. K. Shashurin

Much attention is currently being given to the development and application of cadmium telluride as a detector of ionizing radiations [1,2].

Since the material of cadmium telluride detectors contains ^{113}Cd , which has a large thermal neutron capture cross section, it is assumed that these detectors will have a high efficiency for recording thermal neutrons [3].

Estimates showed that the main mechanism determining the sensitivity of detectors to thermal neutrons is the recording of prompt capture γ radiation [4,5].

An experimental study was made of 5-400-mm³ detectors developed and fabricated at the A. F. Ioffe Physicotechnical Institute of the Academy of Sciences of the USSR. The main characteristics of the detectors studied are listed in Table 1. A standard Pu-Be source surrounded by a paraffin moderator yielded $3 \cdot 10^6$ neutrons/sec. The thermal neutron flux density in the moderator channel was monitored by a calibrated DTN-1 silicon detector. The pulses from the detector were amplified and shaped by a Langer amplifier and fed to an LR-4840 800 channel pulse-height analyzer.

Figure 1 shows typical spectra obtained in the recording of radiation in the moderator channel with detector No.25 with and without a 2-mm boron filter. Because of the ^{10}B content, the boron filter ensured practically

TABLE 1. Experimental Results

Detector characteristics	Detector number							
	11	25	B	2	AKh	6G	3G	A
Volume of sensitive region, mm ³	5	5	13	15.7	31	94	391	396
Surface area, mm ²	20	31	50	58.5	56.4	159	368	285
Energy resolution at E = 662 keV	28	24	*	60	*	*	*	60
Sensitivity of recording thermal neutrons, mm ² : in spectrometric regime at the 558-keV line in counting regime in the range, keV:	0,20	0,28	0,32	0,37	1,3	—	—	8,1
100 — 1500	12	11	24	21	46	67	200	210
400 — 1500	5,0	5,2	11	10	22	34	115	121

* Counting detector, energy resolution > 60 keV.

Translated from Atomnaya Énergiya, Vol.42, No.1, pp.58-59, January, 1977. Original article submitted June 16, 1976.

This material is protected by copyright registered in the name of Plenum Publishing Corporation, 227 West 17th Street, New York, N.Y. 10011. No part of this publication may be reproduced, stored in a retrieval system, or transmitted, in any form or by any means, electronic, mechanical, photocopying, microfilming, recording or otherwise, without written permission of the publisher. A copy of this article is available from the publisher for \$7.50.

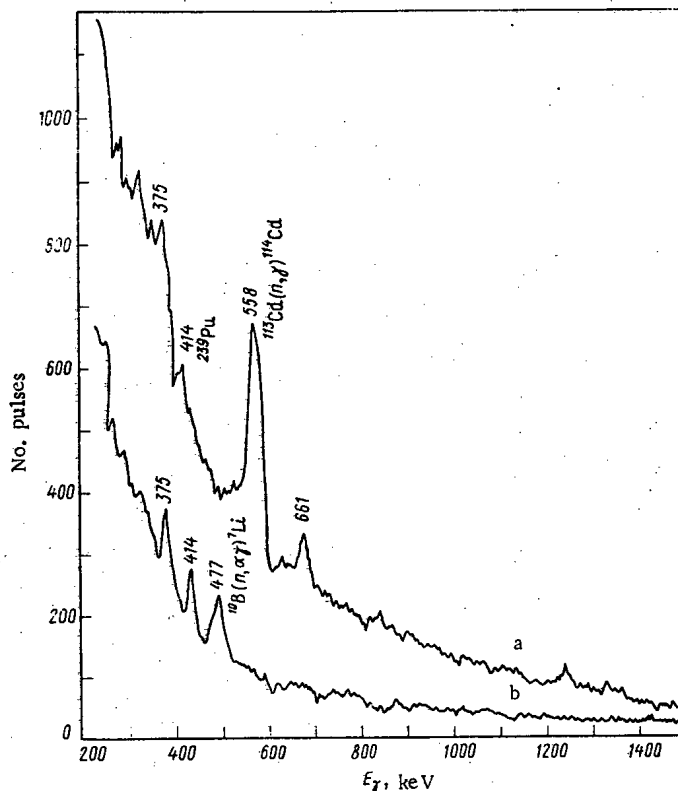


Fig.1. Pulse-height spectra from a Cd-Te detector in a γ -neutron field. a) Detector No.25 without filter; b) with boron filter.

complete absorption of thermal neutrons. In the absence of a boron filter, the peaks resulting from the recording of the 558- and 661-keV lines corresponding to the γ radiation accompanying the radiative capture of thermal neutrons by the ^{113}Cd are clearly identified in the spectrum. When the boron filter is present, the peaks in the spectrum resulting from the recording of capture radiation cannot be distinguished, but the shapes of the peaks corresponding to the 375- and 413-keV radiation from the ^{239}Pu in the neutron source are more clearly visible. The appearance of the peak corresponding to γ radiation of 477-keV energy is related to the recording of radiation accompanying the de-excitation of ^7Li nuclei formed in the interaction of neutrons with ^{10}B nuclei.

Information on thermal neutrons can be obtained by using cadmium telluride detectors in spectrometric and in counting regimes (Fig.1). In using detectors in the spectrometric regime to determine the characteristics of neutron fluxes it is expedient to employ the most intense 558-keV radiation.

Table 1 shows the results of measuring the sensitivity of detectors to neutrons in the spectrometric regime by the peak of the total absorption of 558-keV radiation, and in the counting regime for a different level of discrimination, the choice of which is important in the counting regime for more precise recording of thermal neutrons. The sensitivity of the detectors investigated to thermal neutrons increases as their volume is increased, and is practically independent of the surface area of the detectors. The disparity of the sensitivity measured in the spectrometric regime and the size of some of the detectors appears to be related to the incomplete collection of charge carriers in the sensitive volume, which makes more difficult the clear separation of pulses from the background of the distribution.

The increase of sensitivity to thermal neutrons with an increase in volume of Cd-Te detectors confirms that the recording of neutrons is related to the recording of capture γ radiation.

This is further confirmed by the similarity of the shapes of the pulse-height spectra obtained in recording thermal neutrons by detectors with and without cadmium filters (minus the background of γ radiation).

The Cd-Te detectors were rapidly removed from the neutron field and their induced activity was measured. A study of the nature of the time variation of the induced activity showed that the activation products did not contribute more than 1% to the sensitivity of the detectors to thermal neutrons.

A comparison on the research detectors with those manufactured by industry showed that in the counting regime the efficiency of the Cd—Te detectors was close to that of ^3He -filled and DTN semiconductor detectors. In the spectrometric regime the sensitivity is comparable with that of boron counters [6].

The effect of neutron flux in the spectrometry of γ radiation can be estimated by starting from the interaction mechanism described and the data presented, and comparing the sensitivity of Cd—Te detectors to the γ radiation being analyzed and to neutrons. The high efficiency of Cd—Te detectors in recording thermal neutrons and γ radiation opens up new possibilities for recording them simultaneously in mixed fields. Figure 1 shows that in the pulse-height spectrum obtained without a boron filter the peaks corresponding to the ^{239}Pu γ radiation and those due to the recording of thermal neutrons are clearly identified.

LITERATURE CITED

1. E. A. Ardad'eva et al., Dokl. Akad. Nauk SSSR, 221, 77 (1975).
2. L. Jones and P. Wollam, Nucl. Instrum. and Methods, 124, 591 (1975).
3. V. S. Vavilov et al., At. Energ., 28, No. 6, 505 (1970).
4. L. Groshev et al., Nucl. Data Tables, Vol. 5, Nos. 1-2 (1968).
5. B. S. Dzheleпов, L. K. Peker, and V. O. Sergeev, Decay Schemes of Radioactive Nuclei [in Russian], Izd. Akad. Nauk SSSR, Moscow (1963).
6. L. S. Gorn and B. I. Khazanov, Selective Radiometers [in Russian], Atomizdat, Moscow (1975).

TOTAL CROSS SECTION MEASUREMENT FOR
THE REACTION $T(t, 2n)^4\text{He}$

V. I. Serov, S. N. Abramovich,
and L. A. Morkin

UDC 539.172.14

Tritium is a possible fuel for thermonuclear reactors [1] so the nuclear reactions involving it at low energies of the interacting particles must be well known.

The cross section for the reaction $T(t, 2n)^4\text{He}$ has been measured previously at triton energies of 40–60 keV and above using a gaseous target [2,3]. However, the energy losses by tritons at the inlet windows were large (about 200 keV) so the experimental data at triton energies below 100 keV have large errors.

The differential cross section for this reaction at an angle of 0° with triton energies of 40–200 keV has been measured previously using thin scandium targets saturated with tritium [4]. In view of the differences in the form of the excitation function for the $T(t, 2n)^4\text{He}$ reaction at low triton energies (40–100 keV) [2,3,4], we have measured the differential cross section for this reaction at an angle of 0° for triton energies of 30–160 keV and measured the angular distributions of the emitted neutrons for triton energies of 55–80 keV.

The work was done using an electrostatic accelerator. The energy of the tritons was determined by the magnetic field strength of an analyzer which was calibrated at the resonance of the reaction $^{19}\text{F}(p, \alpha\gamma)^{16}\text{O}$ (proton energy of 340.4 keV). Flat response counters calibrated with a standard Ra— α —Be source were used as neutron detectors. The neutron yield from the $T(t, 2n)$ reaction was measured on a gaseous target with a thin entrance window of roughly $50 \mu\text{g}/\text{cm}^2$ aluminum oxide.

Films of aluminum oxide were obtained by etching a 0.1-mm-thick oxidized aluminum foil attached with BF-2 glue to a glass disk with a drilled hole 8–10 mm in diameter in hydrochloric acid. The 10-mm-diameter input windows for the gas targets prepared in this manner hold a pressure of 10–15 torr and are not destroyed at beam currents of about $10 \mu\text{A}$.

Dummy targets on which LiF targets were attached to determine the energy loss by accelerated particles at the inlet window of the gas target were placed inside and ahead of the target. The gas pressure was determined

Translated from Atomnaya Energiya, Vol. 42, No. 1, pp. 59–61, January, 1977. Original article submitted July 26, 1976.

This material is protected by copyright registered in the name of Plenum Publishing Corporation, 227 West 17th Street, New York, N.Y. 10011. No part of this publication may be reproduced, stored in a retrieval system, or transmitted, in any form or by any means, electronic, mechanical, photocopying, microfilming, recording or otherwise, without written permission of the publisher. A copy of this article is available from the publisher for \$7.50.

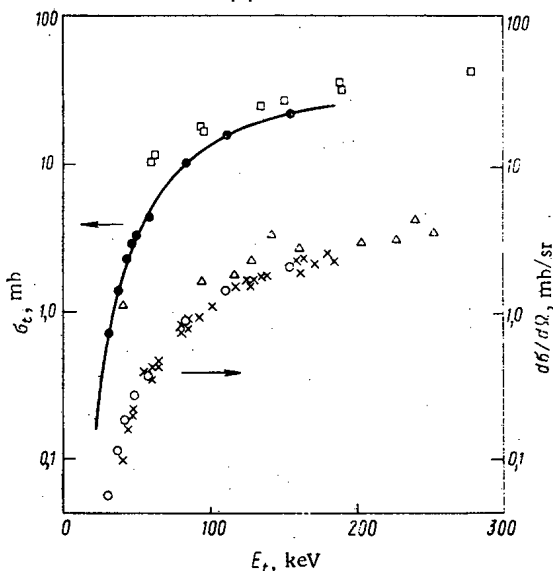


Fig. 1. Dependence of the total and differential (at 0°) cross sections for the reaction $T(t, 2n)^4\text{He}$ on triton energy: Δ, \square, \times data from [2, 3, 4] respectively; \bullet, \circ data for this work; \longrightarrow calculated using Eq. (1).

TABLE 1. Measured Neutron Yields and Triton Energies, keV

E_t^0	E_t	ΔE_t	δE_t	$\delta, \%$	$S(E) \cdot 10^{-22}, \text{cm}^2 \cdot \text{keV}$
60.7	34.2	5.9	± 2.3	13.9	1.84
66.1	39.8	5.6	± 2.1	11.0	2.00
81.6	45.7	5.8	± 2.5	9.9	1.98
76.2	49.8	6.0	± 2.0	6.7	1.98
89.1	53.3	6.0	± 2.4	8.2	1.88
98.9	61.4	6.1	± 2.5	7.6	1.61
126.5	86.5	7.8	± 2.6	6.4	1.69
134.9	113.7	7.7	± 2.6	6.2	1.58
189.9	159.8	8.9	± 2.2	6.0	1.40

with a mercury manometer. The tritium concentration was measured from the current in an ionization chamber initially calibrated at various pressures. The ionization chamber was always connected to the gaseous target volume. Tritium with a small deuterium content (about 0.02%) was used. The contribution of neutrons from the reaction $D(t, n)^4\text{He}$ was determined experimentally by measuring the neutron spectrum with a scintillation counter. Over the range of energies studied it was 6%.

The following measurement procedure was developed. After the airtightness of the gaseous target was verified the thickness of the beam input window was determined by the shift in the resonance of the $^{19}\text{F}(p, \alpha\gamma)^{16}\text{O}$ reaction with $E_p = 340.4$ keV on targets mounted ahead of and behind the input window. Then the background from false targets was measured with the target filled with helium. Then the gas target was filled with tritium and the neutron yield was measured with systematic checking of the gas pressure and ionization chamber current during the time of the measurement. Then the background measurement was repeated. After several of these measurement cycles at various triton energies the location of the resonance in the $^{19}\text{Fe}(p, \alpha\gamma)^{16}\text{O}$ reaction was measured to recheck the thickness of the input window. In the measurements it was found that the input window thickness increased due to formation of a carbon film. At the end of the measurements the thickness of the input window was again measured. The difference between the initial and later measurements of the film was assumed to be proportional to the number of bombarding particles incident on the target and was found by interpolation. To compute the energy lost by the tritons averaged experimental data for the slowing down cross sections of protons and tritons in aluminum, oxygen, and carbon [5-8] were used. The slowing down cross section for tritons at the lowest energies in aluminum were computed on the basis of [6, 7].

During the measurements it was found that the concentration of tritium in the gaseous target changed due to isotopic exchange. An appropriate correction was introduced for the change in gas pressure and tritium concentration.

The experimental data on the change in the neutron yield from the $T(t, 2n)^4\text{He}$ reaction are given in the table, where E_t^0 is the energy of the bombarding particles in front of the window of the gas target, E_t is the energy of the particles on entering the gas target, ΔE_t is the thickness of the gas target, δE_t and δ are the error in determining the energy at the entry to the target and the total random error in the measurement, and $S(E)$ is the astrophysical factor for the reaction cross section computed from the relation

$$N = 2n_1 n_2 S(\bar{E}) \int_{E_1}^{E_2} \frac{1}{E} \exp(-\beta_1/\sqrt{E}) \frac{1}{dE dx} dE.$$

Here N is the total neutron yield; n_1 is the number of target nuclei per cm^3 ; n_2 is the number of incident particles; E_1 and E_2 are the energy of the tritons at the entrance and exit of the gaseous target, respectively ($\bar{E} = (E_1 + E_2)/2$); dE/dx are the specific losses for tritons in tritium; $S(\bar{E})$ is the astrophysical factor for the reaction cross section; $\beta_1 = [2\pi e^2/\hbar] \sqrt{m}$, and m is the reduced mass of tritium.

The angular distributions in the neutron yield were measured at triton energies of 55 and 80 keV over angles from 0° to 150° . For $E_t = 80$ keV the angular distribution is described by the formula $N(\vartheta) = (15.7 \pm 0.6) + (1.1 \pm 0.5) \cos \vartheta$. For $E_t = 55$ keV the anisotropy in the neutron yield decreases by 5%.

From the table it is clear that a slight systematic reduction in $S(E)$ is observed as the triton energy is increased. Thus, its average value for $E_t = 60-114$ keV is 17% less than its average value for $E_t = 30-50$ keV. The experimental values of $S(E)$ obey the formula

$$S(E) = S(0) + \frac{dS}{dE} E. \quad (1)$$

The following values were obtained for the constants from a least squares analysis: $S(0) = (2.10 \pm 0.18) \cdot 10^{-22} \text{ cm}^2/\text{keV}$ (a possible systematic error of $\pm 5\%$ is taken into account) and $dS/dE = (8.8 \pm 1.6) \cdot 10^{-25} \text{ cm}^2$.

The results of a measurement of the total cross section of the reaction $T(t, 2n)^4\text{He}$ in this work and in [3] are shown in Fig. 1. From the figure it is clear that for triton energies $E_t \geq 140$ keV the experimental results are in good agreement. The smooth curve shows the computed variation of the cross section with parameters $S(0)$ and dS/dE .

Also given there are the experimental data on the differential transverse cross section at an angle of 0° for this reaction obtained by us and in [2, 4]. In this case as well the data of all the reports are in satisfactory mutual agreement for $E_t \geq 140$ keV. The observed deviations in the experimental data of [2, 3] at low triton energies are explained by the inaccurate determination of the energy of the interacting tritons.

The basic inaccuracy in the measurements was presumed to be in the determination of the energy of the tritons at the entrance to the gaseous target. The statistical measurement errors and the errors in determining the gas pressure and the tritium concentration were 1-5; ± 3 ; $\pm 5\%$, respectively.

Let us compare the cross sections for the mirror reactions $T(t, 2n)^4\text{He}$ and ${}^3\text{He}({}^3\text{He}, 2p)^4\text{He}$ at small energies. A similar energy dependence

$$\sigma(E) = \frac{S(0)}{E} \exp(-\beta_2 \sqrt{E})$$

is recommended in [10] for the total cross section of the second reaction (neglecting the second term of the expansion in the zeroth approximation) with an astrophysical factor equal to $S(0) = (50 \pm 5) 10^{-22} \text{ cm} \cdot \text{keV}$. From this it follows that the ratio of the astrophysical factors for these reactions will be $S(0)_{TT}/S(0)_{tt} = 24 \pm 2.6$. If we include the pre-exponential coefficient in the expression for the Coulomb barrier permeability, proportional to $z_1^2/z_2^2 = 4$, then the ratio of these factors will be $S'(0)_{TT}/S'(0)_{tt} = 6.00 \pm 0.65$.

This difference in the cross sections is due to the nuclear interaction and seems somewhat surprising. However, it can be qualitatively understood that these reactions involve three particles and that the interaction of the particles in the final state must be taken into account.

In the reaction ${}^3\text{He}({}^3\text{He}, 2p)^4\text{He}$ it is possible to form a quasistationary state of the ${}^5\text{Li}$ nucleus and a virtual state of two protons. In the $T(t, 2n)^4\text{He}$ reaction a quasistationary state of the ${}^5\text{He}$ nucleus and a virtual dineutron, $2n$, are formed in the final state. When a quasistationary state is formed the reaction cross section must be proportional to the integral [11]

$$\int_{E_0 - \Gamma}^{E_0 + \Gamma} \frac{\Gamma^2/4}{(\varepsilon - E_0)^2 + \Gamma^2/4} \varepsilon^{1/2} (Q - \varepsilon)^{1/2} d\varepsilon, \quad (2)$$

where ε is the relative energy of the interacting particles; Q is the reaction energy; E_0 is the energy of the quasistationary state ($E_0 = 0.96; 1.96$ MeV for ${}^5\text{He}$ and ${}^5\text{Li}$); $\Gamma/2$ is the width of the quasistationary state ($\Gamma/2 = 0.58; 1.5$ MeV for ${}^5\text{He}$ and ${}^5\text{Li}$).

Similar expressions may be written for other cases of virtual state formation.

In such a case the ratio of the factors for the cross sections for reactions involving the formation of ${}^5\text{He}$ and ${}^5\text{Li}$ may be equal to $S'(0)_{\tau\tau}/S'(0)_{tt} \approx 3.5$; while for formation of the ${}^5\text{He}^*$ and ${}^5\text{Li}^*$ systems, $S'(0)_{\tau\tau}/S'(0)_{tt} \approx 1-1.5$. From similar estimates for the cases of $2n$ and $2p$ systems being formed in the final state we find that the ratio of the factors will be

$$S'(0)_{\tau\tau}/S'(0)_{tt} \approx 10.$$

From this it follows that the contribution of the channels involving formation of ${}^5\text{He}^*$ and ${}^5\text{Li}^*$ must be small ($\delta < 0.4$) while the contribution of the channels with formation of ${}^5\text{He}$ and ${}^5\text{Li}$ may be $\delta \approx 0.6$. These estimates do not contradict the form of the proton and neutron spectra from these reactions [9,10].

LITERATURE CITED

1. V. Crocer, S. Blow, and C. Watson, in: Proceedings IAEA Symposium on Nuclear Data for Reactors - 1970, Helsinki (15-19 June, 1970), Vol. I, p. 67
2. H. Agnew et al., Phys. Rev., 84, 862 (1951).
3. A. M. Govorov et al., OIYaI Preprint, R-764, Dubna (1976).
4. Yu. V. Strel'nikov et al., Izv. AN SSSR, Fizika, 35, 165 (1971).
5. R. Wolke et al., Phys. Rev., 129, 2591 (1963).
6. J. Phillips, Phys. Rev., 90, 532 (1953).
7. S. Warschaw, Phys. Rev., 76, 1759 (1949); D. Kahn, Phys. Rev., 90, 503 (1953).
8. H. Reynolds et al., Phys. Rev., 92, 742 (1953).
9. C. Wong et al., Nucl. Phys., 71, 106 (1965).
10. M. Dwarakanath, Phys. Rev., 4, 1532 (1971).
11. A. I. Baz', Ya. B. Zel'dovich, and A. M. Perelomov, Scattering, Reactions, and Decay in Nonrelativistic Quantum Mechanics [in Russian], Nauka, Moscow (1966), p. 328.

JOURNAL OF COOPERATION

Meeting of Executive Delegates of COMECON Countries
on Isotope Production (SOP-76)

The meeting took place September 6-9, 1976 in Predal (Rumania). The delegates agreed upon proposals concerning further specialization in the manufacture of 50 isotopic preparates. The meeting also discussed the development and organization of production in the COMECON countries of new products that are now being imported.

In agreement with the operational schedule of the Planning Committee on the Uses of Atomic Energy of the COMECON, model monographs have been prepared on several radioactive pharmaceutical preparates. A list of general methods to be developed on the topic "Radioactivity," their executors, and time schedules have been ratified for 1977-1978.

The meeting discussed proposals on the subject "Unification of Regulations on the Preparation of Materials for Licensing the Use of Sealed Radiation Sources." The desirability of unified certificates on sealed sources has been stressed. The delegates approved the results and recommendations of the Meeting of Specialists conducted during SOP-76 on the cooperation of COMECON countries in the development of compositions for radioimmunoanalysis.

A preliminary agreement has been reached on the discussion of the following standards on "Radioactive Preparates" at the next meeting of the Commission in 1978-1980: 1) marking and certification; 2) gaseous krypton-85; 3) gaseous tritium; 4) tritiated water. At the same time, the meeting considered the desirability of and methods for the development of new regulations for marking labeled organic compounds to conform to international practice, and agreed upon a working schedule on this subject for 1977-1978.

The Session of the Committee of the Council of Science
and Technology — Radiation Engineering

The session took place September 7-10, 1976 in Debrecen (Hungary).

The council coordinated plans for the predicted developments in the basic fields of radiation engineering and technology to 1990, and submitted it for consideration before the next session of the council; approved the Soviet delegation's proposals for methodical recommendations in the field of dosimetry of radiation-engineering facilities using electron accelerators and in the unification of sanitary standards on their locations and operation. The council also approved the structure and unified technical specifications for radiation-engineering facilities: the technical parameters of the radiation process, the basic technical characteristics of the facility, the specifications of radiation sources, the requirements of radiation protection, automation systems, and transportation, and monitoring and measuring instrumentation and automatic devices; general specifications on construction, and on monitoring and measuring equipment. The council discussed the program of comprehensive research in standardization in radiation engineering. It coordinated the reports to be presented at the coming Symposium on Radiochemical Modification of Polymers (Poland, September 1977), put forward a working schedule of the council for 1977-1978, and worked out a preliminary agenda for the next session of the council.

Conference of COMECON Specialists on the Development
of Compositions for Radioimmunoanalysis

The conference took place September 8-9, 1976 in Predal (Rumania). The conference noted that considerable work is in progress on the development and manufacture of compositions intended, first of all, for the

Translated from *Atomnaya Énergiya*, Vol.42, No.1, pp.62-63, January, 1977.

This material is protected by copyright registered in the name of Plenum Publishing Corporation, 227 West 17th Street, New York, N.Y. 10011. No part of this publication may be reproduced, stored in a retrieval system, or transmitted, in any form or by any means, electronic, mechanical, photocopying, microfilming, recording or otherwise, without written permission of the publisher. A copy of this article is available from the publisher for \$7.50.

examination of donors in view of widespread cases of hepatitis, of compositions of triiodothyronin, carcino-embryonic antigen, phytoprotein, and others which can be used in prophylactic examinations of the population.

Conference of the Parties to the Agreement on Multilateral
Specialization and Cooperation in the Manufacture of
Isotopic Products

The conference took place September 10-11, 1976 in Predal (Rumania). The conference heard reports on the execution of primary and secondary orders, on product quality, re-export, etc. The parties coordinated proposals for expanding the list of specialized products, and refined and supplemented the technical specifications and parameters of some of these products.

Participants of the conference expressed satisfaction with the way the agreement is executed and stressed that the work of all negotiating parties on its realization brought appreciable results.

The Tenth Session of the Committee of the Council of Science
and Technology on Processing Irradiated Fuel of Atomic
Power Plants

The session and a meeting of specialists in the technology and construction of plants for regeneration of fuel elements of water-cooled water-moderated power reactors took place September 14-17, 1976 in Budapest (Hungary). The session heard reports of specialists from Hungary, GDR, Poland, Rumania, the USSR, and Czechoslovakia on the work done in the various countries in 1971-1975. In Hungary, anorganic sorbents have been investigated for the extraction of radioactive elements. The importance of further progress of studies in the GDR on the kinetics of extraction of uranium, plutonium, neptunium, zirconium, niobium, ruthenium, cesium, and iodine, and of expanding the studies to conditions with stronger phase mixing has been noted. Polish scientists successfully worked on new methods of extractant regeneration free from the formation of salt wastes. The possibility of using local petroleum fractions as tributylphosphate diluents in extraction technology is studied in Rumania. The Soviet delegation reported on advances in extraction processing of spent fuel elements of water-cooled water-moderated power reactors with short cooling times and on the devising of various extraction equipment (mixer-settlers, pulsating columns, centrifugal extractors). Czechoslovak workers proved the possibility of selective extraction of cesium and strontium, and of trivalent actinide elements with the aid of a cation exchange extractant of a new kind.

The council and conference approved the trend to specialization in the discussed works and stressed the desirability of further concentration of efforts of specialists of the various countries on problems which are expected to yield original results.

Technical tasks in the working schedule for 1976-1980 in the discussed field have been approved.

The preparation of an experiment on comparing the results of determination of elements in solutions of the spent fuel elements of atomic power plants has been discussed. The plan of the experiment prepared by GDR, Soviet, and Czechoslovak specialists and the schedule of the first stage of the experiment have been agreed upon.

The committee reviewed and coordinated the operating schedule of the Planning Committee on the use of Atomic Energy in the COMECON countries on the processing of irradiated atomic fuel for 1977-1978, and redefined the schedules for certain subjects for 1976-1980.

The Seventh Session of the Committee of the Council of Science
and Technology on Nuclear Research Reactors

The session took place in Piestiany (Czechoslovakia) September 27-October 1, 1976. Participants of the session discussed and approved a proposed report on the work of the council and on the results of investigations in the subject "Design and Improvement of Nuclear Research Reactors and Their Use in Reactor Physics and Engineering Research." The session heard a report of Hungarian specialists on the results of a conference of COMECON countries on training personnel for atomic engineering, and agreed upon a plan of cooperation on the topic "Use of Low-Power Research Reactors, and Critical and Subcritical Assemblies for Training Personnel for Reactor and Nuclear Power Engineering." Various fields of cooperation between the

COMECON countries and the IAEA were planned for 1976-1980. A project of a schedule of the council on nuclear research reactors has been approved.

The Tenth Session of the Committee of the Council of
Science and Technology on Fast Reactors

The session took place October 4-8, 1976 in Kiev (USSR). The session discussed the execution of the plan on the topics "Investigation of Fast-Neutron Reactors" scheduled for September 1975 to August 1976.

Participants of the session approved the proposals of Soviet specialists on the creation of a common experimental base for the design of equipment and instrumentation of fast sodium-cooled reactors.

The specialists discussed and approved the proposals of the Soviet delegation on the cooperation in 1976-1980 in the introduction of high-power, sodium-cooled fast reactors after 1980.

The schedule of the work of the council in 1977-1978 has been discussed and coordinated. The session discussed the preparation of a conference of COMECON specialists on the subject "Problems of Technology and Corrosion in Sodium Coolant and Protective Gas" which is planned to take place in Dresden (GDR). A supplementary plan has been agreed upon on nuclear data studies which are carried out for the council. A plan for further studies in the development of methods and programs for physical calculations in fast reactors has been discussed and coordinated with the participation of scientists of various countries.

The Twenty-Third Meeting of the Working Group on Reactor
Science and Engineering and on Atomic Power of the Planning
Committee on the Uses of Atomic Energy of the COMECON

The meeting took place October 5-8, 1976 in Ostrava (Czechoslovakia). Its participants heard a report of the Secretariat on the resolutions of the 14th Session of the COMECON Committee on Scientific and Technical Cooperation associated with the preparation of proposals of long-term programs for cooperation in the provision of economically justified needs of COMECON member countries with the principal kinds of energy, fuel, and raw materials. The Working Group recognized the need of beginning the preparation of technical and economical grounds for the problem.

A list of subjects the work on which is to be carried out separately by agreement between the various countries has been discussed and coordinated.

Reports of Polish and Czechoslovak specialists have been heard and discussed on cooperation in the use of VVÉR-440 water-cooled water-moderated power reactors in nuclear thermal power plants. The possibility of cooperation of COMECON member countries in the development of a reactor plant for an atomic boiler has been discussed. The Working Group plans a seminar devoted to this topic to be conducted in 1977. Proposals on the cooperation in predicting the development of nuclear energy in the COMECON countries have been considered and the principal directions of work on this subject have been determined.

INFORMATION: SEMINARS, CONFERENCES, AND MEETINGS

SOVIET-FRENCH SEMINAR ON FAST REACTORS

P. L. Kirillov

A Soviet-French seminar on "The conception of errors in fast-reactor layouts, and the construction of the basic equipment and auxiliary systems" was held in France in June, 1976. Each side presented 10 papers and reports. The papers presented by the French specialists were concerned with the equipment of the Super Phoenix reactor now under construction (fuel recharging system, control and safety rods, heat exchangers, pumps, and sodium purification systems). They considered methods of strength calculations for reactor assemblies as well as welding of tubes with tube plates for heat exchangers and steam generators. Observations were made about the construction of a fast reactor following Super Phoenix.

The papers delivered by the Soviet specialists were devoted in the main to the equipment of the BN-600 reactor and analysis of the layouts of the BN-350 and BN-600 and a future fast reactor.

The French program provides for the early development of a breeder reactor that would be economically competitive with thermal reactors and organically fueled power stations.

The successful start-up of Phoenix, with a power of 250 MW(E), was a stimulus for the construction of the larger Super Phoenix reactor with a power of 1200 MW(E); the designing has now been completed and a decision has been made to go ahead with its construction. However, the ultimate economic indices (according to the results of the construction, design, and research work) of an atomic power plant with such a reactor, as noted by the designers, are still somewhat inferior to those of atomic power plants with water-moderated water-cooled reactors. The latter circumstance has served as a stimulus for improving the characteristics of Super Phoenix in order that it may be the basis for developing a much more powerful reactor, Super Phoenix 2 (1800-1900 MW), which will not be economically inferior to other electricity-generating facilities. Plans call for the construction of Super Phoenix 2 on the Saône River (5-6 units) without the participation of foreign capital but with the involvement of companies from the German Federal Republic (GFR) and Italy.

A characteristic of the general concept of creating commercial fast reactors is that of using an integrated layout. The French specialists do not deny that neither of the two layouts (integrated, loop) considered at the present time have any significant advantages. The decisive factor in the choice is the experience gained in the design, start-up, charging, and operation of demonstration reactors. Such experience has been accumulated in France as a result of the successful operation of Phoenix with integrated layout. However, even within the framework of such a design there is a large number of alternative solutions. The following were adopted as the most important for Super Phoenix (see Fig. 1).

The reactor tank is suspended by the top from a strong bearing plate, and the heat-exchanger installation is mounted on the sliding support of the pumps on the bearing plate. No in-pile storage is provided for spent fuel assemblies (FA). Consideration was given to unloading spent FA with an after heat of 20 kW from the active zone into an external storage (drum) in a sodium-filled cylindrical case. These are also transported in sodium-filled containers (the heat release of each FA is up to 10 kW).

Graphite is completely excluded from the neutron shielding and is replaced by steel. This is explained by: firstly, the considerable swelling irradiated graphite experiences when it comes in contact with sodium (if the can is unsealed, when the graphite rod is disturbed), which leads to rupture of the can; and, secondly, the increase in the spacing between the active zone and the heat exchangers, as a result of which a sodium layer in combination with steel constitutes effective shielding.

The reactor has no high-speed automatic mechanisms which act on the flow rate. The response time of the slide valves cutting off the flow through pump (check valves were rejected) and heat exchanger is 30-40 sec; the latter are operated by a remote-control manual actuator only if the reactor has been shut down.

Translated from Atomnaya Énergiya, Vol.42, No.1, pp.64-65, January, 1977.

This material is protected by copyright registered in the name of Plenum Publishing Corporation, 227 West 17th Street, New York, N.Y. 10011. No part of this publication may be reproduced, stored in a retrieval system, or transmitted, in any form or by any means, electronic, mechanical, photocopying, microfilming, recording or otherwise, without written permission of the publisher. A copy of this article is available from the publisher for \$7.50.

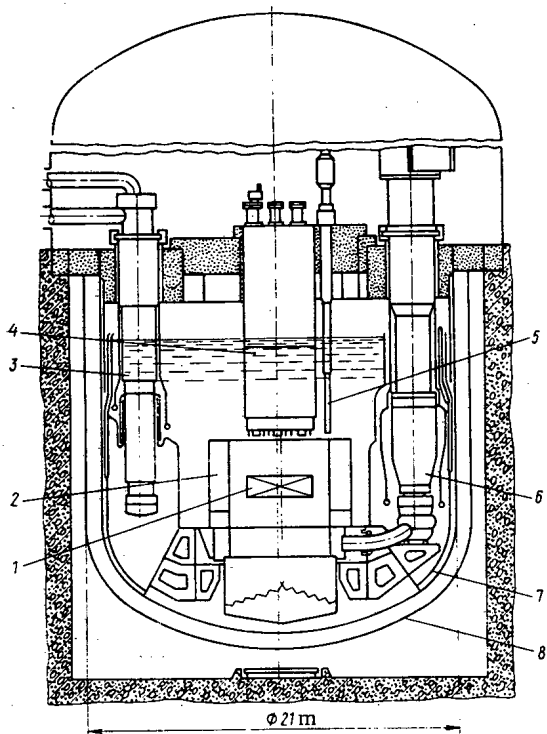


Fig. 1. Diagram of layout of assemblies in the Super Phoenix reactor; 1) active zone; 2) neutron shielding; 3) intermediate; 4) central column; 5) recharging mechanism; 6) primary-circuit pump; 7) reactor vessel; 8) safety housing.

There was a discussion of the various kinds of units and interlocks effecting the automatic transition of the reactor from one set of operating conditions to another. If any pump in the primary or secondary circuit is damaged, the reactor is shut down, the pertinent pump or heat exchanger is cut off, and the reactor is then put at the appropriate power level. It is felt that false responses due to the large number of interlocks are safer than shutdowns as a result of the failure of the basic equipment.

The neutron shielding in the upper part of the fuel assembly is acknowledged to be rational from the point of view of reducing the shielding outside the side shield. However, French specialists are working to produce a packet with dismountable upper shielding suitable for repeated use.

The hydraulic system used has a general collector at the heat-exchanger outlet and the inlet of the pumps. In this system the heat exchangers and pumps function independently; the shutdown of one primary-circuit pump does not entail the shutting down of the corresponding intermediate heat exchangers, secondary-circuit pump, and steam generator (as is the case in the BN-600).

Because of the choice of a rational system for cooling the reactor tank and guided convection in the hot and cold zones of the tank, a comparatively small heat transfer is ensured in the shell separating the cold and hot zones; as a result, more acceptable operating conditions are created for it. Radioactive systems outside the reactor are practically completely eliminated by the placement of all units of the primary circuit, and even the cold traps, inside the reactor tank. Inside the tank is heat insulation consisting of a large number of layers of steel mesh, arranged on the upper bearing plate and the walls of the vessel in an inert-gas medium.

The argon pressure in the gas cavity of the reactor is very low, 0.05 kgf/cm^2 (0.5 kgf/cm^2 in the BN-600).

With allowance for the swelling of the structural materials, the gap between the packets has been increased to 7 mm (the "wrench" size of the hexahedron is 180 mm). During recharging the upper part of a bent packet may deviate from the vertical by 61 mm. The sodium temperature at its outlet is monitored by thermocouples (three thermocouples above each packet). The thermocouples can be replaced during the operation of the reactor.

Further reduction of the costs of an atomic power plant is connected with a reduction in the metal intensity of the assemblies. This is explained to some extent by the transition to the frame construction of the steam generator. As for the reactor, attempts are being made to reduce the size of the vessel (or to significantly increase the power in that vessel) through the rational layout of elements inside the tank, reduction of their number (consolidation), combination of a number of elements (combined pump-heat exchanger unit), changes in the characteristics determining the dimensions (rpm's of pumps, and intermediate heat exchangers), etc.

The Soviet delegation visited the Rhapsodie and Phoenix reactors. A maximum burn-up of 18% was attained with mixed oxide fuel in six fuel elements of Rhapsodie (maximum can temperature 700°C, thermal load 430 W/cm). A small rotating sample will be reconstructed and a new thermometric grid will be established, two thermocouples being installed for each FA to monitor the sodium temperature at the outlet of each fuel assembly. As of June 18, 1976, the power plant with the Phoenix reactor had produced 3.2 billion kW·h of electricity at a cost of 3.5 centimes/kW·h. During the visit to the reactor fuel recharging was under way and the throttle assembly on one of the steam generators was being inspected.

The delegation was also shown two groups of experimental stands in Cadarache and in Grand Quévy (near Rouen).

The seminar enabled specialists to exchange scientific and technical information, and to compare engineering solutions adopted in our country and in France in the development of fast reactors. The consensus was that this had been an extremely useful exchange.

SOVIET—AMERICAN SYMPOSIUM ON FUSION—FISSION REACTORS

V. I. Pistunovich and G. E. Shatalov

A symposium on fusion—fission systems was held at the Lawrence Livermore Laboratory (California) July 13-16, 1976. Twenty-three papers devoted to the physics, technology, and economics of hybrid fusion (or thermonuclear) reactors were presented. Separate discussions were held on the economics of hybrid systems, on the structural designs of various types of reactors, the design of the reactor blanket, safety of reactor operation, and protection of the environment. The American party presented plans for financing the development of projects of hybrid reactors in the USA by both federal organizations (ERDA) and individual firms.

The hybrid fusion reactor is a system in which 14-MeV neutrons produced during the fusion of deuterium and tritium nuclei are used for fission of nuclear raw materials and for producing fissionable isotopes. The vacuum chamber of the fusion reactor is enveloped by a blanket, containing ^{238}U or ^{232}Th , where the bulk of the heat is generated and nuclear fuel is produced. The symposium heard about projects for hybrid reactors based on various fusion devices: open traps, tokamaks, and systems with laser ignition, θ -pinch, and solenoids. All the papers noted that their advantage lies in the possibility of producing a large quantity of fissionable isotopes (^{239}Pu and ^{233}U) for subsequent burning in thermal reactors. A hybrid reactor can yield 700-1000 kg plutonium a year per 1000 MW(T), which is, e.g., 10 times as much as produced by a present-day breeder reactor of the same power, and 3-4 times the possible yield, in principle, of fast breeder reactors. Most projects use natural or depleted uranium in the blanket.

A reactor project based on an open trap was presented by the Lawrence Livermore Laboratory. It considered a modification of spherical blankets for the production of plutonium and ^{233}U . The blanket was designed in spherical form so as to ensure uniform irradiation of the nuclear fuel and to make for easy dismantling. The combination of a hybrid reactor with a water-moderated water-cooled reactor produces electric energy at a cost of about 2.5 cents per kW·h, which is comparable with the cost in the nuclear power industry in the immediate future. The basic design of this reactor is being developed by General Atomic.

The Princeton Plasma Physics Laboratory presented a group of papers on a hybrid reactor based on the tokamak. The plasma parameters are similar to those of the TFTR which is to be built in 1980. The neutron radiated power from the plasma, 0.75 MW/m², is sustained by the injection of 180-keV deuterons. The papers paid much attention to the construction of a divertor for removing contaminants from the plasma.

A paper on the development of a reactor to burn actinides was presented by Westinghouse. The idea of burning radioactive waste and at the same time generating power is an interesting one, but efficient burning requires a high density (up to 10 MW/m²) of the neutron radiation from the plasma. Papers from this area of research are to be presented.

Translated from *Atomnaya Énergiya*, Vol.42, No.1, pp.65-66, January, 1977.

This material is protected by copyright registered in the name of Plenum Publishing Corporation, 227 West 17th Street, New York, N.Y. 10011. No part of this publication may be reproduced, stored in a retrieval system, or transmitted, in any form or by any means, electronic, mechanical, photocopying, microfilming, recording or otherwise, without written permission of the publisher. A copy of this article is available from the publisher for \$7.50.

The Los Alamos and Livermore laboratories presented projects for hybrid fusion reactors based on laser ignition of the target as well as papers on the parameters of such reactors based on θ -pinch and a solenoid with plasma heating by a relativistic electron beam or a laser. The proposed variants provide an opportunity to consider a reactor of convenient geometric form and not very high power level. Thus, a pulsed reactor developed by the Livermore Laboratory has an output electrical power of 400 MW at a total thermal power of 1400 MW and can produce 1.3 tons of plutonium a year. The drawback of most pulsed systems is that a large electrical power circulates in the internal circuit.

Papers presented by the I. V. Kurchatov Institute of Atomic Energy considered problems of the choice of optimal plasma and neutron-physical parameters of hybrid reactors and studies on the possible use of modules in the projected DTRT (T-20) unit.

A lively discussion took place during the symposium on the economic indices of hybrid reactors and the choice of the fuel cycle. Regardless of the fact that the cost of an electric power plant with a hybrid fusion reactor is 1.5-2 times that of an atomic power plant with a breeder reactor, the combined power generation by hybrid fusion and thermal reactors is just as economical (according to price of power plant) as power generation by fast and thermal reactors. Appreciable advantages of the hybrid reactor are the possibility of burning a significant quantity of ^{238}U without recharging fuel, operation with natural or depleted uranium, and the absence of limitations on fuel doubling.

The final outcome of the symposium is a conclusion about the promise held out by the use of hybrid reactors as producers of fuel for thermal reactors while at the same time generating electricity. The reduced requirements with respect to plasma characteristics make it possible to count on the construction of the first commercial hybrid reactors by the end of the century. The type of fusion unit and the range of the optimal parameters of such a reactor will have to be chosen in the near future. It is proposed to discuss these topics at the next symposium.

EIGHTH INTERNATIONAL CONFERENCE ON NONDESTRUCTIVE TESTING

V. V. Gorskii

The eighth international meeting was held in Cannes (France) September 6-10, 1976, with 1245 specialists from 35 countries attending. The plenary and section meetings heard more than 260 papers on practically all methods of nondestructive testing of structural materials, finished products, and equipment in service. However, the majority of the papers were devoted to the theory and practice of methods based on the application of ultrasound, acoustic emission, penetrating emissions, and electromagnetic fields. The subject matter of the papers reflected the main directions in the development of nondestructive testing techniques; increased reliability and accuracy of the techniques; use of computers for gathering, processing, and storing results; mechanization and automation of testing processes; etc. A comparatively large number of papers considered the techniques and technical means of nondestructive testing for the needs of atomic engineering.

Active Zone of Nuclear Reactor. The accelerated development of the nuclear power industry is linked with a significant increase in the production of extremely thin-walled tubes for fuel-element cans. An ultrasonic unit developed in France makes it possible to carry out the flaw detection and check the geometric dimensions of such tubes at one pass. A distinctive feature of this apparatus is that the tube moves progressively whereas the ultrasonic sensors remain immobile. The capacity of the unit is 8-15 times that of units used for the purpose at present. Interesting data were given about the application of computers in the ultrasonic testing of extremely thin-walled tubes when, in addition to their own functions, the computers also perform the functions of the operator (Denmark).

Translated from *Atomnaya Énergiya*, Vol.42, No.1, pp.66-68, January, 1977.

This material is protected by copyright registered in the name of Plenum Publishing Corporation, 227 West 17th Street, New York, N.Y. 10011. No part of this publication may be reproduced, stored in a retrieval system, or transmitted, in any form or by any means, electronic, mechanical, photocopying, microfilming, recording or otherwise, without written permission of the publisher. A copy of this article is available from the publisher for \$7.50.

The stability of fuel elements depends to a significant degree on the quality of the light welded joints. From this point of view an apparatus of practical interest is a 10-MHz one for testing the welded joints of fuel elements in zirconium-alloy cans. With this apparatus it is possible to detect pores of more than 0.2 mm in diameter and zones of poor fusion measuring more than 0.06-0.08 mm in a seam root (France).

A detailed paper was delivered on the technique of inspecting defects, the content and distribution of ^{235}U , thermal conductivity, and distribution of mass along the length of a hexadecagonal fuel element ("wrench" size 12.7 mm, diameter of axial aperture 2.5 mm, length 1.22 mm) based on graphite with fissionable material in the form of a solid solution of uranium carbides with zirconium, designed for operation at 2750°K and a specific power of 4500-5000 MW/m³ (USA).

Neutron radiography has come into increasing use in recent years for studying the condition of irradiated fuel elements. Therefore, particular interest was aroused by a paper containing comparative data about the accuracy with which the diameters of the pellets and radial gaps in fuel elements are measured by radiographic and neutron-diffraction methods, conducted on unirradiated simulators of fuel elements in zirconium cans. Detection of damaged fuel elements in a packet (without dismantling it) was the subject of two papers by American specialists. They reported on the results of research on the detection of fuel elements with defects on simulators of fuel-element assemblies of FFTF and EBR-II fast reactors by neutron-diffraction methods. In assemblies containing ~100 fuel elements it will be evidently possible to detect fuel-element damage. Neutron radiography is also employed in France to inspect working gaps in thermoelectric elements and to determine the hydrogen content in zirconium getter pellets.

Channel-type reactors require apparatus for periodically monitoring the state of the channel tubes. In Canada, longitudinal defects in zirconium-alloy channel tubes in CANDU reactors are detected by an apparatus which has an ultrasonic head with four scanners to move axially, testing a channel tube over its entire perimeter and length (6.5 m) at the rate of 6 m/min during reactor shutdown. Defects of a depth of more than 0.12 mm are detected.

Heat Exchangers. The eddy-current method has found most extensive application in monitoring the state of tubes in heat exchangers in use. Inspection at two or three frequencies makes it possible to enhance the sensitivity to defects in tubes against the background of interference (GFR). Preliminary investigations have been carried out in the USA on ultrasonic testing (from inside tubes) for defects in two-layered tubes, with an inside diameter of 27.6 mm and a wall thickness of 4.6 mm, used in building steam generators for the EBR-II fast reactor. Butt welds in heat exchangers are successfully inspected by the radioisotopic method. A portion of ^{170}Tm measuring 0.5×0.5 mm (half-life 128 days) is inserted into the tube, which has an inside diameter of 14 mm. Panoramic radiography of the welded joint is carried out in six minutes. Pores of diameter greater than 0.18 mm are detected in this way (Great Britain). For these purposes the Baltieu Co. (Belgium) has developed the Nuclex apparatus with panoramic x-ray tube with an external movable anode of outside diameter 12 mm (operating voltage 70-90 kV, focal-spot diameter 0.1 mm).

Reactor Vessel and Structural Elements. As is well known, great difficulties are encountered in the ultrasonic testing of welded joints in components made of austenitic stainless steel. To detect hot cracks in the process of multipass welding of thick-walled tubes during fabrication of atomic power plant equipment, the Guard Co. (USA) irradiates the cracks with acoustic emission. In the Federal German Republic, equipment has been constructed for ultrasonic fault detection of welded seams in the primary circuit of the SNR300 fast reactor; this circuit is made of the austenitic steel Kh6CrNi1811. The inspection is carried out with several inclined scanners operating at 1-2 MHz. Some papers noted the advantages to be gained by employing inclined separate and combined scanners for these purposes (Austria, GFR), and in a number of cases combined or even focused scanners (France, Japan).

Papers presented at the conference also considered the pros and cons of systems developed for testing reactor vessels from the outside (USA, Sweden) and from the inside (GFR, France, Japan, Great Britain, USA). Quite a large amount of experimental material has been accumulated on the acoustic-emission testing of structural elements of the reactors of atomic power plants at Calvert Cliffs (USA), Fessenheim (France), and a boiling reactor in Sweden. The capabilities of the methods for periodic inspection of the primary contour have been well verified and it is now being put into practice. In coming years operating reactors will be equipped with systems for acousto-emission inspection of medium complexity and those to be constructed, with more complex systems. A characteristic feature of the conference was the quite large number of papers on the acousto-emission method of monitoring diverse phenomena which occur during testing of materials (phase transformations, mechanical and thermal effects, corrosion, etc.).

Of great interest to specialists were the papers on the determination of the origin and geometric dimensions of defects detected by various methods (USSR, France, GFR, USA, Czechoslovakia, Polish People's Republic, Bulgarian People's Republic, etc.), the electromagnetic stimulation of ultrasonic vibrations in testing rods (Great Britain), on the determination of grain size by ultrasonic techniques (GFR), on the monitoring of the ferrite content in austenitic steels (Bulgarian P. R.), on an ultrasonic method of monitoring the degree of cold strain, depth of the hardened layer, and surface roughness (France), and many other applications.

As before, radiation methods occupy the leading position among nondestructive testing methods. Almost one-fifth of the papers at the conference were devoted to questions of the theory and practice of the method.

In recent years, much attention has been paid to the automation of the testing processes. An example of the comprehensive solution of the problem is the ultrasonic apparatus constructed by the Krautcrämer company (GFR) for quality inspection of thick plates. The apparatus incorporates all the latest achievements: self-adjustment of the testing zone, automatic control of the sensitivity with the depth of the defect, use of a computer, etc. An original automatic unit for ultrasonic detection of flaws in welded seams in flat structures with digital printout of the results of the testing has been developed in Japan. Many papers gave the technical specifications of automated equipment for testing rolled metal (USSR, USA, Japan, GFR, France, Great Britain, etc.).

A large exhibition of nondestructive testing equipment was organized for the conference delegates. Sixty of the leading companies of Western Europe, the USA, and Japan displayed all sorts of functioning equipment (built mainly as modules), apparatuses and auxiliary equipment for nondestructive testing. Digital readout of the quantity tested and graphical display of the results of the inspection are employed in the apparatus. High quality of manufacture and an eye-pleasing external appearance are features of the apparatus.

On the whole, the conference proceeded in an organized and businesslike manner. Note should be taken of the great attention which the French members of the organizing committee paid to the Soviet delegation.

Meeting during the conference, the International Committee on Nondestructive Testing decided to hold the next conferences in Australia in 1979 and in the USSR in 1982.

CHEMICAL EQUIPMENT AT 'ACHEMA-76 EXHIBITION

S. M. Karpacheva

The purpose of the international exhibition which was held June 21-26, 1976 in Frankfurt-am-Main (GFR), was to demonstrate the newest chemical equipment apparatus in order to complete commercial transactions. All the major manufacturers of such equipment participated.

The latest equipment presented at the exhibition contained a wide assortment of nonmetallic materials such as ordinary and metal-reinforced plastic, fiber plastic, and glass. The Quickfit company (GFR), e.g., showed 5-m³ glass reactors and columns of 1-m diameter. Also shown were compensators made of metal-reinforced rubber and gates closing the flow passage by squeezing a segment of tube of the same material.

As the exhibition showed, particular attention is being paid to the development of installations and apparatus for environmental protection and for building closed technological systems. The Krauss-Maffei company has analyzed the production technology of several thousand chemical products and developed "closed systems" on this basis. A large number of absorbers were proposed for air purification, the most interesting being a Multiventuri scrubber for trapping dust and a fountain scrubber made by Steiler (GFR), for removing NO, HCl, and HBr from air at $D = 1 \text{ m}$, $H_{st} = 0.6 \text{ m}$ 1000 m³/h. The quality of purification is monitored by monitoring and measuring instruments which were well represented at the exhibition.

Translated from *Atomnaya Énergiya*, Vol.42, No.1, pp.68-69, January, 1977.

This material is protected by copyright registered in the name of Plenum Publishing Corporation, 227 West 17th Street, New York, N.Y. 10011. No part of this publication may be reproduced, stored in a retrieval system, or transmitted, in any form or by any means, electronic, mechanical, photocopying, microfilming, recording or otherwise, without written permission of the publisher. A copy of this article is available from the publisher for \$7.50.

Wastewater from plants of various companies is purified according to a scheme incorporating concentration by precipitation, ion exchange or flotation, and filtration and subsequent combustion of the precipitates. This is the scheme by which the BASF company (GFR) operates an installation with a throughput of $10^6 \cdot \text{m}^3/\text{day}$ for the purification of effluents from the company plants in two cities — Ludwigshafen and Friedentahl. For the first operations the companies usually employ standard equipment, and various designs of special-purpose circuits are proposed for combustion. Ion exchange is ensured by ion-exchange resins of helium and macroporous structure, the assortment of which runs to more than 150 brands. An interesting continuously operating installation for effluent purification with activated carbon is produced by the Chiyeda Company (Japan). Sorption is by means of a pseudoliquefied layer of carbon flowing through a plate column; the carbon is regenerated thermally. There also is an evaporation apparatus of special design which ensures distillation purification of water by a factor of 10^6 to 10^7 .

It should be noted that all companies are striving to build apparatuses with the largest possible capacity. Thus, methods are being developed for ensuring high-grade mixing while increasing the volume of reaction vessels to 200 m^3 . For this purpose, several mixers are to be installed in a reaction vessel, at times of different designs, the assumption being that a lower mixing speed imparted uniformly throughout apparatus cross section yields a greater effect than does a centralized high-speed mixer. Various types of mixers and densities of arrangement are proposed for reaction vessels operating at temperatures up to 250°C and pressures up to 15 atm. Reaction vessels for mixing thick pulps and other viscous media were shown at the exhibition.

For liquid—liquid systems there are flow-type reaction vessels, most often horizontal, appropriate for highly viscous media (up to 10^{17} cp) with worm conveyor and so-called static mixers, i.e., tubes with special immobile elements, ensuring contact of the fluids with viscosity ratios of 1:1 to $1:10^6$ cp (the Kenix Company, USA). Heat exchange can also be carried out in these mixers at an efficiency five times that generally accepted, owing to those elements. Such mixer elements are used in vertical reaction vessels for liquid—gas systems.

A variety of extractors was presented at the exhibition, the difference from previous years being that only columns with an auxiliary energy supply were displayed. These were of the following types: rotary-plate (Louva, Switzerland), pulsating vibrating (Montzl, GFR; Robotelle, France) with sieve-plate and filled (Raschig rings) attachments. The Robotelle and Podbilnyak companies, which are famous for their extractors, confined themselves to folders about them; Robotelle displayed a pulsating column and announced that such a column measuring 1 m in diameter had been built for the nuclear fuel reprocessing plant in Marcoule. The Montzl folders described a sieve-plate pulsating column with a diameter of 2.5 m and a capacity of up to 100 m^3 . Louva displayed an asymmetric rotary-plate extractor which was a model of a column with a 1.8-m diameter and 45-m^3 capacity. Only one (glass) mixer—settler for pilot plants (Quickfit) was shown. For purely economic considerations, the company representatives recommend mixer—settlers only for processes with few theoretical stages (3–4).

Among the large number of precipitator centrifuges on show at the exhibition attention was attracted by direct-flow auger-feed centrifuges with hollow rotor, purifying discharge water at a rate up to $120 \text{ m}^3/\text{h}$ as well as program-controlled mechanized centrifuges. Five companies use pulsation or vibration to unload the precipitates.

The numerous filters, pumps, and equipment for loading and unloading solid materials and pulps were not distinguished by any particular novelties.

MEETING OF IAEA EXPERTS ON THE TECHNOLOGY
OF INERTIAL PLASMA CONFINEMENT SYSTEMS

V. M. Korzhavin and V. Yu. Galkin

Much attention has been devoted in recent years to a comparatively new approach to solving problems of controlled thermonuclear fusion, inertial plasma confinement. The basic idea consists in heating a small granule of thermonuclear fuel (target) instantaneously with powerful energy sources to thermonuclear temperature, upon which fusion proceeds while the target disintegrates. This approach has become possible because of the considerable progress made in the construction of high-power lasers and high-current electron accelerators. A distinction is made between laser and electronic thermonuclear fusion, respectively.

A meeting of experts, organized in Dubna July 19-23, 1976, by IAEA in conjunction with the State Committee for Atomic Energy of the USSR, was devoted to a discussion of the state of work on inertial plasma confinement and consideration of the prospects of research in this area. Taking part in the meeting were experts from the USSR, the USA, Japan, France, Great Britain, and GFR. The IAEA was represented by the Deputy Director General, I. S. Zheludev, and the Scientific Secretary, J. Philips. The opening session was attended by the Vice Chairman of the State for Atomic Energy of the USSR, I. G. Morozov.

A survey of the US program up to the year 2000 on inertial confinement was presented by L. Quillian (ERDA). Research on laser thermodynamic fusion is being conducted in the USA by the Lawrence Livermore Laboratory, the Los Alamos Science Laboratory, the KMS-Fusion laboratories, Rochester University, and other scientific centers. A laser fusion board has been organized to coordinate the work in the ERDA. According to the long-term program, it is expected that a reaction with a positive efficiency will be achieved in the 1980's and a demonstration reactor will be built in the 1990's. The main research up to 1986 will be based on multichannel neodymium lasers. At the same time, it is proposed to develop the technique of high-power gas lasers, primarily of the CO₂ type, since neodymium lasers have a low efficiency and their active elements have a short lifetime. Much hope is put in new types of lasers. The long-term program envisages close cooperation between research establishments and industry.

A paper by L. Boose (Los Alamos Laboratory) considered questions of the commercial use of lasers in controlled thermonuclear fusion. Since an energy amplification of more than 100 is impracticable, it is believed that the efficiency of a laser used in a reactor should be no less than 20%. Lasers of the carbon dioxide, chemical, atomic-oxygen, excimer, and iodine types seem to hold out the most promise. The Los Alamos Laboratory intends to construct a high-power CO₂ laser with an energy of 10⁵ J for demonstration experiments in 1979.

The results and prospects of work on laser-produced fusion at the Livermore Laboratory was taken up in a paper by C. Hendrix. The Laboratory specializes in neodymium lasers. Construction is now under way of a powerful 20-channel machine, dubbed Shiva, with a pulse energy of 10⁵ J and an output of 25 TW and it is scheduled to come into service in 1978-1979. Demonstration experiments are planned for the early 1980's.

The KMS-Fusion laboratories (paper by F. Meier) recently conducted experiments to ascertain the nature of the neutron radiation from quasispherical targets with the aid of corpuscular methods of diagnosis. The paper presented a conclusion about the thermal character of the fusion reaction. The laboratories have developed a new method of measuring the laser energy injected into a spherical target by using a spherical calorimeter. The injected energy is 10% of the laser energy.

The foremost US laboratories have now attained an integrated output of 10⁷ neutrons in a pulse during irradiation of quasispherical targets. Much attention is being paid to designs of multilayer targets.

Translated from *Atomnaya Énergiya*, Vol.42, No.1, pp.69-70, January, 1977.

This material is protected by copyright registered in the name of Plenum Publishing Corporation, 227 West 17th Street, New York, N.Y. 10011. No part of this publication may be reproduced, stored in a retrieval system, or transmitted, in any form or by any means, electronic, mechanical, photocopying, microfilming, recording or otherwise, without written permission of the publisher. A copy of this article is available from the publisher for \$7.50.

The Scindia Laboratory is the leader in the domain of electronic thermonuclear fusion. In two papers, J. Jonas, who is heading the work, reported on the equipment being used, on the experimental and theoretical results, and on future plans. An undoubted virtue of electronic beams, as compared to laser beams, is the high efficiency of electronic accelerators (50% as against several per cent). However, there are problems of transporting and focusing the beam on the target. The American program is based on the use of self-focusing of the beam in a diode in two-sided irradiation of the target. Since a thermonuclear microexplosion occurs inside the diode, small targets must be used. The problem of obtaining short pulses arises in this connection. Experiments on irradiation of targets are now being performed at powers of up to 10^{12} W and pulse duration of up to about 20 nsec (Hydra and Proto machines). The yield of 10^7 - 10^8 neutrons per pulse is evidently of nonthermonuclear origin. Demonstration experiments are to be carried out in the early 1980's at a power of 10^{14} W. For the purpose, an electronic accelerator, the EBFA-I ($4 \cdot 10^{13}$ W), is under construction and the EBFA-II (10^{14} W) is under development.

The Japanese program of work on inertial plasma confinement was presented in papers by Ch. Yamanaka, S. Nakaya, and K. Niu. The main research institutions are the universities of Osaka, Nagoya, and Tokyo. There are two projects: the Gekko project, based on the use of high-power neodymium lasers, and the Lekko project, based on electro-ionization CO_2 lasers. At the present time, research is being conducted on the Gekko-II machine (neodymium laser with 150-J beam, pulse duration 3 nsec, and flux density up to 10^{16} W/cm²) and the Lekko machine (CO_2 laser, 200 J, 1 nsec, 10^{14} W/cm²). The researchers are studying the absorbed and reflected energy, the spectral composition, the electron temperature, and the energy spectrum of the ions. A threshold of parametric instabilities was established at 10^{10} - 10^{11} W/cm² for the CO_2 laser. Experiments have begun on the compression of shell targets with laser radiation and the interaction of electron beams with plasma and metal foil.

In France, work on laser-produced thermonuclear fusion is also under way in several laboratories. The meeting heard a paper on the Research Center at Limay (paper by A. Bequarian). Experiments on the interaction of laser radiation with matter are being conducted on the facilities M-3 (CO_2 laser, 10 J, 1.7 nsec) and C-6 (neodymium laser, 100-1000 J, 0.1 nsec). A laser is being built with disk modules to operate in the ultra-short-pulse mode at an output of 1 TW. A great deal of attention is being paid to increasing the radiation contrast and improving the diagnostic means.

A paper by Z. Witkowski (Garching, GFR) discussed problems relating to the use of high-power lasers for thermonuclear fusion. A high-power iodine laser with an energy pulse of 200 J and 2-nsec duration is under construction in Garching. Flash-tube pumping of such lasers ensures good duplication of the radiation parameters. Increasing the radiation contrast remains an unresolved problem. Research on laser-produced plasma with the neodymium laser is being carried out in parallel.

The laboratories in Garching and Limay have recorded a very high coefficient of reflection of laser radiation from plasma (up to 30-50%), which is at variance with measurements made in other laboratories.

According to brief communications by T. Allen (Great Britain) and M. White (Rutherford Laboratory, Great Britain) practically no work on inertial plasma confinement is being done in Great Britain and lasers are used largely to heat plasmas in magnetic traps.

The work done in the USSR on laser-produced thermodynamic fusion was presented in papers by G. V. Sklizkov (P. N. Lebedev Physics Institute of the Academy of Sciences of the USSR) and M. I. Pergament (I. V. Kurchatov Institute of Atomic Energy). The Soviet Union has been first on many fundamental problems in this area, such as the idea of laser-produced thermodynamic fusion obtaining the first neutrons, observation of compression of targets, and maximum reflection coefficient in targets. At present, research is being conducted on the machines Kal'mar, Flora, Delfin, and Mishen with a beam of 100-1000 J (neodymium lasers). A project is being developed for an energy of 10^4 J, at which attempts can be made to obtain a positive energy output in the target.

The results and prospects of research on electron-produced thermonuclear fusion in the USSR were discussed in papers by L. I. Rudakov, V. P. Smirnov, S. D. Fanchenko (I. V. Kurchatov Institute) and M. P. Svin'in (D. M. Efremov Scientific Institute of Experimental Atomic Physics). In contrast to the American program, the Soviet program is based on the technique of generating a long-duration pulse of 100 nsec. Calculations show that if an energy of 3-5 MJ is injected into the outer shell of the target, a thermonuclear reaction ensues with an energy output that is 10-100 times the beam energy. To prevent the destruction of the accelerator by the energy from the thermonuclear microexplosion, the target should be at a distance of several meters. This entails a problem of how to transport the beam to the target. A project is being developed for

a 10^{14} -W accelerator of modular design for demonstration experiments. Simulation experiments carried out on the accelerator Ural (beam energy 1 kJ) confirm the promise held out by this method. A great achievement has been the obtaining of the first thermonuclear neutrons $3 \cdot 10^6$ in a pulse, during irradiation of a quasispherical target in the accelerator Triton (1.5 kJ, 30 nsec). Research on focusing and transporting beams and the interaction with targets is being conducted on the new Kal'mar and Angara-1 accelerators at an energy current density of up to $(5-10) \cdot 10^{12}$ W/cm².

During a visit to the I. V. Kurchatov Institute of Atomic Energy and the P. N. Lebedev Institute the foreign delegates to the meeting had an opportunity to become familiar with the equipment being used.

The results of the meeting show that some countries have long-term scientific programs for solving the problems of controlled thermonuclear fusion on the basis of inertial plasma confinement. The important experimental and theoretical results obtained thus far give reason to hope that within the next 5 to 10 years a thermonuclear reaction with a positive energy output will be achieved.

The next meeting on this topic is to be held in the USA or Japan in 1977.

THIRD SESSION OF SOVIET-AMERICAN COORDINATING COMMISSION ON THERMONUCLEAR ENERGY

G. A. Eliseev

In accordance with the program of exchange between the USSR and the USA in the domain of controlled thermonuclear fusion (CTF) the Soviet-American Coordinating Commission held its third session in Moscow July 1-3, 1976. The session considered the state of the art and the prospects for the development of work in the USA and the USSR on CTF, the results of the collaboration in 1975 were summed up, the program of cooperation for 1976 was made more detailed, and a draft program for 1977 was drawn up.

In the course of the exchange of opinions it was noted that in the year since the last session, significant results had been achieved, giving rise to optimism among the scientists engaged in work on the resolution of the problem. In the first place, note should be taken of the relatively large energy time of plasma confinement (~ 60 msec) in the Soviet tokamak T-10 and the record temperature of the ionic component of plasma (~ 2 keV) in the tokamak TFR in Fontenay-au-Roses (France), successful experiments on heating plasma by injection of neutral beams of ~ 300 kW on the American tokamak ORMAC, a marked increase in the parameter $n\tau$ in experiments in the open magnetic trap 2XPB in the Lawrence Livermore Laboratory (USA). In the area of injection designs for CTF, work has proceeded successfully on the construction of powerful injectors of neutral beams, on the development of a technique for heating plasma in tokamaks with gyrotron generators, and on the development of new superconducting cables and structural materials for thermonuclear systems.

The heads of the thermonuclear centers, M. Gottleib (Princeton), J. Clark (Oak Ridge), T. Fowler (Livermore), and F. Ribby (Los Alamos) reported on the state of research on the principal experimental thermonuclear machines of the USA.

Research has proceeded successfully on systems of the tokamak system. Work on the PLT machine, put in service at Princeton at the end of 1975, has produced a steady-state discharge with a current of up to 600 kA in a 35-kG longitudinal magnetic field. The mean plasma density was $3 \cdot 10^{13}$ cm⁻³, the electron temperature was 2 keV, and the energy lifetime was ~ 40 μ sec. Experiments are to be started with a magnetic field of 50 kG. The first PLT injector (40 kW, 25 A) is to come into service at the end of 1976, and experiments with all four injectors with a total injection power of 2-3 MW are envisaged for March 1977. With the power of the injected neutral beam increased to 300 kW, plasma with an ion temperature significantly above the electron temperature (1500 and 660 eV, respectively) was obtained on the tokamak ORMAC (Oak Ridge).

Translated from *Atomnaya Énergiya*, Vol.42, No.1, pp.71-72, January, 1977.

This material is protected by copyright registered in the name of Plenum Publishing Corporation, 227 West 17th Street, New York, N.Y. 10011. No part of this publication may be reproduced, stored in a retrieval system, or transmitted, in any form or by any means, electronic, mechanical, photocopying, microfilming, recording or otherwise, without written permission of the publisher. A copy of this article is available from the publisher for \$7.50.

TABLE 1. Parameters of US Tokamaks

Machine (laboratory)	R, cm	a, cm	B, kG	I, kA	Commissioning, designation
ISX, Oak Ridge	90	25	18	150	February, 1977, study of contaminants
ALCATOR -B/C, MIT	64	17	100/140	800/1200	December, 1977, high- β experiments
DOUBLET-III, General Atomic	140	45 \times 150	26	5000	February, 1978, plasma of noncircular cross section
ORMAC-V, Oak Ridge	92	30	40	800	April, 1978; powerful injection (2 MW)
RDH, Princeton	145	47	25	500	April, 1978, divertor

It was intended to increase the injection power to 500 kW by the end of 1976. The tokamak ALCATOR at MIT produced a record plasma density ($5 \cdot 10^{14} \text{ cm}^{-3}$) in a 75-kG magnetic field. After modernization of the machine experiments are to begin with a magnetic field of ~ 90 kG. A project is being developed for the reconstruction of the machine, envisaging a subsequent increase in the toroidal field to 100 kG (ALCATOR-B), and then even to 140 kG (ALCATOR-C). Elliptical and doublet configurations of the plasma pinch were obtained on the machine DOUBLET-IIA (a tokamak of noncircular cross section, General Atomic). It was shown that the elongated plasma configuration makes it possible to obtain a large discharge current at the same toroidal field. However, the advantages of elongated configurations are not convincing as yet. The parameters of the new US tokamaks are listed in Table 1.

Considerable progress has been noted in the field of open magnetic traps. A combination of a cold gas stream and cold plasma with intense injection of high-energy neutrals enabled high values of $\bar{\beta}$ (~ 0.7) to be obtained on the machine 2XPB (Livermore). At an injection of 225 equiv. the plasma produced had a density of $1.2 \cdot 10^{14} \text{ cm}^{-3}$ with an ion temperature of 9 keV and $n\tau \sim 10^{11} \text{ cm}^{-3} \cdot \text{sec}$. Experiments with large-dimension plasma with a long pulse duration were proposed for the end of 1976. Moreover, it was decided to extend the open-trap work and, in particular, to begin construction of a huge machine, the MH, designed to obtain $n\tau = 10^{12} \text{ cm}^{-3} \cdot \text{sec}$ at a plasma density of 10^{14} cm^{-3} and an ion temperature of 50 keV.

No noteworthy successes were achieved in experiments with high β systems. Research continued on improving the stability of plasma in the machine SCILLAC. Vertical stabilization of the plasma pinch was achieved with a system of feedbacks. Attempts are being undertaken to ensure horizontal stability by using profiled discharge chambers.

The head of the American delegation E. Kintner (ERDA), reported on the elaboration of a long-range US program on CTF, up to and including construction of a commercial thermonuclear power plant. The ultimate goal of the national program is to incorporate thermonuclear power into the overall energy balance of the USA early into the next century. The program is divided into three successive phases:

1. The immediate tasks up to 1985: obtaining plasma with reactor parameters and study its behavior, and realizing the D-T reaction with positive energy output in the TFTR testing tokamak-reactor.
2. Development of the first energy systems by 1990: obtaining electrical powers of more than 10 MW in one or two experimental reactors.
3. Solution of the problem as a whole by the year 2000: constructing the prototype of a commercial thermonuclear reactor with an electrical output of no less than 500 MW for demonstrating the technical feasibility, economic advisability, and radiation safety of commercial thermonuclear power.

The program has been based on systems of the tokamak type. Open traps as well as pulsed systems based on lasers and relativistic electron beams may be competitive. The total cost of the program (up to the year 2000) is estimated at 14.5 billion dollars. Along with the gradual construction of the principal thermonuclear machines and reactors the program envisages provision of the engineering means for the problem. In particular, it provides for the construction of powerful sources of 14-MeV neutrons, as well as an engineering testing reactor ETR for thoroughly testing structural materials under loads corresponding to those in commercial thermonuclear power reactors.

In discussing the results of the cooperation in 1975 and 1976, the commission noted the successful fulfillment of the agreed programs, bringing unquestionable benefit to both parties. Soviet and American specialists participated in the initial experiments on the PLT and T-10. Fruitful discussions were held during working meetings on the problems of divertors, open traps, contaminants, etc. Joint computational work was done

accelerator. It was found that in the neutrino-energy range from 10 to 30 GeV dimuons are produced at the same level of cross section as recorded in the Fermi National Laboratory. This gives evidence in favor of a value of ~ 2 GeV for the mass of the charmed particles. Interesting results were obtained from searches for another type of lepton pairs, μe , which were carried out with large bubble chambers at CERN and the FNL. The choice of the pair μe as an object of the search was methodologically obvious since bubble chambers with a heavy filling enable electrons (positrons) to be recorded with a high degree of accuracy. In addition, in these instruments it is possible to study the vertices of interactions in detail. In the Gargamel chamber in CERN 16 events with $\mu^-e^+\dots$ of the finite state (with an expectation background of 7 ± 2.5 events) were found in a beam, and three of them were of the type $\mu^-e^+V^0\dots$ (with a background of 1.12 ± 0.5). The cross section proved to be smaller by a factor of 20 than in Serpukhov and the FNL. But this is explained if it is considered that the energy range in the experiment was $E = 3-8$ GeV. At such an energy threshold effects have a considerable influence. Not much later, experiments began on the 15-foot FNL chamber, filled with a neon-hydrogen mixture (20% Ne-80% H_2). The Berkeley-Wisconsin-CERN group found 15 events of the type $\mu^-e^+\dots$ among ~ 5000 neutrino interactions with an energy of ≥ 5 GeV and 11 of these were accompanied by V^0 . As is seen from the data of the two experiments, there is a correlated production of strange particles together with a lepton pair. In the latter experiment, the number of strange particles is as yet too high. The mean number of K mesons accompanying the lepton pair calculated with the isotopic ratios, from the number of neutral K mesons detected, was $\langle N_K \rangle \approx 3.6-4$, which is approximately double the theoretical expectations.

For the present, the mechanism of the production of lepton pairs in an antineutrino beam remains unclear. They were observed with approximately the same intensity as in a neutrino beam, only in the FNL electronic apparatus mentioned earlier. Neither the ITÉF-IFVÉ group working with the Serpukhov accelerator nor the Michigan-FNL-ITÉF-IFVÉ group, analyzing photographs of $\bar{\nu}N$ interactions in the 15-foot chamber, has thus far succeeded in finding lepton pairs at the level of 1% of the total cross section.

The culmination of this section of the conference was a report by the Stanford accelerator group (USA) which is engaged in a search for new particles in colliding e^+e^- beams. This group has detected "narrow" states (width less than the instrumental resolution, $\Gamma < 40$ MeV) in the systems $K^\pm\pi^\mp$ and $K^\pm\pi^\mp\pi^\pm\pi^\mp$ with an effective mass of 1.86 GeV. The production cross section is several per cent of the total annihilation cross section in argon and has a threshold at ~ 4 GeV. Since in e^+e^- collisions charmed states should be produced associatively, it is important what accompanies each of them. No partner of the same mass was observed in the spectrum of the recoil mass, but a partner with a mass of 2-2.15 GeV was clearly seen. The results do not yet have an exhaustive explanation. The variants

$$e^+e^- \rightarrow D^* + \bar{D}^* \text{ or } e^+e^- \rightarrow D^* + \bar{D}, D + \bar{D}^*$$

with the subsequent decay $D^* \rightarrow D + \pi$, are working hypotheses.

One more experimental fact pointing to the production of charmed particles in e^+e^- collisions has been obtained on collision rings in DESY (GFR). According to provisional data individual electrons, accompanied on average by five or six hadrons, were found to be created at a level of several per cent of the total cross section beginning from an energy of ~ 4 GeV. The most natural explanation of the effect is that of associative production of charmed particles with one of them subsequently decaying via semilepton channel $D \rightarrow e + \bar{\nu}_e + \dots$, and the other, via the hadron channel. To date, 22 such cases have been recorded.

Charged Currents. Investigations in the given area have recently been quite orderly. Refinements were made in the data on the total cross sections and structural functions over a wide energy interval, from 2 to 100 GeV. Much information came from groups working on the 15-foot chamber. In the range up to ~ 30 GeV it was found that the interaction cross sections for neutrino and antineutrinos grow linearly with the energy and their ratio is constant, $\sigma_{\bar{\nu}N}/\sigma_{\nu N} \approx 1/3$. The numerous differential relations are in fairly good agreement with each other and do not display noticeable deviations (within 10-15%) from the predictions of the simple parton model. At first, such a tendency was observed at high energies as well. However, the Harvard-Pennsylvania-Wisconsin-FNL group found an anomaly in the distribution of the $\bar{\nu}N$ interaction with respect to the scaling variable y (the relative fraction of energy transferred from the antineutrino to hadrons). Analyzing the data, they arrived at the conclusion that from ~ 40 GeV the ratio of cross sections $\sigma_{\bar{\nu}N}/\sigma_{\nu N}$ begins to deviate from 1/3 and grows to 0.72 ± 0.15 at $E_{\bar{\nu}} = 100$ GeV. With less statistical reliability this result was confirmed by the California Institute of Technology - FNL group (USA) engaged in research on the electronic installation of the FNL accelerator. What is this? Violation of scaling, excitation of a quark-antiquark "sea," or a new type of interaction? Each of these hypotheses requires close study.

Neutral Currents. Since 1973, when they were discovered in "Gargamel," neutral currents have become the object of heightened interest on the part of both theoreticians and experimenters. Widespread currency was gained by the Weinberg—Salam model which has a single free parameter, the Weinberg angle, directly related to the mass of the intermediate boson. Experimentally, the representations were verified in both the inclusive channel and the exclusive channel

$$\nu(\bar{\nu}) + N \rightarrow \nu(\bar{\nu}) + X,$$

and the exclusive channel

$$\begin{aligned} \nu(\bar{\nu}) + p &\rightarrow \nu(\bar{\nu}) + p, \\ \nu(\bar{\nu}) + e^- &\rightarrow \nu(\bar{\nu}) + e^-. \end{aligned}$$

Experiments performed by CERN and the FNL in 1975–1976 established that parity is violated in neutral currents. The ratio of the inclusive cross sections was measured in the energy range from 2 to 40 GeV and found to be $\sigma_{\nu}^{Nc}/\sigma_{\bar{\nu}}^{Nc} \approx 0.5 \pm 0.2$. This value corresponds to a $V-A$ interaction. Using a segmented scintillation calorimeter with drift chambers with a total mass of 33 tons, Brookhaven Laboratory (USA) studied the process of neutrino (antineutrino) scattering on a proton. About 20 cases were recorded in each of these reactions. The value of $\sigma(\bar{\nu}p \rightarrow \bar{\nu}p)/\sigma(\nu p \rightarrow \nu p) = 0.35 \pm 0.2$. The Raines—Hare group (USA), who for many years investigated the scattering of electron antineutrinos on an electron with the aid of a beam of antineutrinos from a reactor were the first to report observation of the effect. The difference found from the $V-A$ theory (by four standard deviations) speaks of a contribution by neutral currents. A "pure" process brought about by neutral currents is the scattering of a muon neutrino (antineutrino) on an electron. To the three events found earlier in an antineutrino beam in Gargamel were added 19 $\bar{\nu}_{\mu}e$ events (background 2.9 events) and 25 $\nu_{\mu}e$ events (background 11.8), recorded in the CERN spark-chamber installation by the Aachen—Padua group (GFR—Italy). The data of all the experimenters, analyzed within the framework of the Weinberg—Salam model, give an "average" value of $\sin^2\theta_W \approx 1/3$ for the parameter.

The conference heard several original papers whose subject matter is marginal, as it were, to the principal directions. A case in point is an experiment recently performed in the ITEP to obtain a more exact value for the mass of the electron neutrino. A new lower limit of $m \leq 35$ eV was fixed. Of the theoretical papers, mention could be made of new approaches to the study of the properties of neutral currents via the effects of the nonconservation of parity in atomic physics.

The conference yielded many interesting results which to a considerable extent reflect the wide thrust of investigations in this area of physics. The next conference has been planned for the summer of 1977 in the USSR.

SECOND SEMINAR ON MÖSSBAUER SPECTROSCOPY

V. A. Povitskii

At their second seminar on Mössbauer spectroscopy, held in Munich (GFR) June 16–26, 1976, Soviet and GFR scientists considered the following topics: relaxation effects, hyperfine interactions in magnetics, experimental techniques, hydrogen in metals, coherent effects, and the application of the Mössbauer effect in biology.

V. D. Gorobchenko (USSR) expounded the elements of the theory developed jointly with A. M. Afanas'ev concerning the time-dependent Mössbauer emission spectra in nonequilibrium systems. The formulas obtained enable experimental spectra to be correctly analyzed when the state of the electron shell of the Mössbauer atom experiences relaxation variations as a result of a previous decay.

W. Wagner (GFR) reported on the experimental study of the kinetics of the processes of radiative after-effect using the example of the transitions of the ions $\text{Eu}^{2+} \rightleftharpoons \text{Eu}^{3+}$ formed after the decay of ^{153}Gd by electron

Translated from *Atomnaya Énergiya*, Vol.42, No.1, pp.74–75, January, 1977.

This material is protected by copyright registered in the name of Plenum Publishing Corporation, 227 West 17th Street, New York, N.Y. 10011. No part of this publication may be reproduced, stored in a retrieval system, or transmitted, in any form or by any means, electronic, mechanical, photocopying, microfilming, recording or otherwise, without written permission of the publisher. A copy of this article is available from the publisher for \$7.50.

conversion. The Gorobchenko—Afnas'ev theory was used successfully to evaluate the relaxation time. Two other papers on this subject demonstrated the broad possibilities of Mössbauer spectroscopy in the study of relaxation processes.

The results of investigations of a new effect, induced magnetic ordering in antiferromagnetics, were presented in a paper by S. S. Yakimov (USSR). Using YFeO_3 as an illustration, it was shown that in a "skewed" antiferromagnetic an external magnetic field of 10 kOe sets up a magnetic structure in the temperature range above the magnetic transformation point. New technical capabilities of Mössbauer spectroscopy were discussed by Yu. V. Baldokhin (USSR). The use of radio-frequency (rf) pumping during a Mössbauer experiment makes it possible to obtain such dynamic characteristics of magnetics as the rf-magnetostriction and rf-mobility of domain boundaries.

Experimental techniques were of greatest interest to the Soviet participants in the seminar. In his paper, M. Calvius (GFR) reviewed the helium cryostats and superconducting solenoids that the Mössbauer Institute at the Technical University of Munich (TUM) has for work in transmission geometry. He reported on a system ensuring high pressure at low temperatures. The pressure on the sample reaches 100 kbar and the temperature can be brought down to 1.6°K. The pressure is of a quasihydrostatic nature; boron carbide is used as the material for the pole pieces.

The institute has an original cryostat for research on amorphous thin films sputtered right in it at a low temperature. It is coupled to a high-vacuum system providing a vacuum of up to 10^{-7} . The lowest temperature 0.035°K, is produced by a cryostat in which the absorber is right in a mixing chamber containing $^3\text{He}/^4\text{He}$. The cryostat is provided with a 50-kOe solenoid.

The experimental equipment described in the papers was shown in the laboratories.

West German scientists presented several papers concerning investigations on metal matrices with hydrogen impurities. Nuclei of ^{57}Fe , ^{181}Ta , ^{197}Au , and ^{237}Np were used in the investigations.

In the review paper "Mössbauer spectroscopy of metal—hydrogen systems," G. Bortmann (GFR) presented data obtained to date in the TUM. Among the most interesting were the abrupt variations in the isomeric shift and hyperfine field observed in iron nuclei and iron—nickel and iron—palladium alloys with comparatively small (several at. %) variations in the hydrogen impurities. This result is related to the redistribution of the electron density in the crystal lattice (because the electrons of the matrix atoms are attracted to hydrogen atoms).

Data on the influence of hydrogen on the isomeric shift and the width of the Mössbauer line of ^{181}Ta nuclei were discussed (A. Heidemann, GFR). Two results are particularly noteworthy: 1) as the hydrogen concentration grows to 0.17 at. % the Mössbauer line of ^{181}Ta nuclei is broadened (five-fold) and shifts towards higher energies (from 1 to 10 mm/sec); 2) as the temperature rises (230–400°K), there is a sharp decrease in the hydrogen-induced line broadening so that when 400°K is reached the line has narrowed down to the width characteristic of pure tantalum. This is explained by the effect of fluctuations in the local fields (produced in tantalum nuclei by hydrogen atoms and their being averaged when the temperature rises).

The results are of undoubted interest since they are essentially the first experimental demonstration of the dynamic narrowing of a Mössbauer line owing to thermal diffusion of an impurity.

Great interest among the participants of the seminar was aroused by papers delivered by R. Mössbauer (France) and V. I. Gol'danskii (USSR). R. Mössbauer presented a review of the basic principles of the interaction of gamma radiation with a solid, after a detailed consideration of the theory of coherent effects during scattering of resonance gamma radiation by ideal single crystals, developed in the works of the Soviet scientists Yu. M. Kagan and A. M. Afnas'ev. In his paper, V. I. Gol'danskii (USSR) dealt with the possibility of employing the effect of inverse electron conversion, i. e., the transfer of energy to the electron shell of a nucleus in order to pump the energy level of isomers with laser pulses. He gave estimates for $^{235\text{m}}\text{U}$ from which it follows that 10^3 excited nuclei can be obtained as the result of a single laser pulse with an energy of ~ 10 J.

F. Parak (GFR) devoted his paper to research on the phase problem by using interference of nuclear and Rayleigh scattering. In particular, analysis of protein by this method has a number of important advantages over the method of isomorphic substitution now in use. The difficulty in determining the phase arises from the low activity of the Mössbauer source in comparison with x-ray sources.

The seminar proved to be extremely productive because of the full scientific program, discussions, and personal meetings. The next seminar is proposed for Moscow in 1977.

BIBLIOGRAPHY

PROBLEMS OF THE METROLOGY OF
IONIZING RADIATION*

Reviewed by M. V. Kazarnovskii

To solve many problems of applied nuclear physics there is a need of sufficiently exact and reliable estimates of fluxes of penetrating radiation (neutrons and gamma rays) in various inhomogeneous and nonstationary media from pulsed and stationary sources. In the process it is often necessary to take account of effects accompanying radiation transfer. Such problems arise, for example, in designing shielding for nuclear-engineering installations and spacecraft and in predicting processes which accompany nuclear explosions for peaceful purposes, as well as in connection with some geo- and biophysical problems. A number of such problems are considered in the compilation under review. It consists of two parts.

The first part is devoted strictly to the metrology of penetrating radiation: the metrological aspect of the estimation of the results of cross sections of nuclear reactions and standard methods of calculating fluxes of neutrons and secondary gamma rays, as well as other secondary effects. Here, in the first place, note should be taken of the new system of nuclear constants for calculating the field of neutrons and the secondary effects they produce in air. This system was obtained on the basis of an analysis of the present-day level of experimental error in nuclear data; this analysis is carried out in the first five papers.

Valuable results are given by A. M. Kovalenko and G. Ya. Trukhanov in a paper in which they present a method of enhancing the efficiency of the Monte Carlo method substantially by using the δ -scattering formalism in calculating particle fluxes in nonstationary and inhomogeneous media, based on a special choice of the form of the dependence of the total cross section on the coordinates and the time.

Three papers in this part are devoted to the further development of the so-called quasidiffusion method of solving the kinetic equation[†] (employing the formalism of the integrated nucleus). These papers consider the space-energy distribution of slow neutrons in homogeneous systems with plane and spherical symmetry. It is demonstrated that the quasidiffusion solution of the kinetic equation can be used for a wide class of thermalization problems as a standard method, and also in metrologically securing the measurement of fields of penetrating radiation and in evaluating the error of approximate methods. An important new physical result is the calculation of the space-energy distribution of slow neutrons in an exponential atmosphere. Of particular interest is a paper by G. G. Vilenskaya in which a solution is found to the model problem about the electromagnetic field excited in air by a nonstationary gamma-ray source on an ideally conducting plane.

The second part of the book is devoted to the physical processes which accompany the penetrating radiation transfer in matter as well as metrological information which can be obtained from the data about these processes. Particular attention should be drawn to a cycle of five papers examining the current problems in the theory of declaration of particles in matter with quite general assumptions about the energy dependence of the losses (provided that the mean energy loss per collision is small in comparison with its energy); an analytic solution is given for a problem about the moderation of neutrons from a stationary source with allowance for inelastic scattering; a study is made of the effect of weak absorption on the space-energy distribution of neutrons from a pulsed source; there is a discussion of the evolution of a nonstationary neutron spectrum in the presence of resonances in the absorption cross section; the elastic moderation of neutrons from a pulsed source in a

* Atomizdat, Moscow (1975).

† The nonlinear iterative method makes it possible to obtain a sufficiently exact solution of the complete kinetic equation with a small number of iterations. This is achieved because part of the calculation is transferred to the solution of a diffusion-type equation with a coordinate-dependent effective coefficient of diffusion (quasidiffusion), recalculated during each iteration.

Translated from *Atomnaya Énergiya*, Vol. 42, No. 1, pp. 75-76, January, 1977.

This material is protected by copyright registered in the name of Plenum Publishing Corporation, 227 West 17th Street, New York, N.Y. 10011. No part of this publication may be reproduced, stored in a retrieval system, or transmitted, in any form or by any means, electronic, mechanical, photocopying, microfilming, recording or otherwise, without written permission of the publisher. A copy of this article is available from the publisher for \$7.50.

heavy, weakly inhomogeneous medium is examined; and an analysis is made of the asymptotic behavior of the solution of the stationary equation for neutron transport in an exponential atmosphere.

The remaining papers consider current problems associated with various electromagnetic effects in air caused by the passage of penetrating radiation. In particular, they first examine in detail the reverse effect of excited electromagnetic fields on the currents exciting them and discuss the processes of the generation of electromagnetic fields by distributed systems of charges moving at the speed of light.

On the whole, the book is a serious scientific work devoted to current problems; it will undoubtedly be of interest to a wide circle of specialists. However, in regard to the appropriateness of new publications of a similar type, the following comment must be made about the editorial makeup of the book: papers devoted to various aspects of one general subject have not been combined into one unit, thus resulting in too many repetitions and making reading difficult.

É. G. Rakov, Yu. N. Tumanov,
Yu. P. Butylkin, A. A. Tsvetkov,
N. A. Beleshko, and E. P. Poroikov

THE PRINCIPAL PROPERTIES OF INORGANIC FLUORIDES*

Reviewed by S. S. Rodin and Yu. V. Smirnov

Recent years have been marked by major successes in the study of the chemistry of inorganic fluorides, especially in connection with their use in the atomic industry.

Moreover, investigations on fluorides (especially of transuranium elements) have had a strong influence on the development of many areas of inorganic chemistry, (ultramicrochemistry, crystal chemistry, and the chemistry of coordination compounds) and many new areas of nuclear physics and chemistry. Fluoride compounds hold pride of place in these investigations.

Many previously unknown fluorides have recently been synthesized and of these particular mention should be made of fluorides of elements in the zero group of the periodic table; and the accuracy with which the physical and chemical constants of fluorides are measured has been increased noticeably. Fluorine compounds are employed widely in many branches of technology. This makes it necessary to publish appropriate handbooks to meet present-day needs.

The handbook under review is the result of a systematic search, compilation, and generalization of numerous sources in the literature. It classifies and systematizes scattered data on the principal physicochemical properties of inorganic fluorides (about 850 compounds).

Six tables give the structural and x-ray characteristics of crystals, the temperatures and thermodynamic parameters of materials in the standard state, vapor pressure and decomposition pressure, the molecular constants of inorganic fluorides, and the thermodynamic functions at temperatures of up to 5000°K. An extensive bibliography is given at the end of each table. The handbook has a formula index and the accepted single numeration of materials, and it draws upon original publications to the end of 1973 (more than 1800 references) and some handbook publications.

Despite the fact that the handbook is not exhaustive and that the tables in individual chapters are of a specific character, the goal set has been achieved: to generalize material on the principal physicochemical properties of the most common inorganic fluorides.

* N. P. Galkin (editor), Atomizdat, Moscow (1975).

Translated from Atomnaya Énergiya, Vol.42, No.1, p.76, January, 1977.

This material is protected by copyright registered in the name of Plenum Publishing Corporation, 227 West 17th Street, New York, N.Y. 10011. No part of this publication may be reproduced, stored in a retrieval system, or transmitted, in any form or by any means, electronic, mechanical, photocopying, microfilming, recording or otherwise, without written permission of the publisher. A copy of this article is available from the publisher for \$7.50.

The handbook is addressed to specialists of scientific institutions and enterprises of the atomic energy and chemical industries as well as nonferrous metallurgy. It will also be extremely useful for teachers, graduate students, and students.

engineering science

continued
from back cover

SEND FOR YOUR
FREE EXAMINATION COPIES

Plenum Publishing Corporation

Plenum Press • Consultants Bureau
• IFI/Plenum Data Corporation

227 WEST 17th STREET
NEW YORK, N. Y. 10011

United Kingdom: Black Arrow House
2 Chandos Road, London NW10 6NR England

Title	# of Issues	Subscription Price
Metallurgist <i>Metallurg</i>	12	\$225.00
Metal Science and Heat Treatment <i>Metallovedenie i termicheskaya obrabotka metallov</i>	12	\$215.00
Polymer Mechanics <i>Mekhanika polimerov</i>	6	\$195.00
Problems of Information Transmission <i>Problemy peredachi informatsii</i>	4	\$175.00
Programming and Computer Software <i>Programmirovaniye</i>	6	\$95.00
Protection of Metals <i>Zashchita metallov</i>	6	\$195.00
Radiophysics and Quantum Electronics (Formerly Soviet Radiophysics) <i>Izvestiya VUZ. radiofizika</i>	12	\$225.00
Refractories <i>Ogneupory</i>	12	\$195.00
Soil Mechanics and Foundation Engineering <i>Osnovaniya, fundamenty i mekhanika gruntov</i>	6	\$195.00
Soviet Applied Mechanics <i>Prikladnaya mekhanika</i>	12	\$225.00
Soviet Atomic Energy <i>Atomnaya energiya</i>	12 (2 vols./yr. 6 issues ea.)	\$235.00
Soviet Journal of Glass Physics and Chemistry <i>Fizika i khimiya stekla</i>	6	\$ 95.00
Soviet Journal of Nondestructive Testing (Formerly Defectoscopy) <i>Defektoskopiya</i>	6	\$225.00
Soviet Materials Science <i>Fiziko-khimicheskaya mekhanika materialov</i>	6	\$195.00
Soviet Microelectronics <i>Mikroelektronika</i>	6	\$135.00
Soviet Mining Science <i>Fiziko-tehnicheskie problemy razrabotki poleznykh iskopaemykh</i>	6	\$225.00
Soviet Powder Metallurgy and Metal Ceramics <i>Poroshkovaya metallurgiya</i>	12	\$245.00
Strength of Materials <i>Problemy prochnosti</i>	12	\$295.00
Theoretical Foundations of Chemical Engineering <i>Teoreticheskie osnovy khimicheskoi tekhnologii</i>	6	\$195.00
Water Resources <i>Vodnye Resursy</i>	6	\$190.00

Back volumes are available. For further information, please contact the Publishers.

breaking the language barrier

WITH COVER-TO-COVER
ENGLISH TRANSLATIONS
OF SOVIET JOURNALS

in engineering science

Title	# of Issues	Subscription Price
Automation and Remote Control <i>Avtomatika i telemekhanika</i>	24	\$260.00
Biomedical Engineering <i>Meditinskaya tekhnika</i>	6	\$195.00
Chemical and Petroleum Engineering <i>Khimicheskoe i neftyanoe mashinostroenie</i>	12	\$275.00
Chemistry and Technology of Fuels and Oils <i>Khimiya i tekhnologiya topliv i masel</i>	12	\$275.00
Combustion, Explosion, and Shock Waves <i>Fizika goreniya i vzryva</i>	6	\$195.00
Cosmic Research (Formerly Artificial Earth Satellites) <i>Kosmicheskie issledovaniya</i>	6	\$215.00
Cybernetics <i>Kibernetika</i>	6	\$195.00
Doklady Chemical Technology <i>Doklady Akademii Nauk SSSR</i>	2	\$65.00
Fibre Chemistry <i>Khimicheskie volokna</i>	6	\$175.00
Fluid Dynamics <i>Izvestiya Akademii Nauk SSSR mekhanika zhidkosti i gaza</i>	6	\$225.00
Functional Analysis and Its Applications <i>Funktional'nyi analiz i ego prilozheniya</i>	4	\$150.00
Glass and Ceramics <i>Steklo i keramika</i>	12	\$245.00
High Temperature <i>Teplofizika vysokikh temperatur</i>	6	\$195.00
Industrial Laboratory <i>Zavodskaya laboratoriya</i>	12	\$215.00
Inorganic Materials <i>Izvestiya Akademii Nauk SSSR, Seriya neorganicheskie materialy</i>	12	\$275.00
Instruments and Experimental Techniques <i>Pribory i tekhnika eksperimenta</i>	12	\$265.00
Journal of Applied Mechanics and Technical Physics <i>Zhurnal prikladnoi mekhaniki i tekhnicheskoi fiziki</i>	6	\$225.00
Journal of Engineering Physics <i>Inzhenerno-fizicheskii zhurnal</i>	12 (2 vols./yr. 6 issues ea.)	\$225.00
Magnetohydrodynamics <i>Magnitnaya gidrodinamika</i>	4	\$175.00
Measurement Techniques <i>Izmeritel'naya tekhnika</i>	12	\$195.00

SEND FOR YOUR
FREE EXAMINATION COPIES

Back volumes are available.
For further information,
please contact the Publishers.

continued on inside back cover